

**LOSS OF TRPML1 ALTERS CELLULAR FUNCTIONS OUTSIDE OF THE
LYSOSOME: DISSECTING THE RELATIONSHIP BETWEEN LYSOSOMAL AND
MITOCHONDRIAL HEALTH IN MLIV**

by

Jessica R. Coblentz

B.S. Pennsylvania State University, The Behrend College, 2010

Submitted to the Graduate Faculty of
the Kenneth P. Dietrich School of Arts and Sciences in partial fulfillment
of the requirements for the degree of
Doctor of Philosophy

University of Pittsburgh

2014

UNIVERSITY OF PITTSBURGH
THE DIETRICH SCHOOL OF ARTS AND SCIENCES

This dissertation was presented

by

Jessica R. Coblenz

It was defended on

October 14, 2014

and approved by

Jon Boyle, Assistant Professor, Department of Biological Sciences

Jeffrey Hildebrand, Associate Professor, Department of Biological Sciences

William Saunders, Associate Professor, Department of Biological Sciences

Claudette St. Croix, Associate Professor, Department of Environmental and Occupational
Health

Dissertation Advisor: Kirill Kiselyov, Associate Professor, Department of Biological
Sciences

Copyright © by Jessica R. Coblentz

2014

LOSS OF TRPML1 ALTERS CELLULAR FUNCTIONS OUTSIDE OF THE LYSOSOME: DISSECTING THE RELATIONSHIP BETWEEN LYSOSOMAL AND MITOCHONDRIAL HEALTH IN MLIV

Jessica R. Coblentz, PhD

University of Pittsburgh, 2014

The transient receptor potential mucolipin 1 (TRPML1) is a lysosomal ion channel permeable to cations, including Fe^{2+} . Mutations in *MCOLN1*, the gene coding for TRPML1, cause the lysosomal storage disease (LSD) Mucopolipidosis type IV (MLIV). Recent evidence from our lab suggests that the lysosome functions as a cytoprotective organelle that works to sequester cytotoxic material to prevent cellular damage to other organelles. However, the role of TRPML1 in the cell is disputed and the mechanisms of cell deterioration in MLIV are unclear. The recent demonstration of Fe^{2+} buildup in MLIV cells raised the possibility that TRPML1 dissipates lysosomal Fe^{2+} and prevents its accumulation. In order to determine the function of TRPML1 and identify the molecular mechanisms leading to MLIV pathogenesis, I have analyzed the involvement of TRPML1 in the cytoprotective function of the lysosome. Since Fe^{2+} catalyzes the production of reactive oxygen species (ROS), I set out to test whether or not the loss of TRPML1 promotes ROS production by Fe^{2+} trapped in lysosomes. My data shows that TRPML1-deficient retinal-pigmented epithelial (RPE1) cells develop elevated levels of oxidative stress that promote lipid peroxidation, activation of mitochondrial fission factors, mitochondrial fragmentation, mitochondrial depolarization, and decreased mitochondrial metabolism. These deleterious effects of TRPML1 deficiency were aggravated by Fe^{2+} exposure, but were reversed by incubation with the antioxidant α -tocopherol. As this data suggests, TRPML1 redistributes Fe^{2+} between the lysosomes and the cytoplasm. This work has led to a better understanding of TRPML1's role in

cellular cytoprotection and in lysosomal transition metal homeostasis with regards to Fe^{2+} . As the oxidative burden in TRPML1-deficient RPE1 cell has been recapitulated in MLIV patient fibroblasts and the MLIV mouse model, this data has also provided new developments into the molecular mechanisms of MLIV pathogenesis. Beyond suggesting a new model for MLIV pathogenesis and identifying novel therapeutic treatments for MLIV, this data shows that TRPML1's role in the cell extends outside of lysosomes.

TABLE OF CONTENTS

| | |
|--|------------|
| PREFACE..... | XIV |
| LIST OF FREQUENTLY USED ABBREVIATIONS..... | XVI |
| 1.0 INTRODUCTION..... | 1 |
| 1.1 OVERVIEW..... | 1 |
| 1.2 LYSOSOMES | 2 |
| 1.2.1 Lysosomal Function | 4 |
| 1.2.2 Lysosomal Regulation..... | 7 |
| 1.2.3 Lysosomal Storage Disorders..... | 8 |
| 1.3 MUCOLIPIDOSIS TYPE IV AND TRPML1 | 9 |
| 1.3.1 Mucopolipidosis type IV | 9 |
| 1.3.2 Clinical Manifestations in MLIV..... | 10 |
| 1.3.3 Cellular Pathology in MLIV | 11 |
| 1.3.4 TRPML1 Molecular Genetics..... | 14 |
| 1.3.5 TRPML1 Structural Characterization | 15 |
| 1.3.6 TRPML1 Functional Characterization..... | 18 |
| 1.3.6.1 TRPML1 “Traffic” Model | 18 |
| 1.3.6.2 TRPML1 “Metabolic” Model | 19 |
| 1.3.6.3 TRPML1 and Transition Metal Toxicity..... | 20 |
| 1.3.7 Treatments for MLIV and other LSDs..... | 22 |
| 1.4 REACTIVE OXYGEN SPECIES | 25 |
| 1.4.1 Types of ROS..... | 26 |

| | | |
|-------|--|-----------|
| 1.4.2 | ROS Function and Oxidative Stress..... | 27 |
| 1.4.3 | Measuring ROS..... | 32 |
| 1.5 | MITOCHONDRIA | 34 |
| 1.5.1 | Mitochondrial Function | 34 |
| 1.5.2 | Mitochondrial Dynamics..... | 36 |
| 1.5.3 | GDAP1 Function..... | 39 |
| 1.5.4 | Mitochondrial Damage and Dysfunction in Disease..... | 40 |
| 2.0 | MATERIALS AND EXPERIMENTAL METHODS..... | 41 |
| 2.1 | CELL CULTURE AND BRAIN TISSUE..... | 41 |
| 2.2 | TREATMENTS | 41 |
| 2.3 | siRNA MEDIATED KNOCKDOWNS..... | 42 |
| 2.4 | RNA ISOLATION AND cDNA SYNTHESIS | 43 |
| 2.5 | REAL TIME QUANTITATIVE PCR (qPCR)..... | 44 |
| 2.6 | QUANTIFICATION OF LC3B-II/LC3B-I RATIO..... | 45 |
| 2.7 | MEASUREMENT OF LIPID PEROXIDATION | 46 |
| 2.8 | MEASUREMENT OF MITOCHONDRIAL MEMBRANE POTENTIAL | 46 |
| 2.9 | FLOW CYTOMETRY AND ANALYSIS..... | 47 |
| 2.10 | CASPASE 3 ACTIVITY ASSAY..... | 48 |
| 2.11 | MITOCHONDRIAL MORPHOLOGY ANALYSIS..... | 48 |
| 2.12 | ROS LOCALIZATION..... | 49 |
| 2.13 | SUPEROXIDE QUANTIFICATION WITH MITOSOX™ RED | 49 |
| 2.14 | SEAHORSE ASSAY FOR CELLULAR METABOLIC ACTIVITY | 50 |
| 2.15 | STATISTICAL ANALYSIS | 51 |

| | | |
|--------------|---|-----------|
| 3.0 | LOSS OF TRPML1 PROMOTES PRODUCTION OF REACTIVE OXYGEN SPECIES..... | 52 |
| 3.1 | INTRODUCTION | 53 |
| 3.2 | RESULTS | 55 |
| 3.2.1 | ROS are generated in RPE1 cells in response to TRPML1 deficit..... | 56 |
| 3.2.2 | TRPML1-KD mediates changes in mitochondrial function and morphology | 62 |
| 3.2.3 | α-Tocopherol as a potential therapeutic treatment for TRPML1-deficient RPE1 cells | 74 |
| 3.2.4 | ROS in TRPML1-deficient cells colocalize with lysosomes | 75 |
| 3.3 | DISCUSSION..... | 79 |
| 3.4 | ACKNOWLEDGEMENTS | 81 |
| 4.0 | OXIDATIVE STRESS INDUCED BY TRPML1 DEFICIENCY ALTERS EXPRESSION OF REGULATORS OF MITOCHONDRIAL DYNAMICS AND REDUCES MITOCHONDRIAL METABOLISM | 82 |
| 4.1 | INTRODUCTION | 82 |
| 4.2 | RESULTS | 84 |
| 4.2.1 | RPE1 cell culture model of oxidative stress as a factor in MLIV pathogenesis extends to the MLIV mouse model | 84 |
| 4.2.2 | Oxidative stress in TRPML1-deficient cells alters gene expression of a mitochondrial fission factor | 85 |
| 4.2.3 | Oxidative stress in TRPML1-deficient RPE1 cells decreases mitochondrial metabolic function..... | 92 |

| | | |
|-----|--|-----|
| 4.3 | DISCUSSION..... | 96 |
| 4.4 | ACKNOWLEDGEMENTS | 97 |
| 5.0 | CONCLUSION AND FUTURE DIRECTIONS | 98 |
| 5.1 | TRPML1 LOSS RESULTS IN ROS ACCUMULATION..... | 99 |
| 5.2 | MITOCHONDRIAL HEALTH IN MLIV | 101 |
| | APPENDIX A | 105 |
| | APPENDIX B | 110 |
| | APPENDIX C | 111 |
| | BIBLIOGRAPHY | 126 |

LIST OF TABLES

| | |
|--|-----|
| Table 1 siRNA gene targets and target sequence..... | 43 |
| Table 2 qPCR primers..... | 44 |
| Table 3 Up and down regulated genes from microarray analysis of TRPML1-deficient HeLa cells | 88 |
| Table 4 Anticipated trafficking defects produced as a result of modulating endocytic proteins | 117 |

LIST OF FIGURES

| | |
|---|----|
| Figure 1 Endocytosis, Autophagy, and Exocytosis | 6 |
| Figure 2 RPE1 cells deficient for TRPML1 accumulate electron dense cellular inclusions | 13 |
| Figure 3 Predicted human TRPML1 structure..... | 17 |
| Figure 4 Nrf2 transcriptional regulation in response to cellular oxidative stress | 31 |
| Figure 5 Schematic representation of mitochondrial fusion and fission proteins..... | 38 |
| Figure 6 siRNA mediated TRPML1-KD in RPE1 cells | 59 |
| Figure 7 TRPML1-KD in RPE1 cells leads to ROS production | 60 |
| Figure 8 TRPML1-KD with Fe ²⁺ leads to increased levels of ROS production | 61 |
| Figure 9 3-MA and TRPML1 959-KD alter autophagic flux in RPE1 cells | 64 |
| Figure 10 TRPML1-KD induces lipid peroxidation in RPE1 cells | 65 |
| Figure 11 Mitochondrial depolarization is induced in TRPML1-KD cells and is potentiated by exposure to Fe ²⁺ | 66 |
| Figure 12 TRPML1-KD is not associated with binding of Annexin V | 67 |
| Figure 13 TRPML1 deficiency in RPE1 cells does not induce activation of Caspase 3 | 68 |
| Figure 14 Mitochondrial morphology image analysis..... | 71 |
| Figure 15 Mitochondrial morphology changes as a function of TRPML1 status, Fe ²⁺ treatment, and ROS | 72 |
| Figure 16 TRPML1 745-KD induces changes in mitochondrial morphology | 73 |
| Figure 17 ROS in Fe ²⁺ treated TRPML1-deficient RPE1 cells colocalizes with lysosomes..... | 76 |
| Figure 18 ROS in TRPML1 deficient RPE1 cells are not localized to mitochondria | 77 |

| | |
|---|-----|
| Figure 19 Model of TRPML1-deficiency in RPE1 cells induces ROS and mitochondrial fragmentation | 78 |
| Figure 20 Oxidative stress in brain isolated from MLIV mouse model | 87 |
| Figure 21 Oxidative stress in MLIV patient fibroblasts induces transcription of <i>GDAP1</i> , a key player in mitochondrial fragmentation..... | 89 |
| Figure 22 siRNA modulation of TRPML1, GDAP1, and PPT1 in RPE1 cells..... | 90 |
| Figure 23 Changes in <i>MFN1</i> and <i>GDAP1</i> mRNA levels are specific to TRPML1 functional status in RPE1 cells and not general lysosomal dysfunction..... | 91 |
| Figure 24 Oxidative stress in TRPML1-deficient RPE1 cells inhibits mitochondrial metabolic function | 94 |
| Figure 25 Mitochondrial depolarization in TRPML1-deficient RPE1 cells is dependent on upregulation of GDAP1 | 95 |
| Figure 26 Model of TRPML1 deficiency in RPE1 cells..... | 104 |
| Figure 27 Oxidative stress is induced in TRPML1-deficient RPE1 cells, but not ATP13A2-deficient RPE1 cells..... | 107 |
| Figure 28 Loss of TRPML1 and ATP13A2 in RPE1 cells induces mitochondrial depolarization | 108 |
| Figure 29 Mitochondrial depolarization is rescued by TFEB overexpression in ATP13A2-deficient HEK cells | 109 |
| Figure 30 TRPML1 deficiency in RPE1 cells induces NF- κ B p50 nuclear translocation in an ROS dependent manner | 110 |
| Figure 31 Localization of proteins and phosphoinositides associated with endocytic traffic | 117 |
| Figure 32 siRNA-mediated down regulation of endocytic proteins | 121 |

Figure 33 Texas red dextran delivery to lysosomes after long load and long chase times does not provide enough resolution to distinguish trafficking delays in TRPML1 and PIP5K3 deficient cells 122

Figure 34 Trafficking assays with Alexa Fluor 488 dextran using short load and chase times can be used to pinpoint the time it takes for cargo to be delivered to the early endosome and lysosome in control cells..... 123

PREFACE

I have several people who I would like to thank for helping me become the scientist I am today. First, I would like to thank my thesis advisor, Dr. Kirill Kiselyov, for his mentorship. Kirill's guidance and support has helped me to develop as a person and a critical thinker, while his trust has allowed me to pursue my own scientific interests. I would also like to thank him for my pink pipettes, which have allowed me to excel at bench work. I would like to thank the members of my lab for their experimental advice and friendship. It has been a pleasure to work with all of the members of the Kiselyov lab, both past and present. I especially want to thank my lab mate and best friend, Karina Peña: you have been a constant source of encouragement, scientific knowledge, and genuine happiness throughout the toughest years of my life. Our morning conversations and your friendship have truly made me a better person and have continually renewed my passion for science, even when I thought I should just quit, teach pure barre, and bake cookies. You are going to excel in your career as a scientist and I hope we remain lifelong friends.

I would like to thank my friends and classmates: you guys have truly made this an enjoyable experience; Tom Harper: for guidance with the Leica; Pat Dean and the fiscal office: for keeping our lab stocked with supplies and me paid; and Cathy Barr and the main office: for keeping me registered and on track. I would also like to thank my thesis committee: Dr. Jon Boyle, Dr. Jeffrey Hildebrand, Dr. William Saunders, and Dr. Claudette St. Croix. I am extremely grateful for all of your guidance and support. Your criticism, advice, and enthusiasm have pushed me to be a better scientist. I would also like to extend my thanks to Charleen Chu's lab, especially Jianhui Zhu, for help with several of the mitochondrial assays.

I must also thank my undergraduate research mentor, Dr. Beth Potter: it was your enthusiasm for endolyn and microbes that changed my career path for the better. You welcomed me into your lab and gave me my first scientific project. I will always be grateful for your encouragement and friendship.

Last but certainly not least, I want to thank my family. To my Mom and Dad: to you I am forever grateful for always supporting me and pushing me to find the answers to my “Why’s?” You have taught me that with hard work I can achieve anything. To my Sisters: each one of you has helped to make me the person I am today. Though you never understood my research, you guys have always supported me and know just how to make me smile. To my girls: you have both brought such joy and happiness to my life. Emmie Jane, you have shown me a new meaning of hard work and unpredictability, without you sleeping through the night, I would not have been able to finish this. I hope that my love for science will instill a desire in you to find your passion in life. To the most important person in my life, my husband Ryan: you have been a never ending source of support, whether running marathons or listening to my crazy ideas and experiments gone bad, you have always pushed me and encouraged me to do my best. You have provided me with never ending love and friendship to get me through this crazy time. Your ability to cook delicious meals, make my stress melt away, and make me laugh is what has made me so successful. To you I am eternally grateful. I love you!

LIST OF FREQUENTLY USED ABBREVIATIONS

| | |
|---|---|
| <i>ActB</i> : Actin, Beta | LSD: Lysosomal Storage Disorder |
| AJ: Ashkenazi Jewish | LE: Late Endosomes |
| AP1-3: Adaptor Protein 1-3 | LEL: Late Endosomes/Lysosomes |
| ARE: Antioxidant Response Element | LMP: lysosomal membrane permeabilization |
| α -Toc: Alpha-Tocopherol | 3-MA: 3-Methyladenine |
| CLEAR: Coordinated Lysosomal Expression and Regulation | <i>MCOLN1</i> : Mucolipin-1 |
| CMT: Charcot-Marie-Tooth Disease | <i>MCOLN2</i> : Mucolipin-2 |
| CQ: Chloroquine | <i>MCOLN3</i> : Mucolipin-3 |
| CTR1: Copper Transporter 1 | MFN1/2: Mitofusin 1/2 |
| DMEM: Dulbecco modified Eagle medium | $\Delta\Psi_m$: Mitochondrial Membrane Potential |
| DMT1: Divalent Metal Transporter 1 | MLIV: Mucopolipidosis type IV |
| DRP1: Dynamin Related Protein 1 | MMF: Mitochondrial Fission Factor |
| EE: Early Endosomes | MRI: Magnetic Resonance Imaging |
| EM: Electron microscopy | mTOR: Mammalian Target of Rapamycin |
| ERT: Enzyme Replacement Therapy | NOX: NADPH Oxidase |
| ETC: Electron Transport Chain | <i>NQO1</i> : NADPH: Quinone Oxidoreductase 1 |
| FIS1: Fission Protein-1 | Nrf2: Nuclear Factor-Erythroid 2-Related Factor 2 |
| FBS: Fetal Bovine Serum | OMM: Outer Mitochondrial Membrane |
| GDAP1: Ganglioside Induced Differentiation Associated Protein 1 | OPA1: Optic Atrophy 1 |
| hTERT: human Telomerase Reverse Transcriptase | PCR: Polymerase Chain Reaction |
| <i>HMOX1/HO-1</i> : Heme Oxygenase 1 | PKA: Protein Kinase A |
| IMM: Inner Mitochondrial Membrane | RPE1: Retinal Pigmented Epithelial 1 |
| Keap1: Kelch-like ECH-Associated Protein 1 | <i>RPL32</i> : Ribosomal Protein L32 |
| | RNAi: RNA interference |
| | ROS: Reactive Oxygen Species |

siRNA: small interfering RNA

SRT: Substrate Reduction Therapy

TBHP: tert-butyl Hydroperoxide

TFEB: Transcription Factor EB

TGN: Trans-Golgi-Network

TRP: Transient Receptor Potential

TRPML1: Transient Receptor Potential Mucolipin-1

XO: Xanthine Oxidase

ZIP1: Zrt-Irt-like Protein 1

1.0 INTRODUCTION

1.1 OVERVIEW

Mucopolysaccharidosis Type IV (MLIV) is a lysosomal storage disease (LSD) associated with the loss of the lysosomal transient receptor potential mucopolysaccharin 1 (TRPML1) ion channel. The exact function of TRPML1 is currently unclear, but recent data suggests that it functions as a divalent ion channel promoting the release of Ca^{2+} and transition metals such as Fe^{2+} and Zn^{2+} from the lysosomal lumen. Although it has been shown to conduct these molecules, the effects of divalent metal permeability through TRPML1 have not been studied. Transition metals, such as Fe^{2+} , have been found to accumulate in patients with MLIV. In order to determine if TRPML1 has a role outside of the lysosome, I am interested in determining if the buildup of transition metals in TRPML1-deficient cells affects any organelle or cellular function outside of the lysosome. My research project is centrally focused on determining what happens in the cell when the lysosomal ion channel, TRPML1, is mutated or deficient. Specifically, I wanted to know if other organelles or cellular functions outside of the lysosome are affected by loss of TRPML1. TRPML1 is encoded by the *MCOLN1* gene and mutations in this gene result in the rare lysosomal storage disorder (LSD), MLIV. This disease has a significant neurodegenerative profile and is associated with microglia activation, motor dysfunctions, and the accumulation of cytoplasmic storage bodies. As with many other neurodegenerative diseases, there are no cures for this disease. By determining if

the loss of TRPML1 damages organelles aside from the lysosome and identifying the specific mechanisms by which this damage occurs I will be able to identify new targets for therapeutics to alleviate MLIV pathogenesis, and hopefully other neurodegenerative disease.

This dissertation is divided into 5 sections: 1) background information, 2) methods and materials, 3) the identification that TRPML1 deficiency in RPE1 cells induces oxidative stress, 4) the identification that oxidative stress initiated by TRPML1 deficiency alters the expression of protein regulators of mitochondrial dynamics to induce changes in mitochondrial morphology and alter mitochondrial metabolic activity, 5) conclusions and future directions. The remainder of Chapter 1 will review general information about lysosomal function, regulation, and dysfunction associated with disease, clinical manifestations in MLIV, and the current state of knowledge with regards to TRPML1 function, ROS, and mitochondrial function.

1.2 LYSOSOMES

The lysosome is a membrane bound intracellular acidic organelle that was first described in the early 1950's by Christian de Duve (1). While his discovery was serendipitous, he was awarded the Nobel Prize. Since the first discovery of lysosomes and the identification that they are degradative organelles containing over 60 hydrolytic enzymes and approximately 25 membrane proteins (1-3), the concentric view has stayed very much the same. It wasn't until the discovery of the transcription factor EB (TFEB), in 2009 that people began to appreciate lysosomes as advanced organelles that are crucial regulators of cellular homeostasis (2,4). With the recent discovery of TFEB, the master regulator of lysosomal biogenesis, autophagy, and lysosomal function, what is known about the role of the lysosome has changed drastically. It is now known that lysosomes

play a critical role in substrate degradation, absorption of endocytosed materials, secretion, plasma membrane repair, and they also participate in the recycling of cellular molecules and damaged organelles (3). In order for lysosomes to maintain their degradative capacity, lysosomal hydrolases need to be maintained at pH of 5. In order to maintain this acidic environment, lysosomes contain several ion channels and transporters that create the functional environment for proper cellular degradation. Specifically, the lysosomal H⁺-ATPase utilizes ATP to pump protons from the cytosol into the lysosomal lumen generating an electrochemical gradient to maintain lysosomal pH (2).

Lysosomes are found in virtually all eukaryotic cells where they appear as dark dense bodies within the cytosol (2). They can range in shape, being spherical or tubular, but they typically form a perinuclear pattern within the cell (2). Lysosomes are typically less than 1 μm in diameter, but depending on cell type they can be several microns (2,3). Lysosomal size and number is very dynamic, as it changes in response to cellular conditions and perturbations (2). They are limited by a single 7-10 nm phospholipid bilayer, but also contain an intralysosomal membrane that is rich in phospholipid bis (monoacylglycero)-phosphate, which is the main site of membrane degradation (5,6). Lysosomal membranes proteins are highly glycosylated and therefore their membrane is high in carbohydrate content (2). As a means of protecting the membrane from the highly lytic enzymes within the lumen, glycosylation at the luminal domains form a glycocalyx (7). The lysosome contains high levels of cellular Ca²⁺ that is necessary for the maintenance of cellular trafficking, recycling, and vesicular fusion (8).

1.2.1 Lysosomal Function

The most important function of the lysosome is the intracellular degradation of biological polymers including proteins, nucleic acids, lipid, and carbohydrates. The lysosome receives both intracellular cargo and extracellular cargo for degradation. As seen in Figure 1, extracellular molecules are ingested through endocytosis and passed from the early endosome to the late endosome and finally to the lysosome. As cargo is delivered to the lysosome, it is exposed to the plethora of lysosomal enzymes, which work to degrade cargo (9). To promote lysosomal degradation the intracellular environment of each vesicle gets proceedingly more acidic as vesicles travel through the endocytic pathway en route to the lysosome. The low pH of the lysosome is not only important for the function of acid hydrolases, but it also promotes membrane trafficking. Therefore, disruptions in lysosomal pH have been associated with alterations in endocytic trafficking of proteins and lipids (2).

In addition to endocytosis, the lysosome also participates in exocytosis, which is the expelling of nutrients into the extracellular environment. Initial data suggested that only specialized secretory cells undergo exocytosis, but recent evidence has shown exocytosis to occur in several cell types (10). Exocytosis facilitates plasma membrane repair and allows for cell-to-cell signaling (11). Exocytosis is a two-step process, where lysosomes relocate to the periphery of the cell and fuse with other lysosomes, which is then followed by fusion with the plasma membrane, an event that is dependent on the release of Ca^{2+} (10).

Lastly, the lysosome is important for sequestration, degradation, and recycling of intracellular molecules and organelles, which occurs via a process known as autophagy (11). During this process a double membrane forms around damaged proteins, cytoplasmic components, and damaged organelles, which results in the formation of the autophagosome (12). Next, the contents

of the autophagosome are transported toward the lysosome, which is facilitated by dynein and microtubules (13). Once at the lysosome, the autophagosome can fuse with the lysosome to form an “auto-lysosome” or can briefly interact to transfer its contents that are ready for degradation (2). If the two vesicles fuse the inner autophagosomal membrane enters the lysosomal lumen where it and its contents are degraded, while the outer membrane fuses with the lysosomal membrane (14). Autophagy is classified into three categories including: chaperone mediated autophagy, microautophagy, and macroautophagy (2). In order to regulate autophagy, the mammalian target of rapamycin (mTOR) is crucial, as it is responsible for sensing the energy status of the cell thus determining when cellular content needs to be recycled. Under normal cellular conditions, mTOR interacts with TFEB and is associated with the lysosomal membrane keeping TFEB in the cytoplasm. However, under conditions of starvation TFEB is released and translocates to the nucleus where it can regulate gene expression in order to meet the needs of the cell (15).

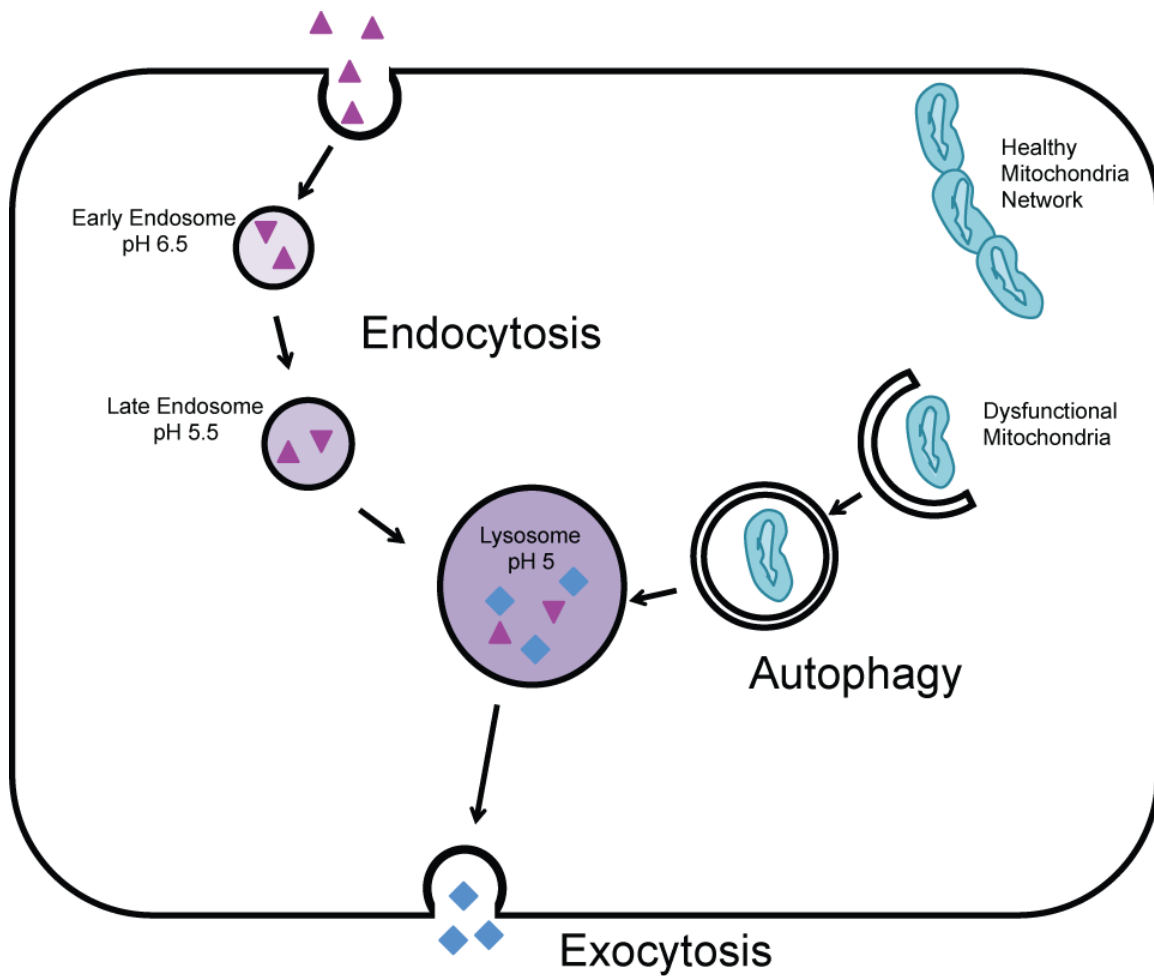


Figure 1 Endocytosis, Autophagy, and Exocytosis

Lysosomes are involved in endocytosis, autophagy, and exocytosis. Endocytosis is important for the internalization of extracellular material, cargo travels through the early endosome (EE) to late endosome (LE) before arriving in the acidic lysosome for degradation. Autophagy is the sequestration, degradation, and recycling of dysfunctional intracellular organelles and macromolecules. Exocytosis is the Ca^{2+} regulated movement and secretion of intracellular material into the extracellular space. Exocytosis aids in plasma membrane repair during injury. Figure modified from Settembre et al (11).

1.2.2 Lysosomal Regulation

As previously mentioned, the lysosome is essential for maintaining cellular homeostasis by regulating cellular clearance and energy production in response to environmental cues. In addition to this task, the lysosome is also important for regulating several physiological processes including cholesterol homeostasis, cytoprotection, cell death, autophagy, and plasma membrane repair. In order for the lysosome to properly regulate these processes, the cell utilizes regulatory gene networks to rapidly respond to environmental cues. Regulatory gene networks are utilized throughout the cell to regulate cellular responses to stress, such as the unfolded protein response.

Until recently, the network regulating lysosomal biogenesis, autophagy, and lysosomal degradation remained unknown. The Coordinated Lysosomal Expression and Regulation (CLEAR) network was the first regulatory gene network associated with the lysosome. Since its discovery, the CLEAR network has been shown to regulate several lysosomal functions including maintenance of lysosomal pH, cellular responses to starvation, lysosomal degradation, and lysosomal biogenesis just to name a few (4,16-18). In 2009, the Ballabio lab showed that in response to conditions of starvation or lysosomal dysfunction via cellular stress or damage, the master transcription factor EB (TFEB) is activated (4). TFEB is a basic helix-loop-helix leucine zipper transcription factor that upon activation enters the nucleus and binds to the CLEAR consensus sequence within the promoter of lysosomal genes (19). This results in the transcriptional regulation of lysosomal genes allowing for the cell to respond to both lysosomal stress by making more functional lysosomes and environmental needs, such as starvation, by inducing autophagy and lysosomal degradation (18-21).

1.2.3 Lysosomal Storage Disorders

Given the complexity of the lysosome, the multitude of cellular activities that it performs, and the number of lysosomal proteins, it is not surprising that defects in any one of these lysosomal components can have deleterious effects on cellular homeostasis. Additionally, defects in any lysosomal hydrolase or membrane protein typically results in impaired lysosomal degradation and the accumulation of storage material, a hallmark of lysosomal storage disorders (14).

Lysosomal storage disorders (LSDs) are a class of rare metabolic disorders caused by deficiencies in specific lysosomal hydrolases or lysosomal proteins involved in lysosomal biogenesis and catalysis. To date, more than 50 hereditary LSD have been described that result in the accumulation of undigested macromolecules in the endocytic pathway (22). While LSDs are generally rare, they do have an incidence rate of about 1:7,000 births (22). While most LSDs are fatal, children typically appear normal at birth but begin to display clinical symptoms at around 12 months of age. In 2/3 of the known LSD the central nervous system is affected. Additionally, other organs including bones, liver, eyes, and skeletal muscle have also been affected in LSDs. As groups of LSDs have similar substrate accumulation, they are typically classified based on substrate accumulations for example sphingolipidoses accumulate sphingolipids, oligosaccharidoses accumulate oligosaccharides, and mucopolysaccharidoses accumulate mucopolysaccharides (14). LSDs can have a mixture of substrates making their classification more challenging (14). Patients suffering from LSDs not only suffer from symptoms as a direct result of lysosomal dysfunction, but the lysosomal accumulations of undigested substrates can also result in secondary defects such as oxidative stress, improper Ca^{2+} handling, perturbed metabolic function, and impaired autophagy (23-25). Unfortunately, the presence of these secondary defects complicates model systems when it comes to research.

1.3 MUCOLIPIDOSIS TYPE IV AND TRPML1

Mucopolipidosis type IV (MLIV) is a neurodevelopmental and neurodegenerative disease caused by mutations in *Mucopolipin-1 (MCOLN1)*, which encodes the lysosomal transient receptor potential ion channel mucopolipin 1 (TRPML1). While the underlying genetic cause of this disease has been identified, the molecular mechanisms leading to disease pathogenesis and neurodegeneration are not well defined. This is due in part to the poor understanding of the role of TRPML1 within lysosomes. Characterizing the loss of TRPML1 is important, as it is not known whether the cellular defects in MLIV are directly caused by the loss of TRPML1 or are an indirect result of the accumulation of lysosomal storage material over time. Several labs are working to understand the exact function of TRPML1 in membrane fusion, Ca^{2+} release, and lysosomal ion homeostasis. Identifying the exact role of TRPML1 within the lysosome will lead to important developments in the molecular pathogenesis of MLIV, as well as general cellular function. The following sections will focus on the characterization of MLIV with regards to clinical manifestations, cellular pathology, molecular genetics, and developments in the structural and functional characterization of TRPML1. Lastly, current treatments and therapeutic approaches for MLIV and other lysosomal storage disorders will be discussed.

1.3.1 Mucopolipidosis type IV

Mucopolipidosis type IV (MLIV) is a rare autosomal recessive lysosomal storage disorder caused by severe or partial loss-of-function mutations in the gene *MCOLN1*, which encodes the lysosomal ion channel transient receptor potential mucopolipin 1 (TRPML1) (26-28). MLIV is characterized by severe neurodevelopmental and degenerative abnormalities with progressive visual impairment

(29). It was first described in the early 1970's when a patient presented with mild developmental delays, cytoplasmic inclusions in cultured cells, and retinal degeneration (30). Since the first diagnosis of MLIV in 1974 it has subsequently been determined to be a pan-ethnic disorder, with approximately 80% of all cases occurring in the Ashkenazi Jewish (AJ) population (26,31). Within this population, it has been estimated that the carrier frequency is 1 in 100, which gives an estimated disease incidence of 1 in 40,000 (32,33). MLIV is only one of several LSDs that commonly occur in the Ashkenazi Jewish population, as Gaucher disease, Tay-Sachs disease, and Niemann-Pick types A and B have also been diagnosed in this population (34).

1.3.2 Clinical Manifestations in MLIV

MLIV is an early onset LSD, with most patients diagnosed within the first year of life with ophthalmological impairments and significant delays in mental and motor development (32,35). As developmental delays are similar to cerebral palsy, MLIV patients are often misdiagnosed (36,37). Normal vision may occur initially, but is often followed by progressive vision impairment within the first decade due to corneal clouding, strabismus, pigmentary retinopathy, and outer retinal degeneration, which ultimately leads to optic atrophy (29,38,39). Visual impairments are likely impacted by the presence of granular material and concentric lamellar bodies within corneal epithelial, conjunctiva epithelial, and retinal ganglion cells, which is discussed in section 1.3.3 (40). While patients may live several decades, the oldest to date being 45, patients typically reach the upper limits of motor and language development by 12-15 months of age but remain neurologically stable later in life (32,34,41). Patients often have trouble speaking and develop spasticity and hypotonia, which significantly reduces motor function and the ability to walk independently (42). In addition to severe motor deficits, MLIV patients also present with iron

deficiency anemia, constitutive achlorhydria, and elevated serum gastrin levels, the latter is typically used as a diagnostic tool for MLIV (35,42).

Neurologically, MLIV patients suffer from white matter dysmyelination and disorganization, dysregulation of neuronal-oligodendroglia interactions, corpus callosum hypoplasia, Purkinje cell death, cerebellar atrophy, reduced maintenance of retinal and optic nerve cells, and decreased signal intensity in basal ganglia (37,43-45). As several of these characteristic neurological features can be identified by magnetic resonance imaging (MRI), MRI has become a useful diagnostic tool (37,46). Unlike other mucopolysaccharidoses, dysmorphic features and organomegaly are not typically reported in cases of MLIV (29,35). Recent work from the Slaugenhaupt lab using the MLIV mouse model has challenged this central view of neurodegeneration in MLIV, as mice were found to have activation of microglia and astrocytes and reduced myelination but no evidence of neuronal loss (41). This study changes our current understanding of MLIV, as it shifts the central idea from the role of the lysosome in neuronal cells to their role in glia cell function. This study presents new possibilities for therapeutic targets in MLIV and other LSDs and additionally provides new avenues for understanding the mechanisms of disease.

1.3.3 Cellular Pathology in MLIV

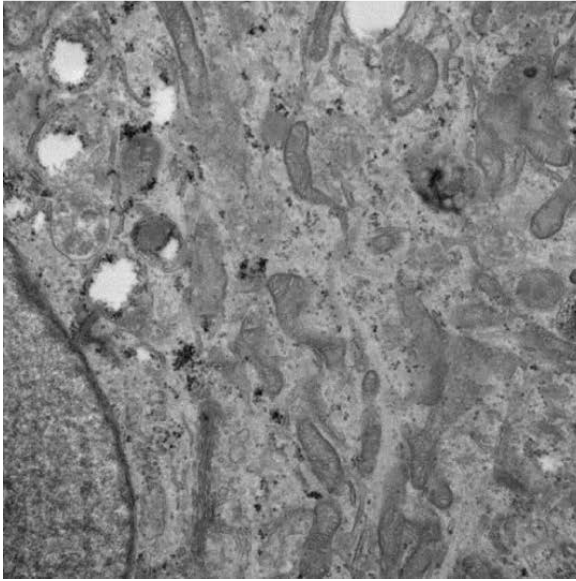
Presentation and severity of ophthalmological impairments, psychomotor retardation, and neurological damage can vary between MLIV patients, but the buildup of undigested substrates in cellular inclusion is one phenotype of the disorder present amongst all patients (32,34,35,47). Electron microscopy (EM) of patient cells show concentric multi lamellar bodies and granulated electron dense vacuoles, indicating the presence of heterogeneous soluble proteins and lipid

aggregates (Figure 2) (32,34,48,49). Pathologically, MLIV is distinguished from mucopolysaccharidoses as there is no excretion of mucopolysaccharide and it is distinct from other mucopolysaccharidoses as lysosomal hydrolases remain functional, the latter may explain the absence of organomegaly (29,50). As with other LSDs, the storage material in patients with MLIV was found to be autofluorescent (51). The distinct morphology and autofluorescent nature of storage material allows for skin biopsies, acid-Schiff staining, and immunofluorescence to be used as diagnostic tools (44,47,51).

While accumulation of cellular material within the lysosome would typically indicate dysfunction of a lysosomal hydrolase, all hydrolases responsible for the catabolism of storage materials are present (52,53). This suggests that the gene associated with MLIV rather than acting as a hydrolase, likely plays a role in regulating endocytic trafficking and/or lysosomal function, inevitably affecting the function of lysosomal hydrolases.

Biochemical analysis has shown abnormal accumulations of sphingolipids, including gangliosides, phospholipids, glycoproteins, and mucopolysaccharides within cells (54). Cellular inclusions are present in cells from every tissue analyzed in MLIV patients, but exact composition of inclusions differs depending on cell type (34). For example, neurons primarily accumulate gangliosides, while hepatocytes and other non-neuronal cells primarily accumulate phospholipids (55). Changes in storage material heterogeneity in different cell types are likely due to cell type specific lipid composition, responses to mutations in TRPML1, and/or different transcriptional profiles present in different cell types (56). In order to understand how the loss of TRPML1 results in cell type specific responses and how different cells respond to endocytic insults, it is crucial to identify the exact function of TRPML1 within the lysosome.

A. Control siRNA Untreated



B. TRPML1 959-siRNA Untreated

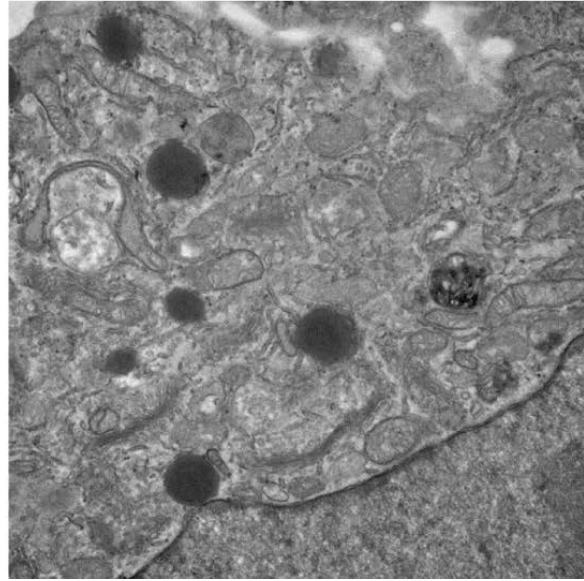


Figure 2 RPE1 cells deficient for TRPML1 accumulate electron dense cellular inclusions

(A) Electron micrograph of control RPE1 cells. (B) Electron micrograph of TRPML1 deficient RPE1. Note the presence of lamellated bodies and electron dense inclusion in TRPML1 deficient cells that are absent in control RPE1 cells.

1.3.4 TRPML1 Molecular Genetics

In 1999, the Gusella lab utilized a genome wide linkage analysis to map the MLIV gene to the short arm of chromosome 19p13.2-13.3 situated between base pair positions 7,587,496-7,598,895 (50). One year later, in 2000, three labs simultaneously cloned the mucolipin-1 (*MCOLN1*, NG_015806.1, NM_020533.2) gene, which encoded a novel protein with high similarity to the transient receptor potential (TRP) family of ion channels (26-28). *MCOLN1* is ubiquitously expressed in all tissues, contains 14 exons, and encodes the transient receptor potential mucolipin-1 (TRPML1) ion channel, which is 580 amino acids in length and has a molecular weight of 65kDa (28). As of August 2014, 28 mutations in both AJ and non-AJ patients have been described, two of these mutations, known as the founder mutations, account for 95% of the MLIV alleles in patients from the AJ population (37,57). These founder mutations include a splice variant (g.5534A→G) and a partial gene deletion (g.511-6944del) (26,29,31,37,50). While some mutations within the *MCOLN1* gene result in complete loss of channel function, other mutations occur that cause channel inactivity and/or mislocalization of TRPML1 within the cell (58,59). Mutations in which the channel is mislocalized or remains inactive are more likely to respond to small molecule therapeutic treatments than mutations that result in the absence of TRPML1 (discussed in section 1.3.7).

Since the identification of the *MCOLN1* gene, no splice variants have been identified in humans, but the mouse gene, *Trpml1*, has two alternatively spliced isoforms (60,61). While no splice variants exist in humans, gene duplications of *MCOLN1* have occurred over time in humans and mice as *Mucolipin-2* (*MCOLN2*) and *Mucolipin-3* (*MCOLN3*) are present in both genomes and encode TRPML2 and TRPML3 proteins, two additional members of the TRPML ion channel

family (54,62). In other model organisms, additional studies have identified only a single gene belonging to the TRPML family in *C. elegans* (*cup-5*) and *Drosophila* (*trpml*, CG8743) (25,60,63).

1.3.5 TRPML1 Structural Characterization

TRPML1 is a member of the mucolipin (TRPML) subfamily of the transient receptor potential (TRP) protein family, which also includes the other subfamilies: TRPC, TRPM, TRPV, TRPA, and TRPP (64). TRP channels are widely distributed in all tissues and act as cellular sensors in response to external or intracellular stimuli such as temperature, sound, light, mechanosensation, PIP₂, Ca²⁺, cyclic nucleotides, pH, phosphorylation potential, and osmotic pressure (64,65). In response to such stimuli, TRP channels are activated and induce depolarization of cellular membranes via the direct or indirect influx of Ca²⁺ and Na⁺ (65). Due to the diverse role of TRP channels, mutations in several TRP genes have been associated with diseases of the intestinal, renal, respiratory, cardiovascular, and nervous systems (65).

While the crystal structure of TRPML1 has not been solved, both bioinformatics and biochemical data from other TRP channels have provided valuable insight about the topology of TRPML1 (Figure 3) (62,66). TRPML1, like other TRP channels, is made of six transmembrane domains (S1-S6) with both amino-terminal (N-) and carboxyl-terminal (C-) tails located within the cytoplasm (28). TRPML1 contains a putative TRP channel pore-forming loop located between S5 and S6 (62). Two negatively charged aspartic acid residues located within this region are predicted to aid in the formation of the pore (67).

Immunostaining and fractionation studies have shown that TRPML1 localization is distinct from most other TRP channels, as it is predominantly localized to late endosomes and lysosomal (LEL) membranes (68-70). TRPML2 and TRPML3, other TRPML subfamily members, are also

localized to the endocytic pathway (71,72). As they are all localized to the endocytic pathway, they have been found to homo- and hetero-multimerize (73,74). Targeting of TRPML1 to LELs relies on the presence of two di-leucine motifs, ETERL¹⁵L and EEHSL⁵⁷⁷L, located within the N- and C-termini, respectively (75). The C-terminal di-leucine motif regulates indirect trafficking of TRPML1 from the Trans-Golgi-Network (TGN) to the plasma membrane followed by endocytic trafficking to the lysosome via interactions with adaptor protein 2 (AP2), while direct trafficking of TRPML1 from the TGN to LEL relies on the interaction of the N-terminal di-leucine motif with clathrin adaptor proteins 1 and 3 (AP1 and AP3) (67,69,76). It has recently been shown that LEL membrane association of TRPML1 is promoted by the palmitoylation of cysteine residues (C⁵⁶⁵CC) located within the C-terminal tail (69). The C-terminal tail also contains two potential protein kinase A (PKA) phosphorylation sites (Ser⁵⁵⁷ and Ser⁵⁵⁹) that are important for regulation of channel activity (77). In addition to phosphorylation by PKA, it has recently been shown that channel activity is highly regulated via the selective binding of specific phosphoinositides at several positively charged amino acid residues within a polybasic domain at the N-terminus (66,78-81). To activate the channel, PI(3,5)P₂ binds to Arg⁶¹ and Lys⁶², while PI(4,5)P₂ binds Arg⁴², Arg⁴³, and Arg⁴⁴ to inhibit channel activity (66,78-81). Similar to its TRP channel relative, polycystic kidney disease protein 2 (PKD-2), TRPML1 contains a large luminal loop between S1 and S2 that may be important for channel regulation (82). Within this loop, TRPML1 contains four N-glycosylation sites in addition to a cleavage site (83-85). The cleavage site is important for the proteolytic cleavage of TRPML1 within the lysosome by cathepsin B and other proteases (83-85).

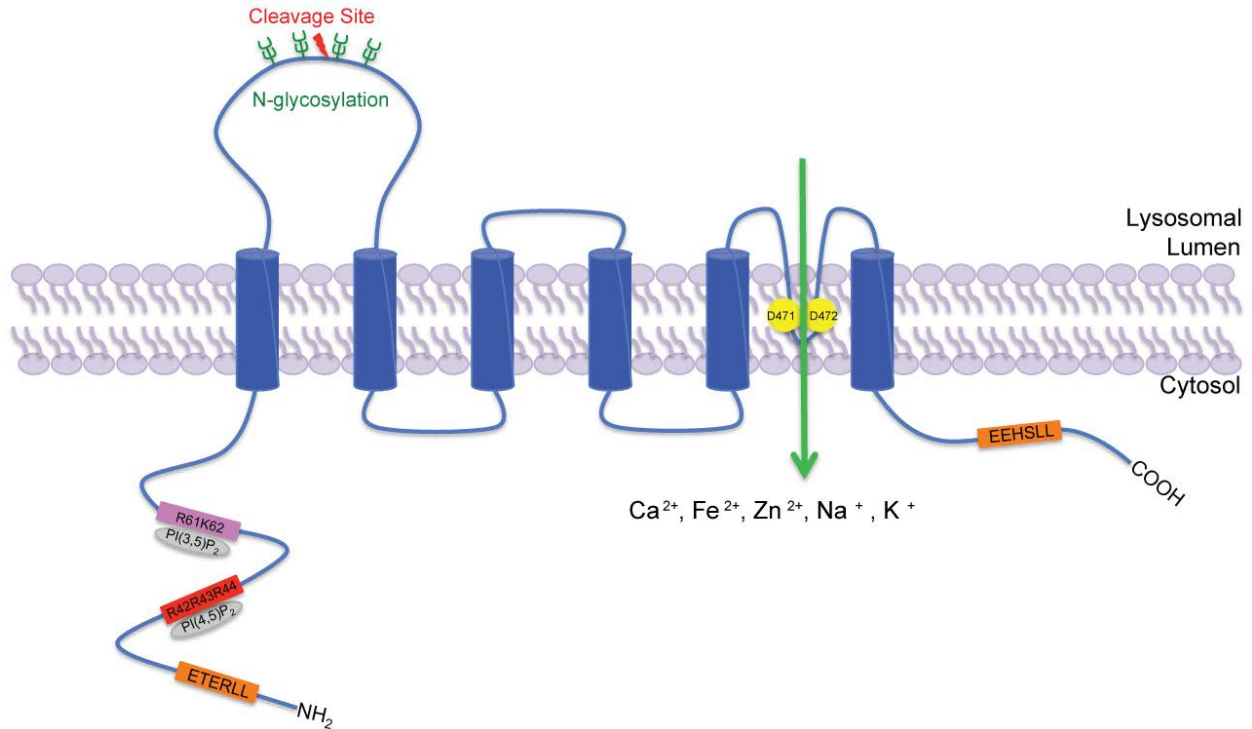


Figure 3 Predicted human TRPML1 structure

Cartoon model of human TRPML1 structural aspects. TRPML1 contains six putative transmembrane domains. Both the N- and C-terminal tails are localized in the cytosol. Two dileucine motifs (ETERL¹⁵L and EEHSL⁵⁷⁷L) are located at the N- and C- terminals, respectively, and are responsible for late endosome and lysosomal localization. Several N-terminal positively charged amino acid residues are predicted phosphoinositide interaction sites (R⁶¹ and K⁶² interact with PI(3,5)P₂ and R⁴²R⁴³R⁴⁴ interact with PI(4,5)P₂). A proteolytic cleavage site and four N-glycosylation sites are located in the large first luminal loop. TRPML1 is a nonselective ion channel and is permeable to Ca²⁺, Fe²⁺, Zn²⁺, Na⁺, and K⁺. The putative pore-forming loop is located between S5 and S6 contains two negatively charged amino acid residues that help form the pore. Model adapted from figure in Wang et al., 2014 (75).

1.3.6 TRPML1 Functional Characterization

While it is known that TRPML1 functions along the endocytic pathway, the exact function of TRPML1 is still up for debate. Studies in MLIV derived patient cells have shown several lysosomal associated defects (discussed in section 1.3.6.1 and 1.3.6.2), but whether these defects are a) directly related to the function of TRPML1 or b) an indirect result of chronic lysosomal dysfunction is not known. It is likely that the answer to this question and others involving TRPML1 will remain unanswered until the exact function of TRPML1 is identified. There are currently two working models of TRPML1 function that explain the primary defect in MLIV. The first model (described in section 1.3.6.1), the “traffic/biogenesis” model, supports the idea that TRPML1 releases Ca^{2+} that drives lysosomal-endosomal fusion necessary for normal degradation of endocytic material (86). The second model (described in section 1.3.6.2), the “metabolic” model, supports the idea that TRPML1 directly regulates lysosomal ion homeostasis necessary for the activity of lysosomal enzymes (86).

1.3.6.1 TRPML1 “Traffic” Model

Initially, the main physiological function of TRPML1 was thought to be the release of Ca^{2+} , which is necessary for the SNARE-mediated fusion of the late endosome and lysosome. This idea led to the development of the “traffic” model, which proposed that TRPML1 directly regulates membrane traffic and when TRPML1 is absent, endocytic material that would normally be targeted for lysosomal degradation accumulates. In support of TRPML1’s role as a Ca^{2+} channel, and in support of the trafficking model, several labs have shown that loss of TRPML1 results in delays of lipid (Lactosyl Ceramide) trafficking in MLIV cells and in *C. elegans* (52,63 ,67,77). The presence of constitutive achlorhydria and increased serum gastrin levels may also be explained by

the proposed role of TRPML1 in lysosomal Ca^{2+} efflux, as Ca^{2+} efflux is important for proper membrane fusion and endocytosis. Inhibition of this cellular event, via the loss of TRPML1, would likely affect normal hydrochloric acid production in gastric parietal cells by preventing parietal cell activation and vesicular trafficking to the membrane (35,42). Whether it is the direct loss of TRPML1 or the secondary accumulation of cellular inclusions causing constitutive achlorhydria remains to be elucidated. Along the same lines, mutations in TRPML1 resulting in the accumulation of undegraded material may be impairing vision in retinal epithelial cells from MLIV patients (54). This model still leaves some open-ended questions, as it does not answer whether the delay in trafficking is a direct result of TRPML1 loss or if the buildup of storage material presents delays in trafficking.

1.3.6.2 TRPML1 “Metabolic” Model

The “metabolic” model relies on the idea that LSDs that are of clear metabolic origin develop delays in membrane trafficking (87). These delays are similar to what has been reported in MLIV. Therefore the function of TRPML1 is mimicking what is observed in other metabolic disorders. The idea of this model relies on the fact that TRPML1 is important for maintaining proper lysosomal ion homeostasis. Therefore in the absence of TRPML1, regardless of the enzymes present, lysosomal ion homeostasis is improperly regulated and enzymes are dysfunctional allowing for the accumulation of storage material similar to other metabolic LSDs. Just as the “traffic” model does not answer all of the questions about the role of TRPML1, neither does the “metabolic” model. While the “metabolic” model does not answer how loss of TRPML1 directly affects lysosomal ion homeostasis, more of the recently published data is in agreement with this model. Recently it was shown that MLIV cells accumulate both Fe^{2+} and Zn^{2+} , which suggest that TRPML1 also plays a role in transition metal homeostasis (79,88). In order to determine which

model better depicts the functional role of TRPML1, more data describing the functional role of TRPML1 in the lysosome is needed.

1.3.6.3 TRPML1 and Transition Metal Toxicity

Transition metals, such as Fe^{2+} , Zn^{2+} , Cu^{2+} , and Ni^{2+} , are essential molecules in all living systems. As an essential nutrient, they are involved in several cellular processes including gene expression, neurotransmission, enzymatic reactions, oxygen transport, energy metabolism, DNA synthesis, and structural maintenance and stabilization of proteins (89-94). While transition metals are indispensable for several cellular processes, their concentrations within the cell needs to be tightly regulated as excess levels cause cellular toxicity and insufficient levels have deleterious effects on the cell. Because of this, transition metals are widely recognized as environmental hazards due to their toxic and carcinogenic effects (93,95).

Iron is the most common transition metal on earth. As a transition metal, iron is an exceptional electron donor as it quickly changes between valances, primarily Fe^{2+} and Fe^{3+} (91). In most cellular conditions, iron exists in the ferric (Fe^{3+}) state and must be reduced to the ferrous (Fe^{2+}) state to become redox active (93). While most metabolically active Fe^{2+} exists in Fe^{2+} binding proteins like hemoglobin and cytochromes, when levels of Fe^{2+} overwhelm Fe^{2+} binding proteins, excess free Fe^{2+} becomes destructive, as it is redox active. Iron contained in the lysosome is often found in the redox active ferrous (Fe^{2+}) state due to the acidic and reducing lysosomal environment (93). Additionally, as the lysosome is responsible for degrading metalloproteins, like transferrin and cytochromes, lysosomes generally contain higher quantities of free metals, specifically redox active metals, making them more susceptible to oxidative stress (93,96). Redox active Fe^{2+} in the lysosome is likely to interact with hydrogen peroxide diffusing into the lysosome,

which catalyzes Fenton reactions. Fenton reactions result in the production of ferryl (Fe^{3+}), hydroxide ions, and ROS in the form of hydroxyl radicals (91). In the case of TRPML1-deficient cells, it is likely the production of these radicals within the lysosome that can have downstream consequences leading to peroxidation of storage material, which generates lipofuscin and ultimately lysosomal membrane damage (91).

Even when Fe^{2+} is maintained at physiological concentrations, the presence of low levels of redox active Fe^{2+} in the lysosome over time can result in the accumulation of lipofuscin, as seen in post-mitotic cells (93,97,98). Accumulation of lipofuscin has been implicated in susceptibility to oxidative stress and decreased lysosomal degradative function (93,99). Impairment of lysosomal degradation ultimately suppresses autophagy and normal recycling of dysfunctional organelles, allowing damaged organelles, like mitochondria, to accumulate. This has been observed in both aging models and LSDs, like MLIV (24,25,49,100,101). Transition metal toxicity has been linked with LSDs and several other neurological diseases including Alzheimer's disease, Parkinson's disease, Huntington's disease, Wilson's disease, and Friedreich's Ataxia (58,88,102-104). The increasing occurrence of transition metal accumulation in diseases of neurological origin emphasizes the importance of proper transition metal homeostasis within cells, as perturbations in this process are detrimental.

Cells have evolved several mechanisms to maintain transition metal homeostasis in order to avoid cellular toxicity. Plasma membrane transporters, such as Copper Transporter 1 (CTR1), Divalent Metal Transporter 1 (DMT1), and Zrt-Irt-like Protein 1 (ZIP1), which aid in the efficient transport of transition metals from the extracellular environment into the cytoplasm (91,102,105-109). Once in the cytoplasm, cells employ chaperones and metal storage proteins, like metallothioneins, to tightly bind metals to reduce their toxic effects (92,110). Additionally,

endocytosis contributes to cellular transition metal levels, as several metal bound proteins, like transferrin, and free metals are endocytosed by cells (93,111). Upon degradation of metal bound proteins in the lysosome, free metals are released into the lumen. Once in the lumen, they remain there and become redox active or are transported to the cytoplasm via lysosomal metal transporters, such as DMT1 (91). Recent data from MLIV patient fibroblasts indicates that DMT1 may not be the only lysosomal metal transporter, as both Zn^{2+} and Fe^{2+} were found to accumulate in cells deficient of TRPML1 (58,88). Interestingly, MLIV patients are also known to accumulate lipofuscin, suggesting that the lysosomal Fe^{2+} is in a redox active state (25,58) While these findings suggest that oxidative stress induced by redox active Fe^{2+} may play a role in MLIV pathogenesis, whether or not the accumulation of metals within the lysosome has detrimental effects on other areas of the cell is not known. Work discussed in Chapter 3 examines the status of oxidative stress and cellular functions outside of the lysosome in TRPML1-deficient cells to determine the extent of cellular damage by accumulation of transition metals, specifically Fe^{2+} (23). These findings have opened new and exciting avenues towards identifying the exact cellular function of TRPML1.

1.3.7 Treatments for MLIV and other LSDs

The search for treatments for several lysosomal storage disorders is an ongoing process, while treatments and therapies for some LSDs have been successful, no specific treatment has been found for MLIV. The search for therapeutic strategies for all LSDs is a difficult process as the underlying molecular causes and disease pathogenesis for LSD are still being discovered. Recent attempts to correct cellular abnormalities associated with MLIV using drugs like Nigericin and Chloroquine (CQ) that lower lysosomal pH have resulted in little success (33). It is likely that therapeutic treatments will remain unsuccessful until the exact function of TRPML1 is elucidated.

More recently, the Grimm lab has utilized small molecules to restore channel function and endolysosomal trafficking defects and to reverse the accumulation of heavy metals in TRPML1 mutants in which the channel is either mislocalized or remains inactive (38). The small molecule MK6-83 was surprisingly able to induce channel activity, rescue aberrant lactosyl ceramide trafficking, and ameliorate zinc accumulation in several mutant expressing cells (F408 Δ and F465L mutants for example) but not TRPML1^{-/-} fibroblasts (38). While not applicable to all MLIV patients, this study suggests possible success in pharmacological treatment of a select group of MLIV patients who retain inactive or mislocalized TRPML1 mutations (38). This study is the first of its kind to rescue channel function, trafficking defects, and transition metal homeostasis defects in MLIV patient cells.

Another exciting pharmacological approach is the use 2-hydroxypropyl- β -cyclodextrin, to induce transcriptional activation of the CLEAR network and TFEB to enhance and restore cellular clearance (112). It has been shown that the activation of TFEB increases lysosomal biogenesis, autophagy, and lysosomal exocytosis via intracellular release of Ca²⁺ by TRPML1 and increasing the population of lysosomes ready to fuse with the plasma membrane (19,113). This increase in exocytosis results in the cellular clearance of stored material and may help to alleviate secondary defects caused by accumulation of stored material within the lysosome. While activation of TFEB has been shown to effectively clear stored material in several LSDs, including Pompe's disease, Batten disease, Neuronal Ceroid Lipofusinos, Multiple Sulfatase Deficiency, Mucopolysaccharideosis Type IIIA. However, it has not produced promising results in MLIV models, as TRPML1 seems to be necessary for TFEB activated clearance (112-114). Not only does activation of TFEB appear to be effective for several LSDs, it has also been used to promote clearance in other neurodegenerative diseases, including both Parkinson's and Huntington's

disease (115,116). While pharmacological activation of TFEB seems promising to treat neurodegenerative diseases, additional studies need to be performed in order to understand the long-term consequences of upregulating TFEB.

Until recently, neuronal health was the central focus of disease pathogenesis in MLIV and therefore therapeutic developments focused primarily on relieving lysosomal abnormalities and dysfunction that results in decreased neuronal health and eventual neurodegeneration. This central paradigm which focused solely on neurodegeneration has shifted since the SLaugenhaupt lab recently showed that the MLIV mouse model revealed activation of glial cells and astrocytes in combination with reduced myelination that does not coincide with neuronal loss (41). This finding will allow for future therapeutic treatments to target neuroinflammation and glial cells via glial progenitor cell replacement therapy (41).

While therapeutic strategies for MLIV patients are unavailable, the most doctors can do for patients is to make them comfortable and improve quality of life. Many MLIV patients undergo intensive physical therapy treatments in combination with vision, speech, and occupational therapies to improve motor function and help with everyday tasks. In addition to physical therapy, iron supplementation is often used to treat iron deficiency anemia, which occurs as a result of the constitutive achlorhydria and poor nutrient absorption (117). Since MLIV patients often suffer extreme eye discomfort in addition to corneal clouding and retinal degeneration, doctors often prescribe increased lubrications and therapeutic contact lenses to decrease pain. In severe cases of MLIV associated with optic atrophy, conjunctiva and corneal transplants have been performed to temporarily correct visual impairments (118).

For several other LSDs, therapeutic strategies have progressed rapidly in the last decade as a direct result of identifying the molecular underpinnings for each disease. For diseases caused by

deficient lysosomal hydrolases several therapeutic options exist, including enzyme replacement therapy (ERT), chaperone treatment, gene therapy, hematopoietic stem cell transplants, bone marrow transplants, and substrate reduction therapy (SRT) (119-122). Enzyme replacement therapy is the most effective and widely used treatment for LSDs. Since it was first approved to treat Gaucher disease, ERT has successfully been used to treat Fabry disease, Mucopolysaccharidosis types I, II, IV, VI, and Pompe's disease (22,119,123,124). While ERT is effective, its inability to cross the blood brain barrier limits its therapeutic potential (14,125). In addition to the treatments above, combination therapy has also proven successful. Combination therapy involves the use of specific treatments, like SRT or ERT, in conjunction with drugs that target secondary effects, like inflammation, in hopes of gaining synergistic effects and managing multiple aspects of the disease (125,126). While all of these strategies have proven effective at altering phenotypes, ameliorating disease symptoms, and improving patient survival, thus far no strategy provides a cure (22). Additionally, as few treatments are accessible to the central nervous system, many strategies are unable to address neurodegeneration associated with most LSDs (14). Identifying therapeutic strategies that address neuropathic symptoms and treat neurodegeneration will pave the way for the future of LSD therapeutics.

1.4 REACTIVE OXYGEN SPECIES

Oxygen is an important component of several biological molecules and it is essential for cellular respiration and the production of energy (127). Given the redox potential of oxygen and the fact that oxygen is essential in the production of cellular energy via the electron transport chain (ETC), it is not surprising that superoxide, a reactive oxygen species (ROS), is produced in the

mitochondria since oxygen can be partially reduced (127). In healthy cells, antioxidant systems are in place to keep levels of ROS in check, but when too many ROS are produced or antioxidants are reduced, oxidative stress can occur (128).

Recently, oxidative stress has been linked to several neurological and neurodegenerative disorders, including several LSDs, Alzheimer's disease, and Parkinson's disease (95). The LSDs associated with elevated levels of ROS include Gaucher, Fabry, GM1 and GM2 (Sandhoff and Tay-Sachs) gangliosidoses, Niemann-Pick type C, Mucopolysaccharidosis Type I and IIIB, Neuronal Ceroid Lipofuscinosis types I, II, III, and VI (129-139). The central nervous system seems to be the perfect environment for oxidative damage, as oxygen requirements in the brain are extremely high and antioxidant systems are generally weaker (127,140). Several mechanisms are responsible for elevated levels of oxidative stress in the brain, by identifying these mechanisms and developing antioxidant therapeutics to alleviate oxidative damage, it is likely I can reduce pathogenic effects associated with several diseases. The following sections will highlight the physiologically relevant reactive oxygen species, their source, their normal cellular function, ROS mediated cellular damage and oxidative stress, regulation of antioxidant systems in response to oxidative stress, the role of oxidative stress in disease, and the means of measuring ROS within the cell.

1.4.1 Types of ROS

Free radicals and reactive molecules derived from molecular oxygen are termed reactive oxygen species (ROS) (95). ROS include superoxide ($O_2^{\bullet-}$), hydroxyl radical ($\bullet OH$), hydrogen peroxide (H_2O_2), and peroxy radical (ROO^{\bullet}). ROS can be generated via non-enzymatic methods through the transfer of electrons directly to oxygen via coenzymes like in the ETC, or via enzymatic

methods by cellular enzymes including NADPH Oxidases (NOX), Xanthine Oxidase (XO), and lipoxygenase (141). Generation of intracellular ROS have been associated with mitochondria, lysosomes, endoplasmic reticulum, peroxisomes, plasma membrane, and the cytoplasm (127).

Superoxide is the most abundant ROS and considered the “primary” ROS as it reacts with other molecules to give rise to “secondary” ROS (95). While the most abundant cellular ROS product is superoxide generated within mitochondria via electron leak in the electron transport chain, it can also arise from irradiation of oxygen (95,142). Hydroxyl radicals are highly reactive and considered very dangerous for the cell as they can react directly with DNA, inducing DNA damage (95,143). Hydroxyl radicals are produced in lysosomes by Fenton reactions, when Fe^{2+} reacts with H_2O_2 molecules resulting in the production of Fe^{3+} , $\cdot\text{OH}$, and OH^- (95,127). The resulting hydroxyl radicals promote intralysosomal oxidation, which eventually damages the lysosomal membrane allowing hydrolytic enzymes to move into the cytosol, where they can activate apoptotic cascades (100). Hydrogen peroxide is produced in peroxisomes as a result of oxygen consumption (95). It is known that peroxisomes not only produce hydrogen peroxide but they also contain catalase, which functions to prevent toxic accumulation of hydrogen peroxide (95). In cells, hydrogen peroxide acts as a signal molecule to modify signaling proteins (127). Peroxyl radicals are the protonated form of superoxide and include hydroperoxyl ($\text{HOO}\cdot$), which has been shown to be associated with lipid peroxidation (95).

1.4.2 ROS Function and Oxidative Stress

Energy production is an essential cellular function, as such; living cells are continually in the presence of ROS. In order to prevent cellular damage from high levels of ROS, cells must maintain their redox state by balancing the rate of ROS production and their removal (127,128). Low levels

of ROS, prove to be beneficial for cells, as they are important for physiological processes, since they function as second messengers in signal transduction pathways to promote cell survival, proliferation and migration (127,144,145). High concentrations of ROS, however, have been shown to be very damaging for cells as they interact with biological molecules promoting DNA damage, lipid peroxidation, and oxidation of proteins, that ultimately induces oxidative stress (140). As a way of combating this process, cells have developed antioxidant mechanism to reduce cellular levels of ROS (95). The antioxidant systems that cells use to maintain ROS include enzymatic antioxidants, like super oxide dismutase, glutathione peroxidase, thioredoxin reductase and catalase, and non-enzymatic antioxidants, like ascorbic acid, α -tocopherol, glutathione, and flavonoids (127). While enzymatic antioxidants primarily function by converting ROS into a non-reactive species, non-enzymatic antioxidants work by neutralizing ROS, preventing lipid peroxidation, becoming radicals themselves, or by terminating free radical chain reactions (127). With these systems in place, healthy cells are able to maintain low to moderate levels of ROS.

When cells are challenged with elevated levels of ROS, whether endogenous or exogenous, in order to avoid detrimental effects, they must be able to rapidly alter their antioxidant capacity. To do so, cells have employed the transcription factor nuclear factor-erythroid 2-related factor 2 (Nrf2), which is considered the master regulator of antioxidant and cytoprotective genes (146-148). Under normal physiological conditions, Nrf2 is bound to its inhibitor Kelch-like ECH-associated protein 1 (Keap1) and is localized to the cytoplasm where it is continuously degraded by the proteasome upon ubiquitination of Nrf2 (Figure 4) (146,147). The inhibitor contains cysteine residues that act as redox sensors to detect changes in cellular ROS levels (146). Upon initiation of oxidative stress, the cysteine residues within Keap1 are oxidized inducing a conformational change that releases Nrf2 and prevents farther ubiquitination of Nrf2 (146,147).

Newly synthesized Nrf2 is then translocated to the nucleus and forms a heterodimer with other transcription factors, like Jun and Maf. The heterodimer then binds to antioxidant response elements (ARE) in the promoter region of several genes to activate their transcription (146). Target genes of Nrf2 include but are not limited to *Superoxide Dismutase 1 (SOD1)*, *Glutathione S-transferase alpha-1 (GSTA1)*, *Metallothioneines (MTs)*, *NAD(P)H: quinone oxoreductase 1 (NQO1)*, and *Heme oxygenase-1 (HMOX1)*. As *NQO1* and *HMOX1* expression was used as an indirect measurement of cellular ROS in Chapters 3 and 4, I will elaborate on their cellular function (149).

Heme oxygenase-1 (*HMOX1/HO-1*) is a ubiquitous inducible cellular stress protein, which functions in oxidative catabolism of heme to produce biliverdin, which is converted into the antioxidant bilirubin. Upon interaction with additional ROS, bilirubin is converted back into biliverdin promoting the neutralization of ROS thereby reducing cellular oxidative stress. Recently, *HMOX1* has been recognized for its role in cellular defense mechanisms, as it is known to confer antioxidant, anti-inflammatory, and anti-apoptotic effects (150).

NAD(P)H: quinone oxoreductase 1 (*NQO1*) is a highly inducible antioxidant and cytoprotective enzyme (151). It is a flavoenzyme responsible for the reduction of quinones, which results in reduced potential for reactive oxygen intermediates to form via redox cycling (151). *NQO1* has also been found to act as a scavenger for superoxide, a gatekeeper for the 20S proteasome, and promotes stabilization of microtubules (151).

While antioxidants systems are very good at alleviating the cellular burden of ROS, sometimes they are unable to overcome the accumulation of ROS. When antioxidants systems can no longer maintain the balance between ROS production and removal, this induces oxidative stress, which can have deleterious effects on cells (127). There are two mechanisms that lead to

oxidative stress. The first involves the generation of too many ROS, which has been associated with aging, inflammation, and chronic diseases (95). The second mechanism stems from inhibition of cellular systems important for eliminating ROS, which has been associated with diseases like Parkinson's disease and some LSDs, which exhibit reduced levels of glutathione (95,152,153). Oxidative stress in cells results in several detrimental phenotypes including lipid peroxidation, cross-linked proteins and protein dysfunction, DNA peroxidation and gene mutations, and ultimately cell death (127).

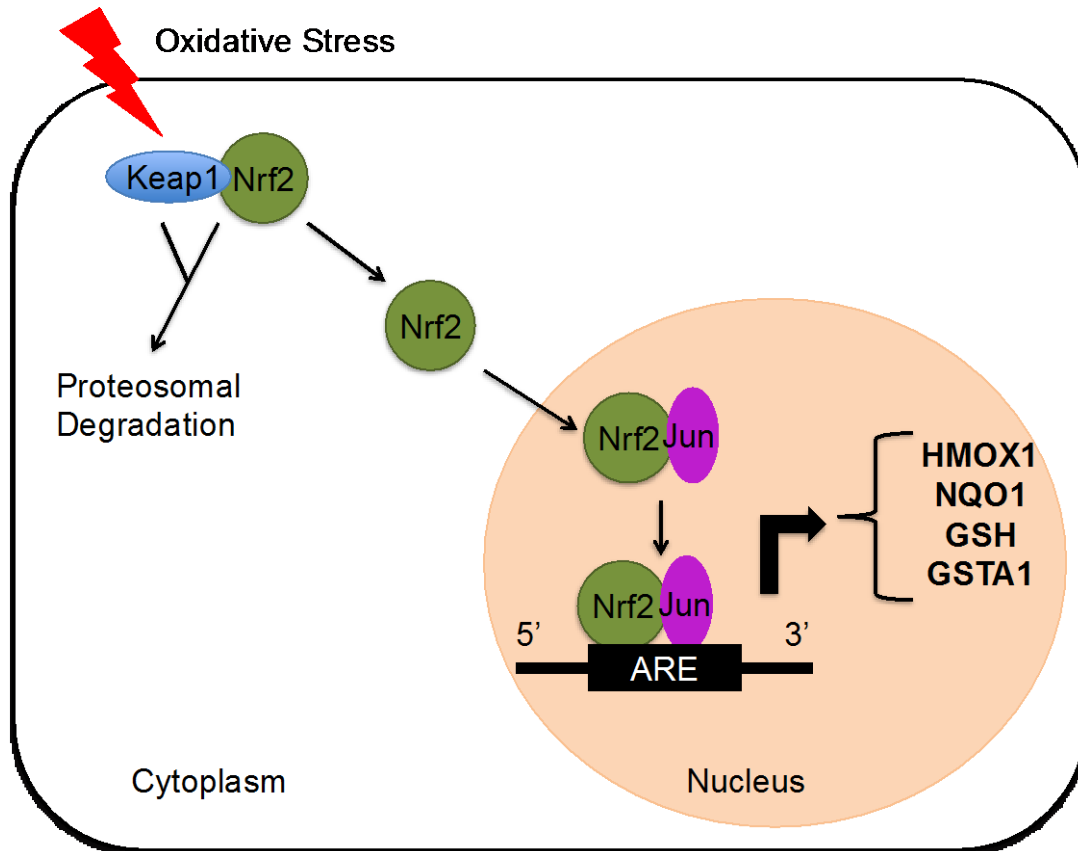


Figure 4 Nrf2 transcriptional regulation in response to cellular oxidative stress

Under normal cellular conditions, Nrf2 is bound to its inhibitor Keap1 and is localized to the cytosol where it is continuously degraded. Keap1 contains cysteine residues that act as redox sensors to detect changes in cellular oxygen levels. Upon initiation of oxidative stress, the cysteine residues within Keap1 are oxidized inducing a conformational change that releases Nrf2. Nrf2 is then translocated to the nucleus and forms a heterodimer with transcription factors, like Jun. The heterodimer then binds to antioxidant response elements (ARE) in the promoter region of several genes, which activates transcription. Figure adapted from Bataille et al (146).

1.4.3 Measuring ROS

A substantial challenge in ROS biology is the ability to measure ROS levels and to determine their cellular localization. While several labs are working on developing new probes to clearly identify specific types of ROS, the tools that are currently available limit the extent of ROS research. The following section will discuss the current techniques available for measuring ROS within the cell, the benefits of each technique, and their limitations.

The first technique that I will discuss is an indirect measurement of ROS, where the ROS burden is measured by examining gene expression of ROS responsive and antioxidant genes. This method relies on the idea that cells challenged by ROS must alter their antioxidant capacity in order to combat new levels of ROS. This process is initiated by the transcription factor Nrf2 as previously discussed. This method requires the isolation of RNA, synthesis of cDNA, and analysis of transcript levels via quantitative polymerase chain reaction (qPCR). While this technique is rather useful in determining if cells are undergoing oxidative stress, it does not provide any information about the level of ROS present nor the type of ROS being generated. In Chapters 3 and 4, this technique was used to examine the abundance of both *HMOX1* and *NQO1* mRNA abundance, which reflects the presence of oxidative stress.

The next technique to examine ROS is the use of a fluorescent ratiometric probe called BODIPY® 581/591 C₁₁ undecanoic acid. This dye is useful for assessing the impact ROS have on the cell. When cells are challenged with increased levels of ROS that are not opposed by antioxidants, ROS are able to damage the cell by oxidizing lipids, proteins, and DNA. This technique is used to examine cellular levels of lipid peroxidation. This fatty acid probe works by reacting with radicals generated by cellular oxidative stress. Upon oxidation, the fluorophore shifts fluorescence from red to green, which is indicative of lipid peroxidation (154). This method is also

an indirect measurement of oxidative stress and does not provide any information about the level of ROS nor the type of ROS present. Additional techniques are also available to measure lipid peroxidation such as the measurement of malondialdehyde (MDA) and 4-hydroxy-trans-2-nonenal (HNE), which are produced as byproducts of lipid peroxidation (155).

The next technique is used to measure several ROS through the use of the cell permeant dye 2',7'-dichlorodihydrofluorescein diacetate (H₂DCFDA). This dye is used to measure intracellular ROS including superoxide, hydroperoxy radical, singlet oxygen, hydroxyl radical, and various peroxides (156). While this technique is widely used and relatively simple to examine localization of several ROS within the cell, it lacks specificity and therefore cannot be used to specifically identify ROS. A major drawback of using this dye is that it is easily photo-oxidized and can result in further production of ROS (156). Dihydroethidium (DHE) is another redox sensitive fluorescent probe. DHE emits blue fluorescence until it is oxidized by superoxide when it shifts to red emissions. While DHE can be used to assess the presence of ROS, it cannot be used to determine localization, as it is known to intercalate with DNA generating a fluorescent signal within the nucleus (157). MitoSOX Red is a variant of DHE, which is targeted to mitochondria to detect mitochondrial superoxide species. While MitoSOX Red can be used to determine the presence of mitochondrial superoxide, it cannot be used to determine exact levels of mitochondrial superoxide species (158). Additionally, genetically encoded ROS probes have recently been developed (142). While these techniques encompass the most common methods to examine intracellular ROS, as more probes are developed it will become easier to determine spatial and temporal intracellular ROS production.

1.5 MITOCHONDRIA

Mitochondria are dynamic organelles that produce most of the cell's energy. While mitochondria are most notably known for their role in energy production via the electron transport chain (ETC) and oxidative phosphorylation, which will be discussed later, mitochondria are also an essential component of signaling pathways as they act to integrate cellular signals and respond by regulating energy supply, ROS signaling, cellular homeostasis, autophagy and intrinsic apoptotic pathways. In addition to acting as integrators of cellular signals, mitochondria also play a role in Ca^{2+} homeostasis, nutrient metabolism, and heme biosynthesis. In order to perform these functions, mitochondria form highly dynamic networks that are continuously remodeled by fission and fusion (159-161).

1.5.1 Mitochondrial Function

Mitochondria are considered the power plant of the cell, as they are essential sites of aerobic energy production in eukaryotic cells (162). Mitochondria maintain energy production through oxidative phosphorylation that couples the flow of electrons through the electron transport chain to generate a proton gradient across the inner mitochondrial membrane (IMM). Throughout this process, an electro-chemical gradient is generated by a series of subsequent steps using 5 protein complexes containing several redox centers. The protons generated from the electron transport chain then travel from the matrix space via a proton-motive force through ATP synthase resulting in the production of ATP (162). As highly efficient ATP producers, cytosolic localization of mitochondria is not random, but rather mitochondria are often found where high amounts of ATP are needed by the cell (163). While most of the electrons generated in the ETC are utilized to

produce ATP, it is possible for electrons to leak out and be transferred to oxygen, which results in the production of superoxide (164). Superoxide generated within mitochondria has the potential to generate additional ROS and reactive nitrogen species, which at low levels are used for cellular signaling but when improperly controlled can be damaging to mitochondria and ultimately the cell (164). To determine if mitochondria are meeting the energy demands of the cell, assays have been developed to assess cellular metabolic activity. One such assay is the Seahorse Extracellular Flux assay, which has the ability to measure mitochondrial metabolism in an isolated environment providing a comprehensive view of cellular metabolism in an extremely sensitive manner among the same cell population. This assay monitors several aspects of cellular metabolism including basal respiration, ATP production, proton leak, maximal respiration, spare respiratory capacity, and glycolytic function. An additional assay often used to examine mitochondrial function and mitochondrial health is the measurement of mitochondrial membrane potential using fluorescent dyes.

In addition to ATP production, mitochondria are dynamic organelles that maintain cellular homeostasis through regulation of cellular maintenance, survival, Ca^{2+} signaling/storage, metabolite synthesis, and apoptosis (165-167). The dynamic nature of mitochondria is important for several of these functions, as mitochondria respond to these cues by changing morphology, connectivity, size, and distribution (168). Mitochondrial dynamics need to be stringently regulated and depend on the balance between fission and fusion machinery. As imbalances between fission and fusion have been shown to negatively impact the viability and physiology of cells (169,170). In addition to regulated fusion and fission, the biogenesis of functional mitochondria and the elimination of dysfunctional mitochondria must be a tightly regulated process in order to ensure that cells are always equipped with healthy ATP generating mitochondria (167,171). One

mechanism of mitochondrial quality control and a cellular survival pathway used to monitor and regulate the elimination of dysfunctional mitochondria is known as mitophagy (172). It is essential to constantly monitor dysfunctional mitochondria, as a buildup of several damaged mitochondria within a cell can activate apoptosis (173).

1.5.2 Mitochondrial Dynamics

Maintenance of mitochondrial morphology is crucial for energy production and cellular homeostasis, therefore mitochondria must be able to rapidly adjust their morphology in response to the metabolic needs of the cell (165). In healthy cells, mitochondria are continuously cycling between fragmented and tubular networks throughout the lifetime of a cell (174). However, when cells are challenged with cellular stressors, such as oxidative stress, apoptosis, necrosis, and autophagy, this intricate balance between fusion and fission shifts toward fission and often results in fragmented unhealthy mitochondria (159,175). The proteins responsible for maintaining this delicate balance in mitochondrial morphology are separated into two groups, the fission proteins and the fusion proteins (Figure 5).

Fission of mitochondria is important for cellular health, as it ensures that damaged mitochondria are targeted for autophagy and promotes generation of new organelles (176). Mitochondrial fission is mediated by the cytoplasmic dynamin-related protein 1 (DRP1) which interacts with the outer mitochondrial membrane (OMM) proteins including, Fission protein-1 (FIS1), Mitochondrial Fission Factor (MFF), and Ganglioside induced differentiation associated protein 1 (GDAP1), the latter will be discussed in section 1.5.3 (168). DRP1 is a large GTPase that is translocated to mitochondria to promote fission (168). FIS1, MFF, and GDAP1 have all been proposed to recruit DRP1 to the OMM scission site, but their exact role in mitochondrial fission

remains unknown (177). At this site, DRP1 promotes fission by forming multimeric ring complexes, which constrict following GTP hydrolysis resulting in fission of mitochondria (166). Recent evidence suggests that FIS1 and MFF influence the number of DRP1 proteins found on the OMM (177). Mitochondrial translocation of DRP1 is highly regulated by post-translational modifications which include phosphorylation by Cdk1/cyclin B kinase at Ser⁶¹⁶ promoting fission, phosphorylation by cAMP PKA at Ser⁶³⁷ inhibiting fission, dephosphorylation by calcineurin at Ser⁶³⁷ increasing fission, polyubiquitination by Parkin, and sumoylation by MAPL to stabilize DRP1 on the mitochondria, thus promoting fission (166).

As elongation of mitochondria favors maximal ATP synthesis, cells that rely heavily on oxidative phosphorylation are constantly undergoing mitochondrial fusion (176). Mitochondrial fusion is regulated by the OMM dynamin-like GTPases Mitofusins 1/2 (MFN1/2) and the IMM GTPase Optic Atrophy 1 (OPA1). MFN1/2 are integrated into the OMM, of the two, MFN1 is required by OPA1 to promote mitochondrial fusion (166). Mitochondrial fusion occurs when MFN1/2 tethers the OMM together, facilitating the remodeling of membrane lipids by hydrolysis of cardiolipin by mitochondrial PLD. This results in the formation of phosphatidic acid, which facilitates fusion by altering membrane curvature (166). Mitochondrial fusion is dependent on GTP hydrolysis to provide energy (178). OPA1 functions to promote IMM fusion. Upon the availability of GTP, OPA1 oligomerizes promoting fusion of the IMM (166). Regulation of mitochondrial fusion occurs through proteasome degradation or proteolytic cleavage of fusion machinery (166). Mitochondrial fusion typically occurs as part of a stress response but fusion also offers a method to evenly maintain organelle populations (166,174,179).

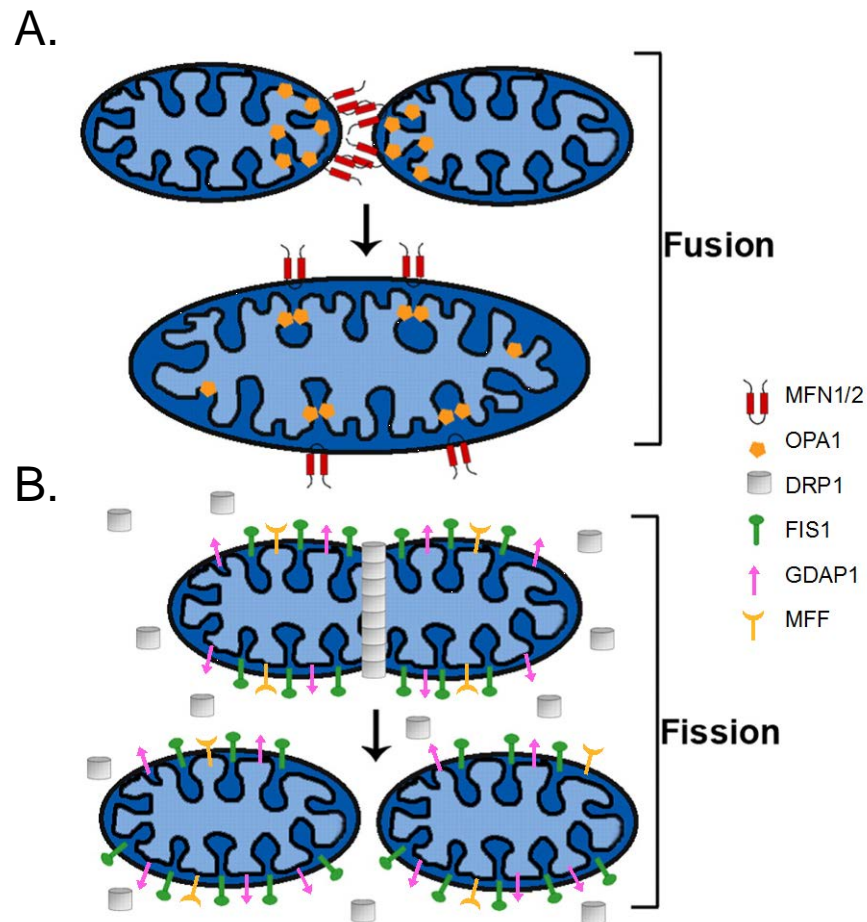


Figure 5 Schematic representation of mitochondrial fusion and fission proteins

(A) During mitochondrial fusion, MFN1/2 link two adjacent mitochondria via their coiled-coil domains promoting OMM fusion. IMM fusion is regulated by OPA1 and occurs upon the hydrolysis of GTP. (B) During mitochondrial fission, post-translational modification of cytosolic DRP1 initiates its recruitment to mitochondria. At the OMM, DRP1 directly interacts with MFN and FIS1, which leads to formation of multimeric ring complexes that promote fission upon the hydrolysis of GTP. GDAP1 is known to function in mitochondrial fission and is anchored in the OMM via a transmembrane domain at the C-terminus (180). Figure adapted from Mandemakers et al (181)

1.5.3 GDAP1 Function

The *GDAP1* gene maps to chromosome 8q21.1 and encodes the ganglioside induced differentiation associated protein 1 (GDAP1), which is expressed primarily in neurons (76,182-184). The GDAP1 protein is involved in mitochondrial fission, as it has been shown to localize to the OMM, and more recently has been shown to affect Ca^{2+} homeostasis and possibly mitochondrial transport (65,183,185). Over expression of GDAP1 has been shown to induce mitochondrial fragmentation, without activating apoptosis in COS-7 cells (183,185). Mutations in *GDAP1* are associated with both dominant and recessive forms of Charcot-Marie-Tooth (CMT) neuropathies (185). GDAP1 is characterized as a new member of the glutathione S-transferase (GST) family based on sequence similarity (182). Members of the GST family promote cellular detoxification by catalyzing reactions of the antioxidant glutathione to detoxify peroxide metabolites (186). Whether or not GDAP1 actually has GST activity is not known, but recent data indicates that GDAP1 expression was critical for protection against oxidative stress in response to low glutathione levels, as cells expressing mutant GDAP1 did not survive (187). This result indicates that GDAP1 may have a protective effect under oxidative stress conditions and suggests that CMT could be linked to oxidative stress. Interestingly, data in Chapter 4 also supports this hypothesis. Recent work with GDAP1L1, the cytosolic GDAP1 paralog expressed primarily in the central nervous system but also in neurons, suggests that GDAP1-family members act in a protective manner against stress caused by elevated levels of oxidized glutathione (185). Interestingly, overexpression of GDAP1 increased total cellular glutathione concentrations in a manner that elevated mitochondrial membrane potential, suggesting that GDAP1 promotes protection from oxidative stress (187). As little is known about the regulation of GDAP1 and its

exact cellular function, future work in this area will provide valuable insight into the protection that GDAP1 provides in instances of cellular and oxidative stress.

1.5.4 Mitochondrial Damage and Dysfunction in Disease

As mitochondria are responsible for producing most of the cells energy and maintenance of mitochondrial dynamics are important for energy production, it is not surprising that several neurological diseases are associated with mitochondrial dysfunction, as the brain is one of the most energy demanding organs in the body (188). Several neurological and neurodegenerative diseases are associated with mitochondrial dysfunction such as mitochondrial morphology defects, increased sensitivity to apoptosis, electron transport chain induced oxidative stress, and reduced metabolic function (188). Interestingly, several of these neurodegenerative diseases associated with mitochondrial dysfunction, are also associated with brain metal accumulations (188). While all of these diseases have similar physiology and disease phenotypes, it is still unclear if metals accumulation causes mitochondrial dysfunction, or if mitochondrial dysfunction causes metal accumulation. As my data in Chapter 3 and 4 suggests that MLIV is a member of this disease class, the impact of my findings can be applied in a much broader context outside of general LSDs. Additionally, recent evidence in several neurological and neurodegenerative diseases not typically associated with mitochondrial dysfunction have linked disease pathogenesis to alterations in mitochondrial morphology and metabolism.

2.0 MATERIALS AND EXPERIMENTAL METHODS

2.1 CELL CULTURE AND BRAIN TISSUE

Human retinal pigmented epithelial 1 (RPE1) cells immortalized with hTERT were cultured in Dulbecco modified Eagle medium (DMEM)/Ham F12 ((DMEM/F12), 1:1 mix) (HyClone, Logan, UT) supplemented with 10% fetal bovine serum (FBS) (Atlanta Biologicals, Norcross, GA) and grown at 37°C in 5% CO₂. HeLa cells and WGO987 (Control) and WGO0909 (MLIV) patient fibroblasts were cultured in DMEM (Sigma-Aldrich, St. Louis, MO) supplemented with 10% FBS and grown at 37°C in 5% CO₂. Brain tissue isolated from two and six month old TRPML1^{-/-} knockout mice and wild-type (WT) littermate controls (n=4 for each condition), was obtained as a collaboration with Susan Slaughaupt's lab at Harvard Medical School.

2.2 TREATMENTS

All Fe²⁺ treatments were performed in DMEM/F12 with 100 μM iron (II) chloride tetrahydrate (Sigma) for the indicated times. All Zn²⁺ treatments were performed in DMEM with 100 μM zinc chloride (Sigma) for the indicated times. All α-Tocopherol (α-Toc) treatments were performed in DMEM/F12 with 100 nM α-Toc (Sigma) for 24 hours prior to experiments. Mitotracker, mitosox, C₁₁-BODIPY staining and imaging, and JC-1 fluorescence reading were performed in regular buffer which contained, in mM: 150 NaCl, 5 KCl, 1 CaCl₂, 1 MgCl₂, 10 HEPES, pH 7.4, and 1 g/L glucose. All tert-Butyl hydroperoxide (TBHP) treatments were performed for 4 hours with 200

μ M TBHP (Invitrogen, Carlsbad, CA). For analysis of Annexin V binding and Caspase 3 activity, cells were treated with 100 nM Staurosporine for 12 hours prior to analysis.

2.3 siRNA MEDIATED KNOCKDOWNS

For all KD's, the following genes were targeted with the siRNA indicated in Table 1, *MCOLN1*, *PPT1*, *GDAP1*, *DRP1/DNM1L*, *RAB5A*, *RAB7A*, *FIG4*, *VAC14*, *PIP5K3*, *TPC1*, and *ATP13A2* (189,190). Non-targeting control siRNA#1 purchased from Sigma was used as a negative control. For knockdown of endogenous genes, RPE1 cells were plated in either 12 well plates (qPCR) or 35 mm dishes (with or without glass coverslips for all other experiments) and grown to ~70% confluency. As described by manufacturer's protocol, cells were transfected with either control or appropriate siRNA using Lipofectamine RNAiMAX (Invitrogen). Transfections were performed using 300 nM siRNA per 35 mm dish 72 hours prior to analysis. To confirm the efficiency of each knockdown, SYBR-green based qPCR was performed. In the case where appropriate antibodies were available, protein levels were also examined.

Table 1 siRNA gene targets and target sequence

| Gene Target | Supplier | Target Sequence | Target Location |
|----------------------|-------------------------------|---------------------------------|-----------------|
| Control siRNA #1 | Sigma SIC001-10NMOL | Non-targeting | Non-targeting |
| <i>MCOLN1 959</i> | Dharmacon Custom KISKD-000001 | 5'-CCCACATCCAGGAGTGTA-3' | 959-977 |
| <i>MCOLN1 745</i> | Dharmacon J-006281-08-0010 | 5'-GAUCUCACCCUCUUGGAAA-3' | 745-763 |
| <i>PPT1</i> | Dharmacon COLGA-000013 | 5'-GGUACUCACAUAAAUGCUIUUU-3' | 1556-1575 |
| <i>GDAP1</i> | Sigma SASI_Hs02_00309162 | 5'-GAAAGUCUUGGAUCAGGUU-3' | 718-736 |
| <i>DRP1/ DNM1L</i> | Sigma SASI_Hs02_00340086 | 5'-GUAUACUGAGACUUGUU-3' | 2198-2216 |
| <i>TPC1</i> | Dharmacon J-010710-07-0005 | 5'-CCAUCGAGCUGUAUUUCAU-3' | 1321-1339 |
| <i>RAB5A</i> | Dharmacon J-004009-08-0005 | 5'-AGAGUCCGUGUUGGCAA-3' | 616-634 |
| | Dharmacon J-004009-05-0005 | 5'-GCAAGCAAGUCCUAACAUU-3' | 895-913 |
| <i>RAB7A</i> | Dharmacon J-010388-08-0005 | 5'-GGGAAGACAUCACUCAUGA-3' | 290-308 |
| | Dharmacon J-010388-05-0005 | 5'-CUAGAUAGCUGGAGAGAUG-3' | 527-545 |
| <i>FIG4/KIAA0274</i> | Dharmacon J-019141-12-0010 | 5'-AGCUAGGUAUCUACGAAUA-3' | 656-674 |
| | Dharmacon J-019141-11-0005 | 5'-GGGCUUAAUUCGAGCGGUU-3' | 467-485 |
| <i>VAC14</i> | Dharmacon J-015729-05-0010 | 5'-GAACACCUCUGGUACCAA-3' | 1789-1807 |
| | Dharmacon J-015729-06-0010 | 5'-CCAGAACAUAACCGUGCAA-3' | 397-415 |
| <i>PIP5K3</i> | Dharmacon J-005058-12-0005 | 5'-UCUGAGCCAUCCUGGUUUA-3' | 1542-1560 |
| | Dharmacon J-005058-15-0005 | 5'-GAUGGACGUUGGCUGGAUU-3' | 1002-1020 |
| | Dharmacon J-005058-13-0010 | 5'-GGCACAAGCUAUAGCAAUU-3' | 1367-1385 |
| <i>ATP13A2</i> | Invitrogen hss118711 | 5'-CCAACGUGAUCAGCAUACCGGUCAA-3' | 887-911 |
| | Invitrogen hss118712 | 5'-GGACUUGAAGAUGGUGGAGUCUACU-3' | 1953-1977 |
| | Invitrogen hss118713 | 5'-CAGAGCUGGUGUGCGAGCUAGAGAA-3' | 2813-2837 |

2.4 RNA ISOLATION AND cDNA SYNTHESIS

Total cellular RNA was extracted from cultured RPE1 cells or patient fibroblasts grown in 12 well plates using TRIzol (Invitrogen) as per the manufacturer's instructions. For isolation of RNA from mouse brain tissue, tissue was homogenized in Trizol as per the manufacturer's instructions. For cDNA synthesis, 2 µg total RNA was annealed with 0.5 µg oligo (dT)₁₈ primer (Thermo Scientific, Waltham, MA and IDT, Coralville, IA) followed by reverse transcription with MuLV Reverse Transcriptase (Applied Biosystems, Foster City, CA).

2.5 REAL TIME QUANTITATIVE PCR (qPCR)

qPCR was performed using 1:1000 dilutions of cDNA, 2X SYBR green (Fermentas, Glen Burnie, MD), and 4 μ M primer per 10 μ l reaction. The following genes were amplified using the primers indicated in Table 2; *RPL32*, *MCOLN1*, *HMOX1*, *PPT1*, *GDAP1*, *MFN1*, *NQO1*, *ActB*, *TPC1*, *RAB7A*, *RAB5A*, *PIP5K3*, *VAC14*, *FIG4*, *DRP1/DNM1L* and *ATP13A2*. All IDT primers were designed to span exons and negative RT controls were tested to ensure amplification of cDNA only. qPCR was performed using the Relative Quantification method on the 7300 Real Time System (Applied Biosystems). Reactions were run on the following parameters: 2 minutes at 50°C, 10 minutes at 95°C, and 40 cycles at 95°C for 15 sec followed by 60°C for 1 minute. All biological assays were run in triplicate. Relative gene expression were calculated using the $2^{-\Delta\Delta C_t}$ method, where C_t indicates cycle threshold (191). Data are presented as percent difference in expression upon normalization to the house keeping genes, *RPL32* or *ActB* where indicated, and relative to control-KD cells, WGO987 (control) fibroblasts, or WT littermate controls.

Table 2 qPCR primers

| Gene Name | Supplier | Species | Forward Primer | Reverse Primer |
|-------------------|----------|---------|------------------------------------|------------------------------------|
| <i>RPL32</i> | Qiagen | Human | QT01668198 | QT01668198 |
| <i>MCOLN1</i> | IDT | Human | 5'-TCTTCCAGCACGGAGACAAC-3' | 5'-AACTCGTTCT GCAGCAGGAAGC-3' |
| <i>HMOX1</i> | IDT | Human | 5'-GAGACGGC TTCAAGCTGGTGAT-3' | 5'-CCGTACCAG AAGGCCAGGTC-3' |
| <i>PPT1</i> | IDT | Human | 5'-CCTGTAGATTCG GAGTGGTTTGATT-3' | 5'-CAGGCGGTC CTGTGTGTACA-3' |
| <i>GDAP1</i> | IDT | Human | 5'-CCAGAAGAGGG CCAGCAAC-3' | 5'-CTCAAGACACGCTCG TAATAGGTTTCC-3' |
| <i>Mfn1</i> | IDT | Human | 5'-TCAGATGAAAAA AAGAGTGTGAAGAC-3' | 5'-ACATCTGTGCCT GGAAGTGTACTA-3' |
| <i>RPL32</i> | IDT | Mouse | 5'-CACCAGTCAGAC CGATATGTGAAA-3' | 5'-TGTTGTCAATGCCTC TGGGTTT -3' |
| <i>HO-1</i> | IDT | Mouse | 5'-CACAGATGGCG TCACTTCCGTC-3' | 5'-GTGAGGACCCAC TGGGAGGAG-3' |
| <i>NQO1</i> | IDT | Mouse | 5'-GGTAGCGGCTCC ATGTACTC-3' | 5'-CATCCTTCCAGGA TCTGCAT-3' |
| <i>ActB</i> | Qiagen | Human | QT00095431 | QT00095431 |
| <i>TPC1</i> | AB | Human | Hs00330542_m1, 4331182 | Hs00330542_m1, 4331182 |
| <i>RAB7A</i> | IDT | Human | 5'-GAGATTCTGGAGTC GGAAGACATC-3' | 5'-TGCTGTGCCCA TATCTGCATTGTG-3' |
| <i>RAB5A</i> | IDT | Human | 5'-GAGTACCATTGG GGCTGCTTTTCTAAC-3' | 5'-CTCTTGCAAAGGA CTCCTCATTGTGA -3' |
| <i>PIP5K3</i> | IDT | Human | 5'-TGGCCTGGCAAAG TTTGATTCATC-3' | 5'-ATGCTGGCTGATC TATTTGAGCA-3' |
| <i>FIG4</i> | IDT | Human | 5'-TGTGGCAGTCA AAGCTGTTGATCTA-3' | 5'-CAACATCACCTC ACAGTTTGCAC-3' |
| <i>VAC14</i> | IDT | Human | 5'-ATCATCTCCTGGA TCCTGGTCTG-3' | 5'-GAACAACCTCAC ACATTTTGCGAATCT-3' |
| <i>DRP1/DNM1L</i> | IDT | Human | 5'-TGTAGCAATTAC AGTACACAGGAATT-3' | 5'-TTCAATTGCCA CTAAGTTATGGACCAT-3' |
| <i>ATP13A2</i> | IDT | Human | 5'-AGTGTCTGGACAGAAGCGG-3' | 5'-ACCTGGTAGAAGGCTTGCTG-3' |

2.6 QUANTIFICATION OF LC3B-II/LC3B-I RATIO

Autophagic flux was analyzed by measuring the ratio of LC3B-II and LC3B-I in RPE1 cells. As described in Wang et al., RPE1 cells were plated in 6 well plates and separately transfected with control or appropriate siRNA for 72 hours prior to collection (192). RPE1 cells were treated with 20 μ M Chloroquine for 12 hours prior to isolation as a positive control used to obtain the maximal LC3B ratio. As a negative control, RPE1 cells were pretreated with 2.5 mM 3-MA for 24 hours to prevent the initiation of autophagy, thus producing the minimal LC3B ratio. Prior to isolation, cells were washed one time with cold PBS and then scraped in 1 ml of cold PBS. The suspension was placed in a centrifuge tube and centrifuged at 2,000-x g to collect the cells. Cells were then resuspended in cold lysis buffer that contained: 20 mM Tris-HCl, pH 7.6, 150 mM NaCl, 2% Triton X-100 with 2 mM phenylmethanesulfonyl fluoride (PMSF) in 2-propanol. Cells were incubated on ice after resuspension and then centrifuged at 16,000-x g for 10 minutes at 4°C. The supernatant was collected and the protein concentration was measured using the Bradford (Bio-Rad) protein assay. Samples were resuspended in 4X SDS, boiled for 5 minutes, and then 20 μ g of protein were loaded on to a precast 12% Tris-Glycine gel, ran, and then transferred to PVDF membranes. The membranes were blocked with 10% (w/v) non-fat dry milk in TBS-T and then probed with polyclonal rabbit anti-LC3B antibody (Abcam, ab48394) diluted 1:1000 or monoclonal β -actin (Abcam, AC-15) diluted 1:5,000, washed, and probed with HRP conjugated goat-anti-rabbit secondary antibody (Amersham, Piscataway, NJ) diluted 1:5,000. Immunodetection was performed with the Luminata Forte HRP substrate (Millipore) and band densities were measured using ImageJ (Bethesda, MD) software. Levels of LC3B-II and LC3B-I were normalized to actin and the LC3B ratio was calculated by dividing LC3B-II by LC3B-I. Note that for analysis of LC3B-II, lower exposure times were used in quantification.

2.7 MEASUREMENT OF LIPID PEROXIDATION

RPE1 cells were plated onto glass coverslips and transfected with control or TRPML1 959 siRNA 72 hours prior to staining with 3 μ M BODIPY 581/591 C₁₁ undecanoic acid in regular buffer for 30 minutes at 37°C in 5% CO₂. Cells were washed with regular buffer prior to live cell imaging using a Leica TCS SPF confocal microscope. Probes were excited with an argon ion laser set at 488 nm while emission was detected at 498-544 nm for peroxidated probe and 580-620 nm for nonoxidized probe. Image analysis was completed using ImageJ to calculate oxidation % = 100%*Green/(Green + Red), where Green and Red are pixel values of images.

2.8 MEASUREMENT OF MITOCHONDRIAL MEMBRANE POTENTIAL

RPE1 cells were plated onto 35 mm dishes and separately transfected with control or appropriate siRNA for 72 hours prior to staining for 20 minutes at 37°C in 5% CO₂ with the mitochondrial membrane potential sensitive dye, JC-1 (5 μ g/ml in DMEM/F12 supplemented with 10% FBS). In the presence of mitochondrial membrane potential, JC-1 forms aggregates that fluoresce with an emission peak at 590 nm, while mitochondria that have lost their membrane potential favor the monomeric form of JC-1, which has an emissions peak at 530 nm (193,194). Cells were dissociated with 0.05% trypsin (Invitrogen) and washed once with room temperature regular buffer prior to measuring fluorescence. Fluorescence of JC-1 monomers and aggregates were measured using a fluorometer with the excitation/emission set at 485/530 nm and 535/590 nm, respectively. $\Delta\Psi_m$ was inferred from the ratio of fluorescence at 590 nm (Red) and 530 nm (Green). Carbonyl cyanide

m-chlorophenylhydrazine (CCCP, Sigma, 10 μ M), which collapses the $\Delta\Psi_m$, was used as a positive control.

2.9 FLOW CYTOMETRY AND ANALYSIS

The Vybrant™ Apoptosis Assay Kit #3 (Invitrogen, V-13242) was used for analysis of cell death by measuring green fluorescence in Annexin V positive cells via flow cytometry. Briefly, RPE1 cells were grown in 6-well plates and transfected separately with control or TRPML1 959 siRNA 24 hrs prior to treating with 100 μ M Fe^{2+} for 24 hrs. To count the cells prior to flow cytometry, cells were washed in PBS (Lonza, Basel, Switzerland) and trypsinized in 0.05% trypsin (Invitrogen). To stain cells, 5×10^5 cells were resuspended in the Annexin Binding Buffer and loaded for 15 minutes with 2 μ l of FITC Annexin V and 1 μ l of propidium iodide (PI). Cells were sorted at the University of Pittsburgh Cancer Institute Cytometry Facility on the BD Accuri™ C6 (Becton Dickinson, Franklin Lakes, New Jersey). To analyze the data the BD Accuri C6 software, side scatter, and forward scatter were used to gate events to exclude debris but include both healthy and apoptotic cells. Annexin V binds to cells that are undergoing apoptosis and express phosphatidylserine on the outer layer of the cell membrane, while PI enters cells with a compromised cell membrane and binds to cellular DNA (195). The staining of cells with these dyes allows for the separation of live cells (unstained), apoptotic cells (FITC Annexin stained, and necrotic cells (PI stained cells).

2.10 CASPASE 3 ACTIVITY ASSAY

For analysis of Caspase 3 activity, RPE1 cells were plated in 6 well plates and separately transfected with control or TRPML1 959- siRNA for 72 hours prior to assay, some samples were treated with 100 μM Fe^{2+} for 48 hours prior to analysis. As a positive control, cells were treated with 100 nM Staurosporine for 12 hours prior to analysis. Cells were prepared and measured using the EnzChek Caspase 3 Assay Kit #1 (Invitrogen, E13183) following the manufacturer's instructions. AMC substrate fluorescence was measured using a fluorometer at an excitation wavelength of 342 nm and an emission wavelength of 441 nm. Data are normalized to control and presented percent of control.

2.11 MITOCHONDRIAL MORPHOLOGY ANALYSIS

RPE1 cells grown on glass coverslips and transfected separately with control or TRPML1 siRNA were stained with 100 nM Mitotracker Green® FM (Invitrogen, Carlsbad, CA) in regular buffer at 37°C in 5% CO_2 for 25 minutes followed by live cell imaging using a Leica TCS SPF confocal microscope. For data analysis, since each image contained complete cells and parts of cells, raw images were segmented using ImageJ, with each segment containing one complete cell (Figure 14A). Each segment was then binarized using the thresholding function of ImageJ (Figure 14B). Threshold settings ranged between 55 and 255, to preserve the mitochondrial network characteristic of each specific cell. Mitochondrial morphological characteristics, including AR and FF, were calculated by obtaining the major and minor axes of the ellipse equivalent to the mitochondria, area, perimeter, and number of mitochondria using the analyze particle function in

ImageJ. All mitochondrial morphological analysis was completed using three biological replicates on three separate days.

2.12 ROS LOCALIZATION

To determine the localization of ROS species in TRPML1-deficient RPE1 cells, RPE1 cells on glass coverslips were transfected separately with control or TRPML1 siRNA 72 hours prior to imaging. Some samples were treated with 100 μM Fe^{2+} for 24 hours prior to imaging. Using the Image-IT® LIVE Green ROS Detection Kit for microscopy (Invitrogen, I36007) cells were loaded with 25 μM carboxy- H_2DCFDA according to the manufacturer's protocol. Cells were also loaded with LysoTracker® Red DND-99 using a 1:10,000 dilution in regular buffer then live cell imaging was performed using a Leica TCS SPF confocal microscope. Images were analyzed using ImageJ software.

2.13 SUPEROXIDE QUANTIFICATION WITH MITOSOX™ RED

Cells were plated on MatTek (Ashland, MA) dishes and transfected with siRNA to induce TRPML1 KD. Cells were exposed to Fe^{2+} , $\alpha\text{-Toc}$, or TBHP for indicated times prior to loading with superoxide probe MitoSOX™ Red (5 μM , Invitrogen) for 15 minutes at 37°C in conjunction with Mitotracker Green® FM (1.5 μM , Invitrogen). MitoSOX™ Red and Mitotracker Green® FM were then imaged by mounting coverslip bottom dishes on a Nikon TiE inverted fluorescent microscope (Nikon, Melville NY) with a X60, 1.4NA optic equipped with a temperature-

controlled chamber (Tokai Hit, Japan). Mitotracker Green® FM and MitoSOX™ Red dyes were excited using 488 and 513 nm and detected using appropriate filters for GFP and TRITC, respectively. For Mitotracker Green® FM, images were collected with the following settings: Light source 10%, 14 Bit: No binning, exposure: 40ms. For MitoSOX™ Red, images were collected with the following settings: Light source 20%, 14 Bit: Binning 2 x 2, exposure: 100 ms. Images were analyzed in NIS-Elements by adjusting the binary threshold to include appropriate mitochondrial localized TRITC signal, indicating actual MitoSOX™ Red signal. The threshold was set at low: 245 and high: 16383, smoothed 1X, cleaned 1X, and converted to a binary image. Measurements were obtained using the automated measurement tab; counts for mean TRITC intensity were exported to excel for statistical analysis. For each experiment at least 10 stage positions were measured. Experiment was repeated three times for most samples: n=3 for control untreated, control + α -Toc, TRPML1-959 untreated, TRPML1-959 + α -Toc; n=2 for control + Fe^{2+} and TRPML1-959 + Fe^{2+} ; n=1 for control TBHP. Quantification for TRPML1-959 + TBHP not included.

2.14 SEAHORSE ASSAY FOR CELLULAR METABOLIC ACTIVITY

To assess cellular metabolic activity with regards to basal oxygen consumption, glycolysis, ATP turnover, and mitochondrial respiration the Seahorse XF24 Extracellular Flux Analyzer was used (Seahorse Bioscience, North Billerica, MA). RPE-1 cells were transfected with control or TRPML1-959 siRNA 48 hours prior to plating cells (100,000 cells/well) in 24 well Seahorse cell culture microplate 24 hours prior to experiment. Cells were treated with either 100 μM Fe^{2+} for 48 hours or 100 μM Zn^{2+} for 24 hours prior to experiment. One day prior to experiment, the sensor

cartridge was hydrated with calibration buffer. Prior to the start of the experiment, each well was washed with unbuffered DMEM, replaced with a final volume of 700 μ L DMEM, and incubated at 37°C for 60 minutes. Upon cartridge calibration, basal extracellular acidification rates (ECAR) and cellular oxygen consumption rates (OCR) were measured followed by subsequent measurements upon the addition of 1 μ M oligomycin, 300 nM CCCP, and 1 μ M antimycin A (196-198). For each compound in addition to basal measurements, three readings were recorded. For each experimental condition four replicates were averaged, normalized to total protein levels (measurement of cell number) per well, and compared using a one-tailed, unpaired t-test. Normalization of data at the cellular level with total protein provides information about the bioenergetic differences between cell populations (199).

2.15 STATISTICAL ANALYSIS

Data are summarized as mean \pm standard error of the mean (S.E.M.) of three independent experiments, unless explicitly stated. The statistical significance was assessed using a one-tailed, unpaired t-test with $p \leq 0.05$ considered significant. * indicates $p \leq 0.05$, while ** indicates $p \leq 0.01$.

3.0 LOSS OF TRPML1 PROMOTES PRODUCTION OF REACTIVE OXYGEN SPECIES

The work discussed in this chapter was originally published in the Biochemical Journal and has been modified and reprinted with permission from © the Biochemical Society. The citation for the original publication is:

Jessica Coblentz, Claudette St. Croix, and Kirill Kiselyov, “Loss of TRPML1 promotes production of reactive oxygen species: is oxidative damage a factor in Mucopolidosis type IV?” Biochemical Journal. 2014; 457: 361-368 © the Biochemical Society (23).

TRPML1 is a lysosomal ion channel permeable to cations, including Fe^{2+} . Mutations in *MCOLN1*, the gene coding for TRPML1, cause the lysosomal storage disease (LSD) Mucopolidosis type IV (MLIV). The role of TRPML1 in the cell is disputed and the mechanisms of cell deterioration in MLIV are unclear. The recent demonstration of Fe^{2+} buildup in MLIV cells raised the possibility that TRPML1 dissipates lysosomal Fe^{2+} and prevents its accumulation. Since Fe^{2+} catalyzes the production of reactive oxygen species (ROS), I set out to test whether or not the loss of TRPML1 promotes ROS production by Fe^{2+} trapped in lysosomes. My data shows that retinal-pigmented epithelial (RPE1) cells develop a punctate mitochondrial phenotype within 48 hours of siRNA-induced TRPML1 knockdown (KD). This mitochondrial fragmentation was aggravated by Fe^{2+} exposure, but was reversed by incubation with the ROS antioxidant α -tocopherol (α -Toc). The exposure of TRPML1-KD cells to Fe^{2+} led to: loss of mitochondrial membrane potential ($\Delta\Psi_m$), ROS buildup, lipid peroxidation and increased transcription of genes responsive to cytotoxic oxidative stress in TRPML1-KD cells. This data suggests that TRPML1 redistributes Fe^{2+} between the lysosomes and the cytoplasm. Fe^{2+} buildup caused by TRPML1 loss

potentiates ROS production and leads to mitochondrial deterioration. Beyond suggesting a new model for MLIV pathogenesis, this data shows that TRPML1's role in the cell extends outside lysosomes.

3.1 INTRODUCTION

TRPML1 is a member of the mucolipin family of transient receptor potential (TRP) ion channels (62,86). TRPML1 is encoded by the *MCOLN1* gene, mutations in this gene result in the rare lysosomal storage disease MLIV (26-28). The disease has a significant neurodegenerative profile and is associated with motor dysfunction and the accumulation of cytoplasmic storage bodies (32,34). How the loss of TRPML1 causes severe neurodegeneration is currently unclear, but delineating the role of TRPML1 within the cell may provide insight into the pathogenesis of MLIV. TRPML1 is localized to lysosomes due to the presence of two lysosomal localization signals in its N- and C-termini (69,84). These signals are not evident in its relatives TRPML2 and TRPML3, as their localization appears to be wider (68,200,201). In addition to localization signals, TRPML1 is potentiated by a low lysosomal range of pH and its regulation by lysosomal phosphatidylinositol 3,5-bisphosphate further limits its physiological context to the lysosome (58,80,202).

TRPML1 conducts monovalent as well as divalent cations such as Fe^{2+} , Zn^{2+} , and Ca^{2+} (58,202). Its Ca^{2+} permeability has attracted the most interest, primarily in the context of its possible role in endocytic membrane fusion (67,203,204). A variant of this has also been discussed with regards to TRPML1's role in lysosomal secretion (113,205). TRPML1's role in membrane fusion has been discussed before (85,86,190,206).

Although TRPML1 was shown to conduct Fe^{2+} and TRPML1-deficient cells have been shown to accumulate Fe^{2+} , its role in Fe^{2+} homeostasis have not been actively pursued (58). The pathways of Fe^{2+} entry into cells include endocytosis of protein-bound Fe^{2+} , followed by its liberation and absorption in the late endocytic pathway. It may also enter lysosomes via autophagy of Fe^{2+} -containing organelles and Fe^{2+} -bound proteins. Fe^{2+} catalyzes production of ROS due to Fenton-like reactions, and ROS are damaging to several key aspects of cellular function, including DNA and mitochondrial damage and the buildup of lipofuscin (99). Therefore, I sought to answer whether or not TRPML1 loss has an effect on mitochondria and whether ROS mediate such an effect.

Mitochondria are dynamic organelles that produce most of the cell's energy and are essential components of signaling pathways that maintain cellular homeostasis and regulation of cellular responses to stresses. In order to maintain these functions, mitochondria form highly dynamic networks that are continuously remodeled by fission and fusion (159,160). When mitochondria become damaged, whether it is due to altered $\Delta\Psi_m$, loss of mtDNA, or ROS buildup, they need to be degraded in order to prevent the activation of downstream apoptotic cascades and cell death (170,207-209). The loss of mitochondrial membrane integrity is associated with collapsing $\Delta\Psi_m$, which can be ascertained using voltage-sensitive dyes targeted to mitochondria, such as JC-1 (193,194). Several means of mitochondrial damage have been identified including ROS, which have been implicated in mitochondrial permeabilization in a variety of systems. Damage like this to mitochondrial membranes takes place during stroke and ischemia, under which conditions of oxygen deprivation leads to ROS production and oxidation of mitochondrial lipids (170,210-214). Other causes of mitochondrial damage include overload with Ca^{2+} during excitotoxicity (215).

Mitochondrial shape is another readout of their status. Under resting conditions, the size (length) of mitochondria is dictated by the balance between mitochondrial fusion and fission events (159,160). The shape of mitochondrial networks can be altered by multiple cellular perturbations, including apoptosis, necrosis, and autophagy (159). In order to focus directly on the effects that the loss of TRPML1 has on mitochondria, I utilized a range of experimental conditions that do not induce marked increases in apoptosis, as apoptosis is often associated with fragmentation of mitochondria.

Here I aimed to answer whether or not TRPML1 has a role beyond lysosomes and whether its functional status directly affects other organelles. I chose to utilize the expression of oxidative stress induced genes, ROS levels, lipid peroxidation, $\Delta\Psi_m$, and mitochondrial morphology as readouts of TRPML1's impact on the cell beyond lysosomes. My data suggests that TRPML1 loss facilitates ROS production, in a manner that is aggravated by Fe^{2+} exposure. I propose that this mechanism is a contributing factor in the pathogenesis of MLIV. It should be noted that since TRPML1 inactivation has been suggested in a range of diseases involving lipid metabolism, this mechanism is possibly a contributing factor in the pathogenesis of other diseases outside of MLIV (203).

3.2 RESULTS

It has previously been shown that TRPML1 is responsible for the transport of Fe^{2+} as TRPML1 loss has been associated with the buildup of Fe^{2+} (58). However, the impact of Fe^{2+} dysregulation in TRPML1-deficient cells has not been comprehensively described. Under normal conditions, it is suggested that TRPML1 functions to release lysosomally accumulated Fe^{2+} into the cytoplasm

(58). There it is then scavenged by ferritin and exported out of the cells through ferroportin (216). Since Fe^{2+} catalyzes ROS production, I propose that Fe^{2+} retention in TRPML1-deficient cells leads to ROS production (99). If this model is correct, then: 1) the effects of Fe^{2+} exposure will potentiate the cellular consequences of TRPML1 loss, and 2) the addition of the ROS antioxidant α -tocopherol should eliminate such consequences.

3.2.1 ROS are generated in RPE1 cells in response to TRPML1 deficit

In these studies, I used human RPE1 cells that were immortalized with hTERT. Among several reasons for choosing this cell type was the fact that MLIV involves ocular abnormalities. While most abnormalities involve corneal and conjunctiva epithelial, some damage to retinal epithelial does occur in MLIV (40,217). In order to test the effects of TRPML1 loss, two siRNA probes were utilized as previously described (189,190). These probes, TRPML1 959 siRNA and TRPML1 745 siRNA, produced consistent results, which are discussed throughout this report. In RPE1 cells, TRPML1-KD with TRPML1 959 siRNA resulted in the loss of $87.5 \pm 1.7\%$ of *MCOLN1* mRNA, while TRPML1 745 siRNA resulted in the loss of $93.8 \pm 1.2\%$ of *MCOLN1* mRNA (Figure 6A). Towards testing the cell-wide effects of TRPML1 loss and aggravation by Fe^{2+} accumulation, I exposed control and TRPML1-KD cells to $100 \mu\text{M}$ Fe^{2+} for the period of 24 to 48 hours. I subjected these cells to a series of tests aimed at detecting ROS and cellular dysfunctions induced by ROS.

The first set of experiments focused on answering whether TRPML1-deficient cells produce ROS and whether Fe^{2+} exposure elevates ROS levels when cells lack the TRPML1 ion channel. When cells are challenged with elevated ROS levels, the cytoprotective transcription factor, nuclear factor erythroid 2-related factor 2 (Nrf2) is activated, which in turn activates the transcription of several genes involved in cytoprotection from oxidative stress and inflammation

(148). Expression levels of mRNA coded by such genes have previously been used as a readout of ROS production and oxidative stress. I selected heme oxygenase-1 (*HMOX1*), which is a well-characterized gene known to be transcriptionally regulated by Nrf2 in response to oxidative stress (78). Cells were transfected with control and TRPML1 siRNA and treated with chemicals prior to measurement of *HMOX1* mRNA levels using quantitative PCR.

When RPE1 cells were incubated with the positive control tert-Butyl hydroperoxide (TBHP), *HMOX1* mRNA was upregulated, indicative of a strong response to oxidative stress (Figure 7A). Analysis of *HMOX1* mRNA levels in TRPML1 959-KD cells indicate that *HMOX1* mRNA levels were consistently increased, averaging $341.1 \pm 60.6\%$ more than the levels detected in control cells (Figure 7B, $p < 0.0001$). Furthermore, exposure of TRPML1 959-KD cells to Fe^{2+} for 48 hours caused a significant increase in *HMOX1* mRNA levels, far exceeding the levels detected in TRPML1 959-KD cells. In Fe^{2+} -treated TRPML1-KD cells, *HMOX1* mRNA levels averaged $1068.4 \pm 99.1\%$ more than levels detected in control untreated cells ($p < 0.0001$). Transfection with TRPML1 745 siRNA resulted in a significant loss of *HMOX1* mRNA, but exposure to Fe^{2+} significantly upregulated *HMOX1* mRNA levels in these cells (Figure 8A). While exposure of control-KD cells to $100 \mu\text{M}$ Fe^{2+} for 48 hours did not result in a statistically significant change in *HMOX1* mRNA levels ($10.38 \pm 1.9\%$ gain), Fe^{2+} treatment with both TRPML1 siRNA constructs resulted in statistically significant changes in *HMOX1* mRNA levels (Figure 8B, $159.8 \pm 19.1\%$ gain, $p < 0.001$ for TRPML1 959 siRNA and $110.7 \pm 21.3\%$ gain, $p < 0.005$ for TRPML1 745 siRNA). This data suggests that exposure to Fe^{2+} potentiates the production of ROS in TRPML1-deficient cells.

Autophagic issues were previously shown in TRPML1^{-/-} patient skin fibroblasts (24,218). Such issues were linked to a buildup of dysfunctional mitochondria (24,218). Since the latter can

produce ROS, I sought to answer whether or not autophagic deficits impact ROS buildup in TRPML1-KD cells. For this purpose, I treated RPE1 cells with the autophagy inhibitor 3-Methyladenine (3-MA) and analyzed *HMOX1* mRNA levels. Prior to analysis of *HMOX1* mRNA, I confirmed the effectiveness of the 3-MA treatment and the effects of TRPML1-KD on autophagic flux by measuring the ratio of LC3B-II and LC3B-I proteins (Figure 9A) (192,219). Western blot analysis was used to measure this ratio and Figure 9B shows that both 3-MA and TRPML1-KD have reduced ratios of LC3B-II/LC3B-I, suggesting that both of these conditions alter normal autophagic flux. A reduction in this ratio can indicate reduced number of autophagosomes, delays in trafficking to the lysosome, reduced fusion with the lysosome, or impaired proteolytic activity. While reduced ratios in 3-MA treatments are likely due to a decrease in autophagosomal number, the exact cause of reduced autophagic flux in response to TRPML1 959-KD is unknown. To determine if an autophagic deficit alone was responsible for the generation of ROS, *HMOX1* mRNA levels were then analyzed. Figure 7B shows that TRPML1-KD induces an increase in *HMOX1* mRNA, while 3-MA does not, which indicates that general inhibition of autophagic flux alone is not enough to induce the production of ROS.

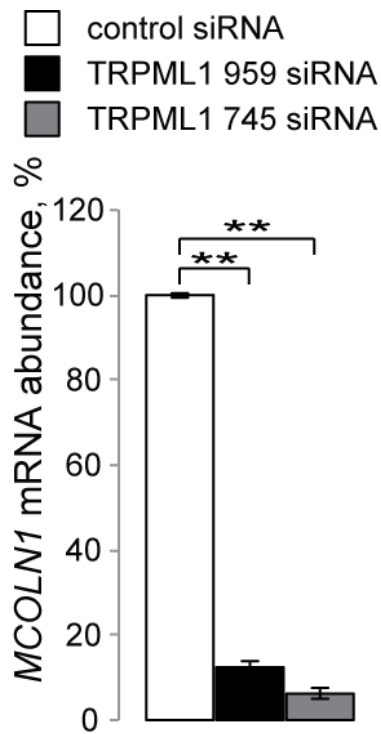


Figure 6 siRNA mediated TRPML1-KD in RPE1 cells

MCOLN1 mRNA expression assessed by qPCR in RPE1 cells in control-KD, TRPML1 959-KD, and TRPML1 745-KD conditions. Cells were exposed to siRNA for 72 hours prior to isolation of RNA. Data were normalized to values detected in untreated control-KD cells, which were taken as 100%. Data are means \pm S.E.M. from three or more experiments for all conditions, ** $P < 0.01$ between values indicated by brackets.

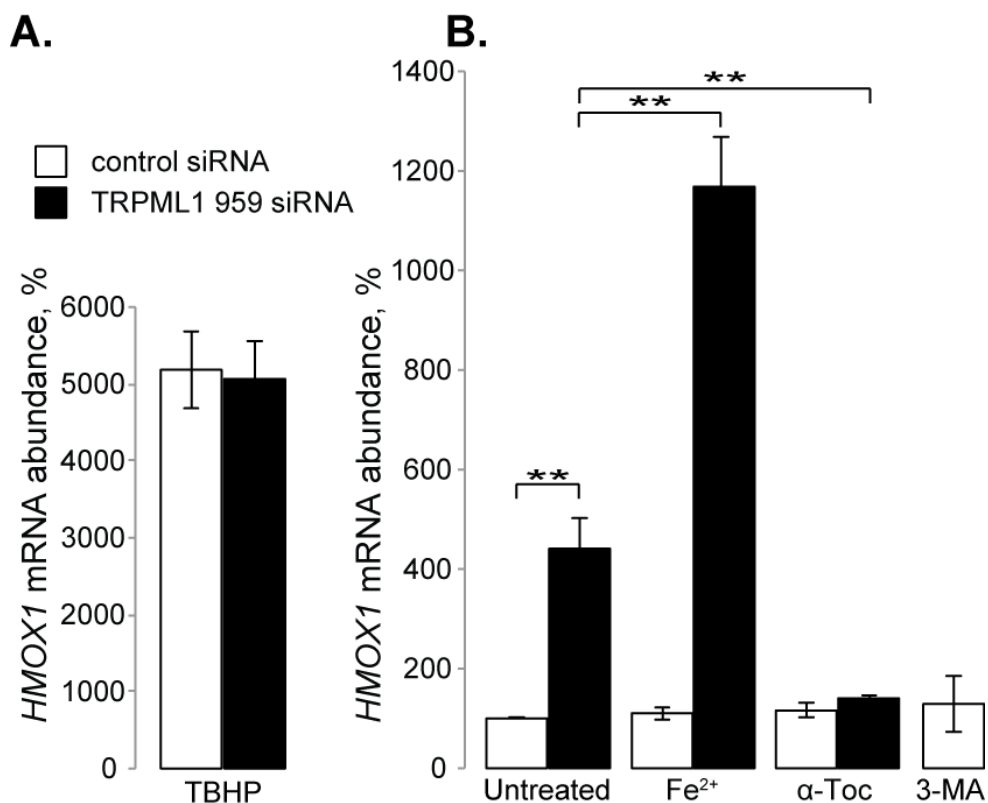


Figure 7 TRPML1-KD in RPE1 cells leads to ROS production

(A) *HMOX1* mRNA expression assessed by qPCR in control and TRPML1-KD cells exposed to 200 μ M TBHP for 4 hours. Data were normalized to values detected in untreated control-KD cells, which were taken as 100%. (B) *HMOX1* mRNA expression in control and TRPML1-KD cells exposed to 100 μ M Fe²⁺ for 48 hours or 100 nM α -Toc for 24 hours. Control-KD cells were also exposed to 2.5 mM 3-MA for 24 hours prior to analysis. Data were normalized to values detected in untreated control-KD cells, which were taken as 100%. Data are means \pm S.E.M. from three or more experiments for all conditions, ** P<0.01 between values indicated by brackets.

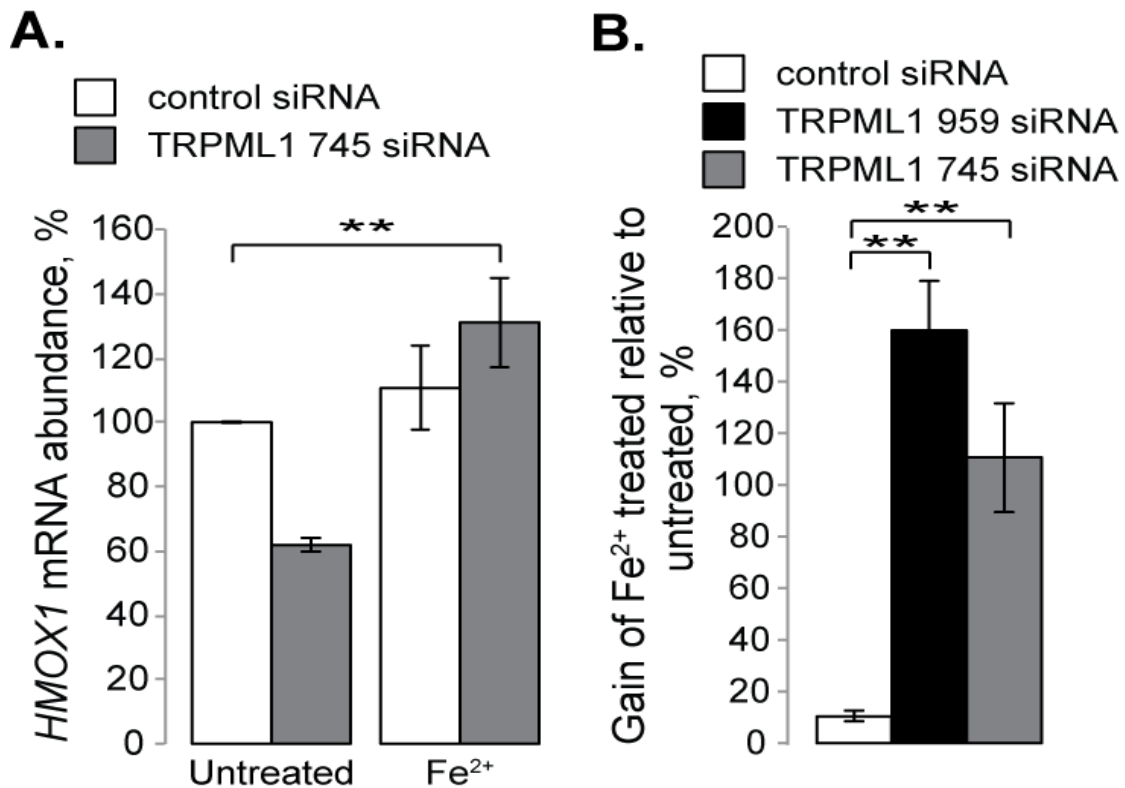


Figure 8 TRPML1-KD with Fe²⁺ leads to increased levels of ROS production

(A) *HMOX1* mRNA expression assessed by qPCR in control and TRPML1 745-KD cells exposed or not to 100 μ M Fe²⁺ for 48 hours. (B) The percentage gain of *HMOX1* mRNA expression between Fe²⁺ and untreated cells. Data were normalized to values detected in untreated control-KD cells, which were taken as 100%. Data are means \pm S.E.M. from three or more experiments for all conditions, ** P < 0.01.

To assess the impact of ROS on membrane lipid peroxidation in RPE1 cells, the fluorescent ratiometric probe BODIPY® 581/591 C₁₁ undecanoic acid was used. When this fatty acid probe reacts with radicals generated by oxidative stress, there is a shift in fluorescence of the fluorophore from red to green, indicative of lipid peroxidation (154). Figure 10 shows that lipid peroxidation is significantly upregulated in TRPML1 959-KD cells both unexposed and exposed to Fe²⁺ for 24 hours compared to control-KD. I was unable to detect a statistically significant increase in oxidation between Fe²⁺-treated and untreated TRPML1 959-KD cells, as the degree of oxidation was relatively high in untreated TRPML1 959-KD cells initially. However, compartmentalization of oxidized lipids in Fe²⁺-treated TRPML1 959-KD cells is evident (Figure 10).

3.2.2 TRPML1-KD mediates changes in mitochondrial function and morphology

One of the main targets of oxidative damage is mitochondria (220). Oxidation of mitochondrial lipids was previously shown to lead to the loss of $\Delta\Psi_m$, which is a pre-apoptotic event (170,210-214,220). To test whether TRPML1 loss causes mitochondrial depolarization, I measured changes in $\Delta\Psi_m$ using the fluorescent dye JC-1. As a positive control, RPE1 cells were exposed to CCCP, a proton gradient uncoupler, which decreased $\Delta\Psi_m$ by 78.9±0.5% relative to control (Figure 11, p<0.0001). Measurement of $\Delta\Psi_m$ in TRPML1-KD cells indicated that loss of TRPML1 induced a significant decrease in $\Delta\Psi_m$ for both TRPML1 siRNA constructs. When compared to control-KD, TRPML1 959 siRNA decreased $\Delta\Psi_m$ by 13.1±1.8%, while TRPML1 745 siRNA decreased $\Delta\Psi_m$ by 19.6±4.4% (Figure 11, p<0.0001 for both). Additionally, exposure of TRPML1-KD cells to Fe²⁺ for 48 hours potentiated the loss of $\Delta\Psi_m$ compared to untreated control-KD for both siRNA, as TRPML1 959 siRNA with Fe²⁺ decreased $\Delta\Psi_m$ by 27.2±1.9% and TRPML1 745 siRNA with Fe²⁺ decreased $\Delta\Psi_m$ by 34.0±2.2% (Figure 11, p<0.0001 for both). Such a decrease was

undetectable in control-KD cells, as Fe^{2+} only decreased $\Delta\Psi_m$ by $4.0\pm 2.3\%$ (Figure 11, not significant). To rule out the possibility that loss of $\Delta\Psi_m$ was inducing apoptosis in these cells, induction of apoptosis was analyzed. Using both annexin V staining via flow cytometry and Caspase 3 activity, it was determined that apoptosis was not significantly activated in any of my siRNA-KD conditions (Figure 12 and Figure 13).

Our lab has previously shown that in cells affected by LSDs, including MLIV, mitochondria are fragmented (24,218). I attributed this phenotype to the buildup of effete mitochondria, which are not processed in time due to an autophagy block in cells affected by LSDs. Since suppressed autophagy is a significant factor in explaining pathogenesis of LSDs (49,200,209,221-224), this model connected lysosomal deficiencies in MLIV to autophagy, to deficits in mitochondrial function, and to cell death. The original force causing mitochondrial fragmentation under these conditions remained unidentified. Specifically, it was not clear whether fragmentation is a passive result of mitochondrial aging and delayed cleanup, or whether it is caused by lysosomal deficiencies in LSDs. Towards answering this question, I compared mitochondrial phenotypes in control cells and cells acutely deficient of the lysosomal ion channel TRPML1. In agreement with the previously published data, TRPML1-KD caused a punctate mitochondrial phenotype. Figure 15A shows confocal images of RPE1 cells stained with Mitotracker Green® FM. While mitochondria in control-KD cells look like long threads, such threads are broken in both TRPML1 959-KD and TRPML1 745-KD cells (Figure 15A and Figure 16A).

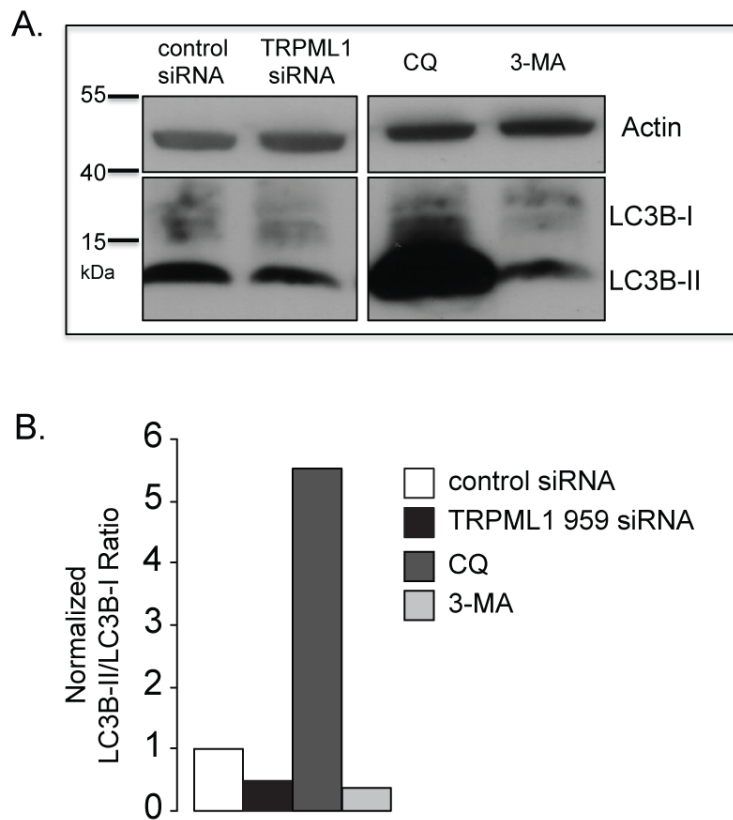


Figure 9 3-MA and TRPML1 959-KD alter autophagic flux in RPE1 cells

(A) Representative western blot indicates processing of LC3B. Expression levels of LC3B-I, LC3B-II, and actin were analyzed following control-KD, TRPML1 959-KD, treatment with 20 μ M Chloroquine (CQ) for 12 hours, or 2.5 mM 3-MA for 24 hours. Actin was used as a loading control. (B) Autophagic flux was measured by quantifying the ratio of the band intensities of LC3B-II and LC3B-I, which reflects autophagic flux. Levels of LC3-II and LC3-I were normalized to actin loading control.

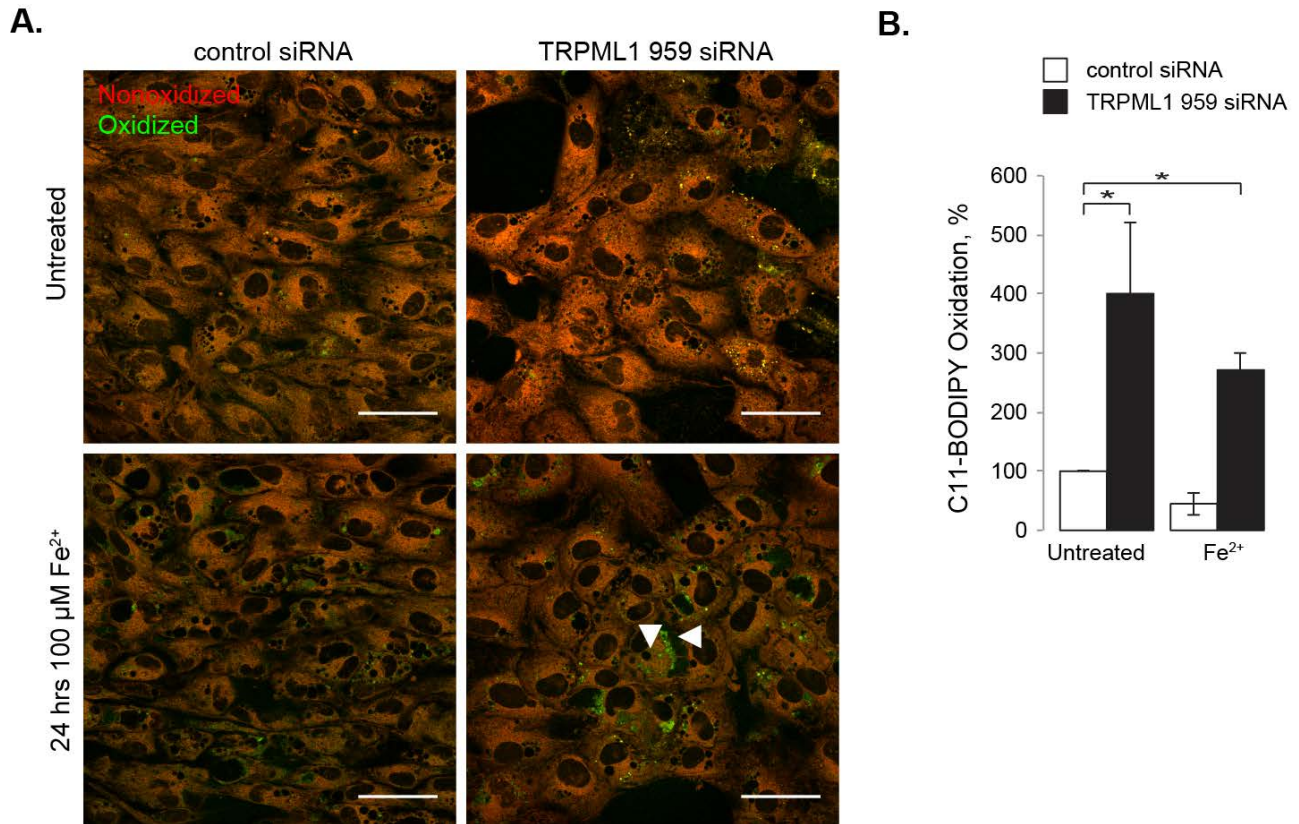


Figure 10 TRPML1-KD induces lipid peroxidation in RPE1 cells

(A) Confocal images of RPE1 cells, 72 hours post transfection with control or TRPML1 siRNA, exposed to 100 μM Fe^{2+} for 24 hours. Cells were stained with 3 μM of C_{11} -BODIPY undecanoic acid. $n=3$. Scale bar corresponds to 50 μm . Note increased green stain in TRPML1-KD cells exposed to Fe^{2+} , compared to control cells exposed to Fe^{2+} . Arrowheads indicate accumulation of oxidized lipids. (B) Quantification of oxidation% of C_{11} -BODIPY, where oxidation% = $100\% \times \text{Green}/(\text{Green} + \text{Red})$, where Green and Red are pixel values of images recorded with an excitation of 488 nm and emissions at 498-544 nm for peroxidated probe and 580-620 nm for the intact probe (154). Data were normalized to values detected in untreated control-KD cells, which were taken as 100%. Data obtained from 3 separate experiments of 5 images containing 3 or more cells, * represents $p < 0.05$.

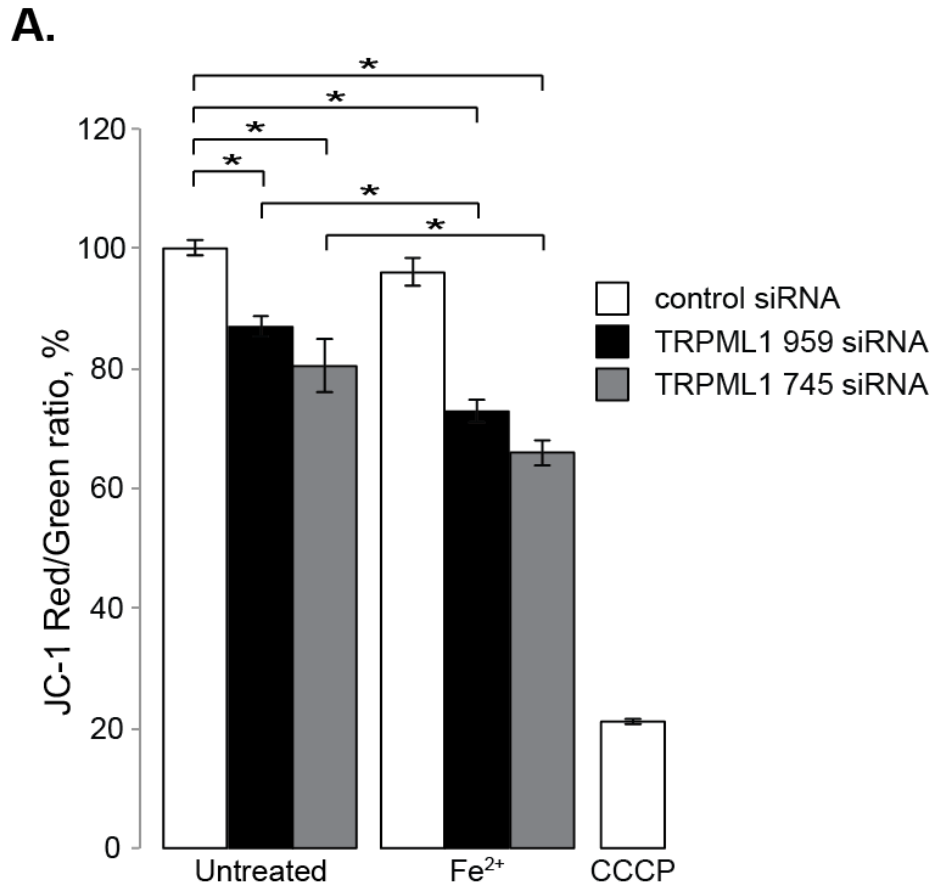


Figure 11 Mitochondrial depolarization is induced in TRPML1-KD cells and is potentiated by exposure to Fe²⁺

(A) Fluorometric analysis of JC-1 fluorescence in control and TRPML1 959 and 745-KD cells exposed to 100 μ M Fe²⁺ for 48 hours. 10 μ M CCCP for 15 minutes was used as a positive control. Data were normalized to values detected in untreated control-KD cells, which were taken as 100%. n=5. * represents p<0.01.

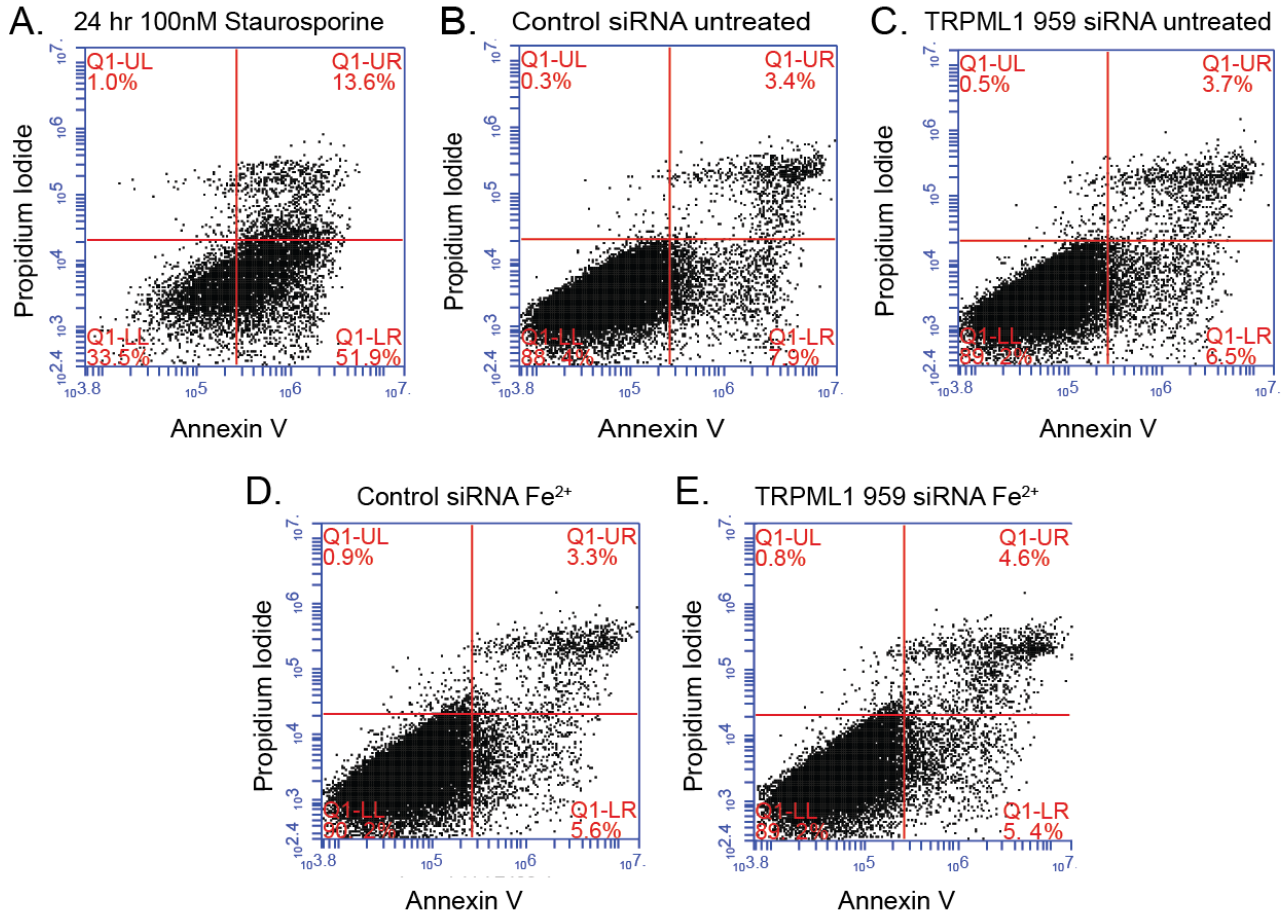


Figure 12 TRPML1-KD is not associated with binding of Annexin V

(A) Positive control for cell death induced by 100 nM Staurosporine. (B-E) Cells transfected with control (B, C) and TRPML1 959-siRNA (D, E), untreated (B, C) and treated with Fe²⁺ (D, E). Note an increase in stain positive for Propidium Iodide and Annexin V, indicating late apoptosis in cells treated with Staurosporine.

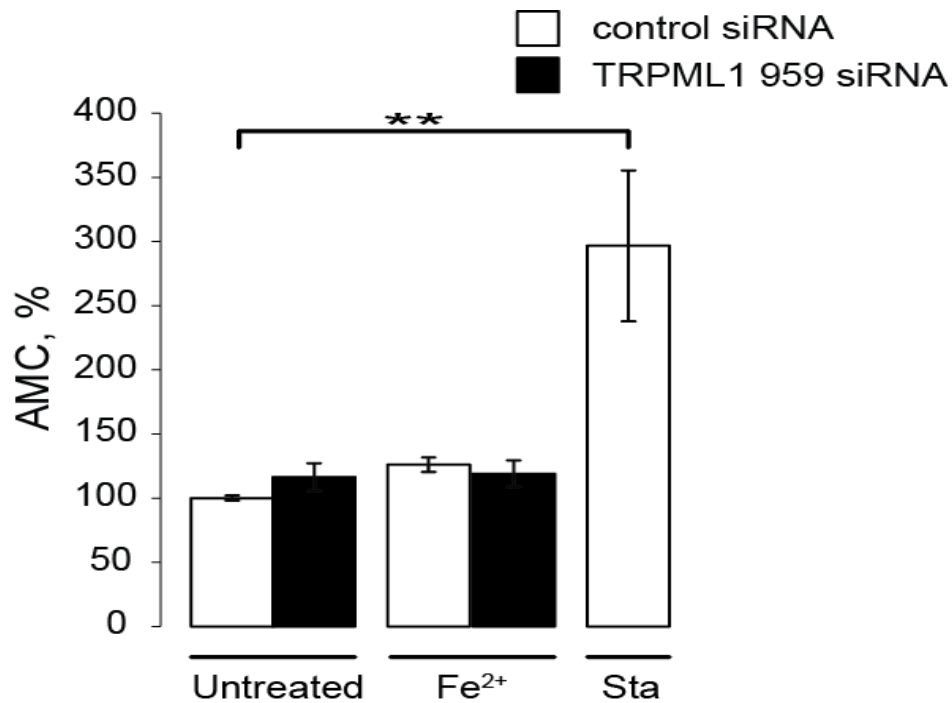


Figure 13 TRPML1 deficiency in RPE1 cells does not induce activation of Caspase 3

(A) Apoptosis was measured using the EnzChek Caspase 3 Apoptotic assay in RPE1 cells 72 hours post transfection with control or TRPML1 siRNA. Cells were also treated with 100 μ M Fe²⁺ for 48 hours prior to analysis. As a positive control, cells were treated with 100 nM Staurosporine for 12 hours prior to analysis. Caspase 3 activity is shown as AMC fluorescence and as a % of untreated control cells. n=3. ** represents p<0.01

To quantify the differences in mitochondrial morphology between control and TRPML1-KD cells, I utilized previously defined characteristics of mitochondrial morphology (225,226). I used two descriptors of mitochondrial shape: aspect ratio (AR) and form factor (FF), as both give a full picture of differences in the structure of mitochondrial networks. My method of analysis is described in Figure 14. All images used in this analysis were obtained using Mitotracker Green® FM, since this stain does not depend on membrane potential and gives an accurate representation of shape. Image analysis was performed in ImageJ. The particle counting function of ImageJ was used to yield mitochondrial number as well as specific characteristics of mitochondria including area, perimeter, AR, and FF.

AR is a ratio that represents mitochondrial length. Elongated objects have higher AR than shorter circular objects and thus AR is frequently used to compare mitochondrial lengths in cells with well-ordered mitochondrial network, such as neurons. Figure 15B shows AR comparisons between control and TRPML1 959-KD cells, in addition to treatments that will be described below. In TRPML1 959-KD cells a statistically significant decrease in length was evident, as AR decreased by $15.4 \pm 1.5\%$ relative to control ($p < 0.0005$).

FF was used as a measurement of mitochondrial network complexity as it took into account the degree of mitochondrial branching and overlap. Healthy mitochondrial networks are often longer and more complex, thus individual mitochondria branch more and overlap with each other; resulting in higher FF. While unhealthy, shorter mitochondria are less likely to overlap and branch. Therefore higher FF is indicative of healthy mitochondria. FF is defined by the formula: $FF = P^2 / \pi \times S$, where P is perimeter, and S is area of the particle. Figure 15C compares FF between control and TRPML1 959-KD cells, in addition to treatments that will be described below. In TRPML1 959-KD cells a statistically significant decrease in complexity was evident, as FF decreased by

34.9±3.2% relative to control ($p<0.0005$). In summary, these data show that TRPML1 959-KD leads to shorter mitochondria with significantly less complexity in regards to branching and overlap.

Figure 15A shows that exposure of TRPML1 959-KD cells to Fe^{2+} for 24 hours leads to a more pronounced punctate mitochondrial phenotype than in untreated control-KD or TRPML1 959-KD cells. Quantification of this difference in Figure 15B indicates that mitochondrial length (AR) in TRPML1 959-KD cells treated with Fe^{2+} is significantly decreased compared to both untreated control-KD (22.0±1.2% decrease, $p<0.0001$) and TRPML1 959-KD cells (7.81% decrease, $p<0.05$). FF decreased in Fe^{2+} -treated TRPML1 959-KD cells, although this difference was not statistically significant compared to control-KD cells (Figure 15C). I attribute this to the fairly high degree of fragmentation and reduction in branching already present in untreated TRPML1 959-KD cells.

Analysis of AR and FF in TRPML1 745-KD cells was not performed, however the morphological trend observed was similar to TRPML1 959-KD but was much less dramatic (Figure 16A). The effects of TRPML1 745 siRNA and TRPML1 959 siRNA on mitochondrial morphology may be correlated with lower *HMOX1* mRNA levels, indicative of lower ROS levels, upon TRPML1 745-KD.

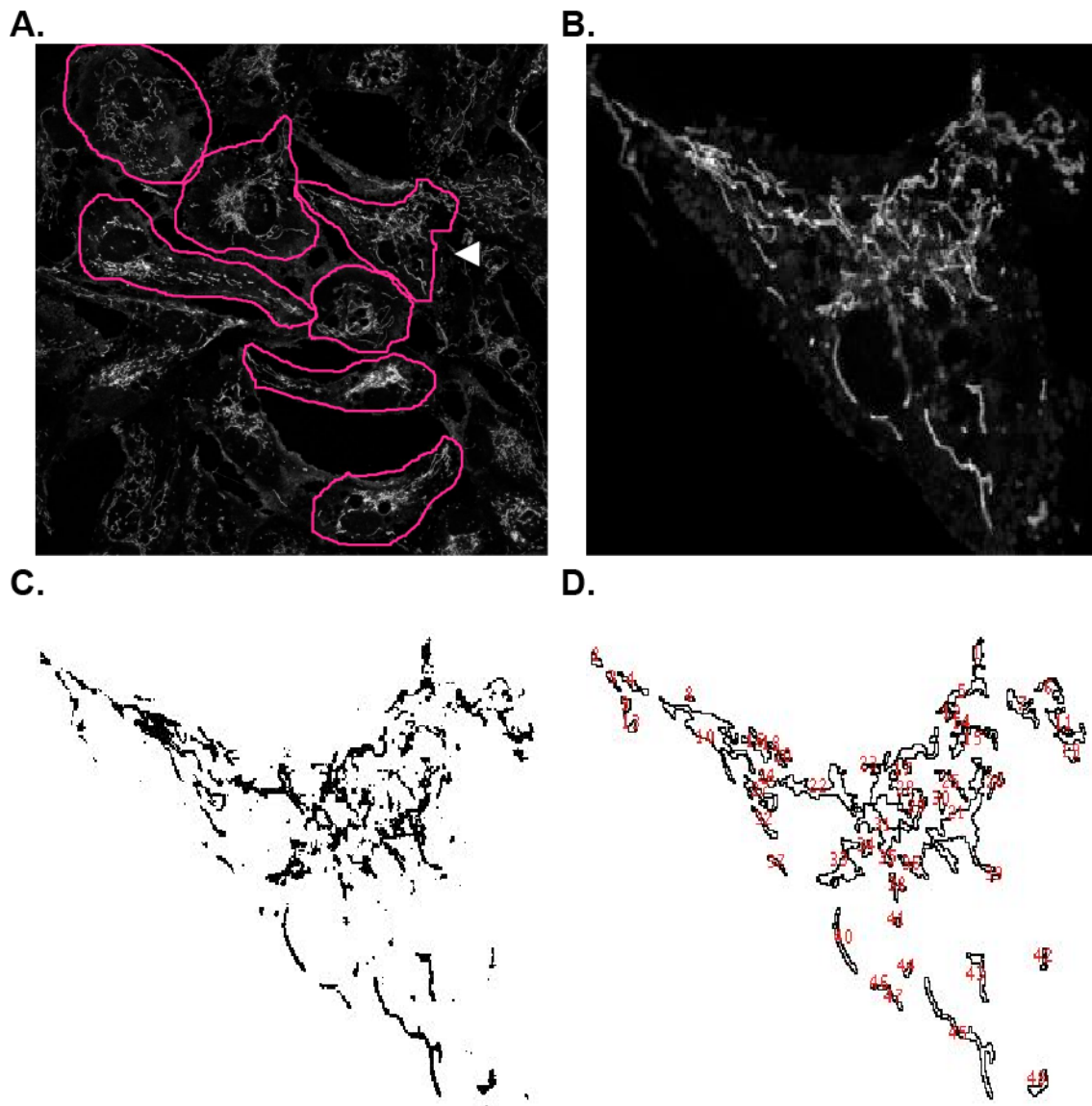


Figure 14 Mitochondrial morphology image analysis

(A) Confocal images of RPE1 cells stained with the mitochondrial marker Mitotracker Green® FM. In this example, cells 72 hours post transfection with control siRNA are shown. Outlined are cells selected for further analysis. They are complete cells, with defined mitochondria, present in similar focal planes. (B) An example of a cell selected for analysis. (C) Binary image of the cell from panel B. (D) Outcome of the “particle counting” function of ImageJ applied to the same cell. Red numbers indicate individual particles.

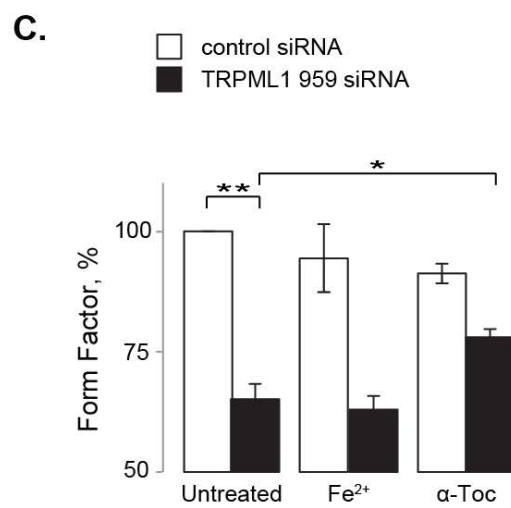
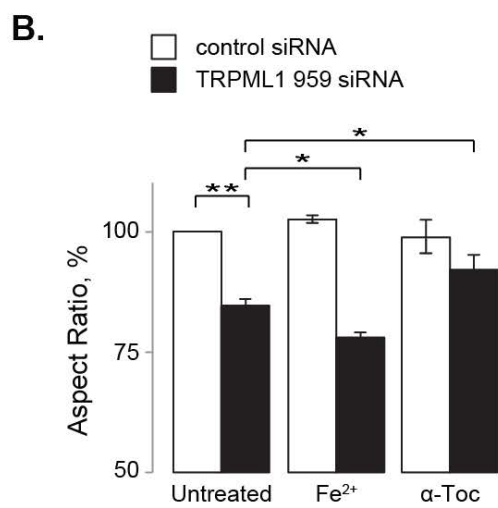
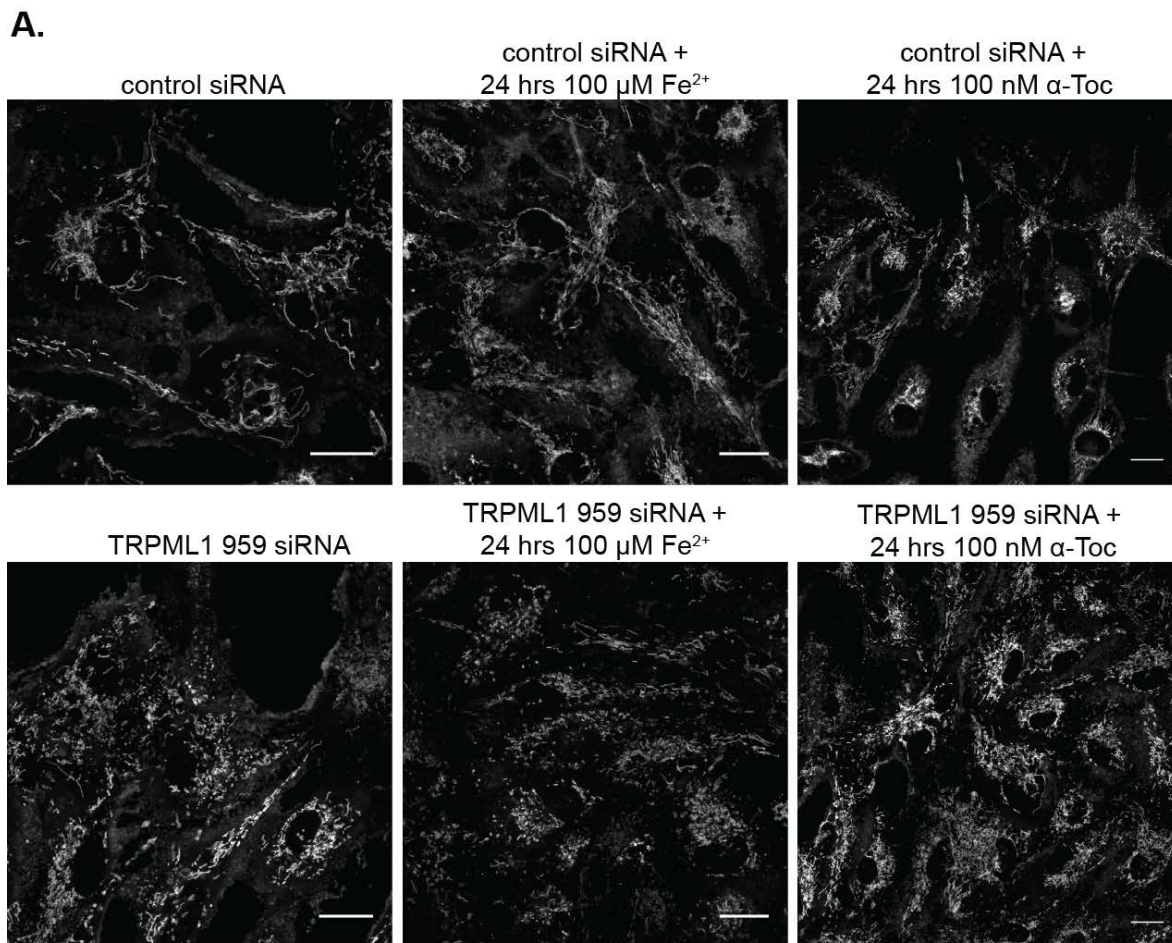


Figure 15 Mitochondrial morphology changes as a function of TRPML1 status, Fe^{2+} treatment, and ROS

(A) Confocal images of RPE1 cells stained with the mitochondrial marker MitoTracker™ Green FM. At 72 hours post-transfection with TRPML1 959 siRNA, cells were exposed to 100 μM Fe^{2+} or 100 nM $\alpha\text{-Toc}$ for 24 h. Scale bar, 20 μm . Brightness was adjusted in some images for better presentation. n=3. (B and C) Statistical analysis of AR (B) and FF (C) of mitochondria from untreated Fe^{2+} or $\alpha\text{-Toc}$ treated RPE1 cells transfected with control siRNA and TRPML1 959 siRNA. Data were normalized to values detected in untreated control-KD cells, which were taken as 100%. For control-KD, data were obtained from 835 mitochondria from 23 cells; for TRPML1 959-KD, data were obtained from 1500 mitochondria from 22 cells; for TRPML1 959-KD with Fe^{2+} , data were obtained from 1434 mitochondria in 27 cells; for TRPML1 959-KD with $\alpha\text{-Toc}$, data were obtained from 1313 mitochondria in 23 cells. Results are \pm S.E.M.; * $P < 0.05$ and ** $P < 0.01$.

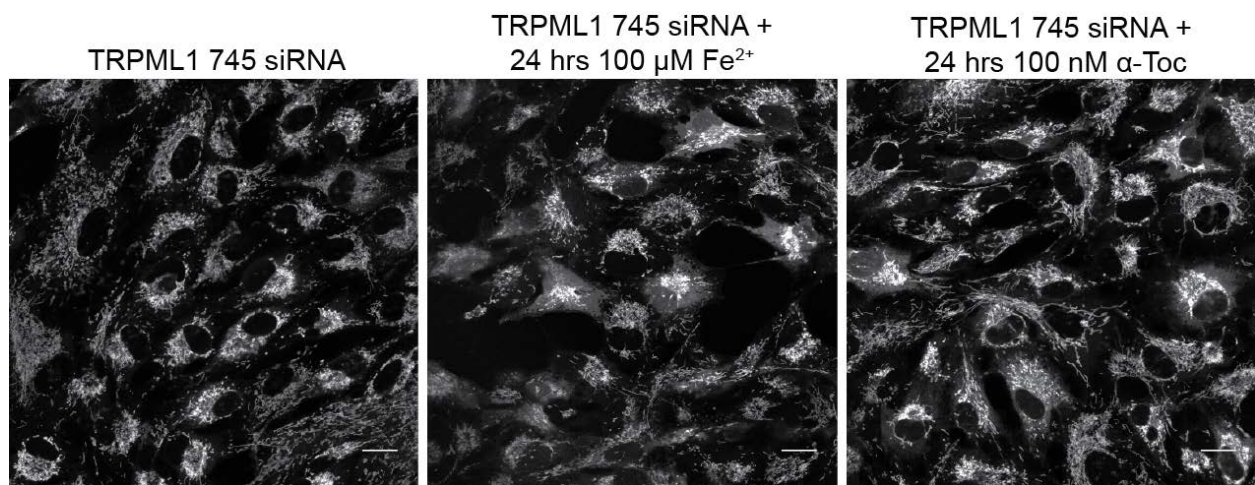


Figure 16 TRPML1 745-KD induces changes in mitochondrial morphology

Confocal images of RPE1 cells stained with mitochondrial marker MitoTracker™ Green FM. At 72 hours post-transfection with TRPML1 745 siRNA, cells were exposed to 100 μM Fe^{2+} or 100 nM $\alpha\text{-Toc}$ for 24 h. Scale bar, 20 μm . n=3.

3.2.3 α -Tocopherol as a potential therapeutic treatment for TRPML1-deficient RPE1 cells

To determine if the increase in ROS levels due to the loss of TRPML1 is reversible, TRPML1-deficient cells were subjected to antioxidant treatment. The antioxidant α -Toc was selected for use as it is known to be lipophilic in nature and thus associates with lipoproteins, fats, and cell membranes and works to protect the polyunsaturated fatty acids from peroxidation reactions (227). Since lipid peroxidation occurred as a result of TRPML1 loss, I hypothesized that the use of α -Toc may reduce the ROS burden. Figure 7B shows that incubation with 100 nM α -Toc for 24 hours in TRPML1 959-KD cells reduced the expression levels of *HMOX1* mRNA compared to untreated TRPML1 959-KD cells alone (68.2% decrease, $p < 0.01$).

If mitochondrial fragmentation is a direct consequence of ROS production due to Fe^{2+} buildup in lysosomes in TRPML1-deficient cells, I predict that ROS reduction should reverse the mitochondrial fragmentation, as ROS reduction was shown above to decrease *HMOX1* mRNA levels. While mitochondria in control-KD cells were unaffected by α -Toc treatment, α -Toc significantly reversed the punctate mitochondrial phenotype in TRPML1 959-KD cells (Figure 15A). This reversion of mitochondrial fragmentation is supported by a significant increase in mitochondrial length in TRPML1 959-KD cells treated with α -Toc, as AR was 8.8% higher than TRPML1 959-KD cells alone (Figure 15B, $p < 0.05$). Additionally, mitochondrial complexity increased significantly with the addition of α -Toc to TRPML1 959-KD cells, as FF was 19.8% higher than TRPML1 959-KD alone (Figure 15C, $p < 0.05$). In conjunction with Fe^{2+} exposure in TRPML1 959-KD cells, these results strongly suggest that the loss of TRPML1 drives mitochondrial fragmentation and ROS generation that may play a strong role in the pathogenesis of MLIV. The reversibility of these phenotypes induced by TRPML1-KD indicates that

antioxidant therapy may alleviate some aspects of MLIV pathogenesis. While α -Toc successfully reduced the oxidative stress burden and reversed the mitochondrial punctate phenotype, it remains to be determined if α -Toc treatment can alleviate other aspects of TRPML1 loss or if it can improve channel activity in TRPML1 mutants.

3.2.4 ROS in TRPML1-deficient cells colocalize with lysosomes

In order to determine if Fe^{2+} accumulation in lysosomes of TRPML1-deficient cells promote ROS production within the lysosome, I examined the localization of ROS within my RPE1 model system. While the methods available to determine ROS localization are currently limited, I was able to pinpoint the site of ROS production in my model. Using carboxy- H_2DCFDA , a fluorescent ROS sensitive probe, I determined that the signal colocalized with lysosomes (Figure 17). To support this data, and to rule out the possibility that ROS are generated/localized to the mitochondria, I analyzed mitochondria in TRPML1-deficient cells for the presence of superoxide using the dye MitoSOX™ Red. Supporting my hypothesis that ROS are produced in the lysosome as a result of Fe^{2+} accumulation in cells deficient of TRPML1; no mitochondrial superoxide production was observed in any condition except the positive control (Figure 18). As more ROS probes become available I will be able to better support my finding and my hypothesis that ROS in this model are lysosomally localized.

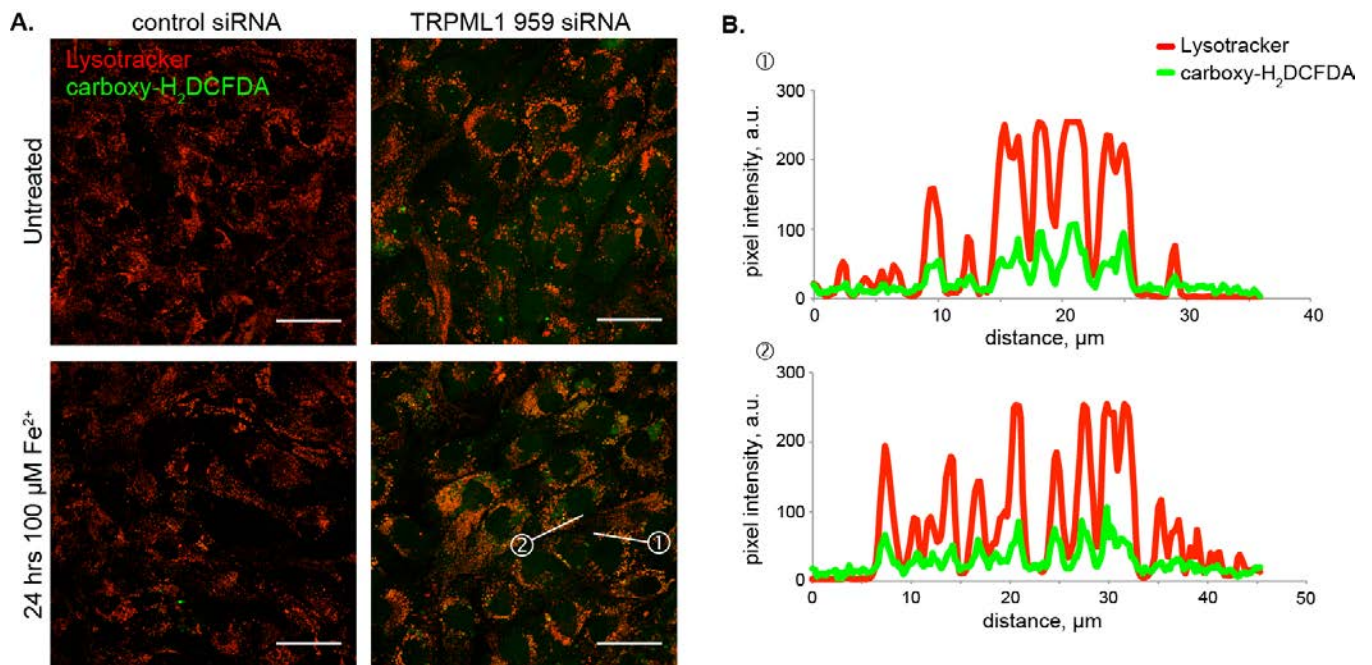


Figure 17 ROS in Fe^{2+} treated TRPML1-deficient RPE1 cells colocalizes with lysosomes

(A) Confocal images of RPE1 cells, 72 hours post transfection with control or TRPML1 959 siRNA, exposed to 100 μM Fe^{2+} for 24 hours. Cells were stained with 25 μM of carboxy- H_2DCFDA . $n=3$. Scale bar corresponds to 50 μm . (B) Plot profiles of cells sectioned for analysis in panel A.

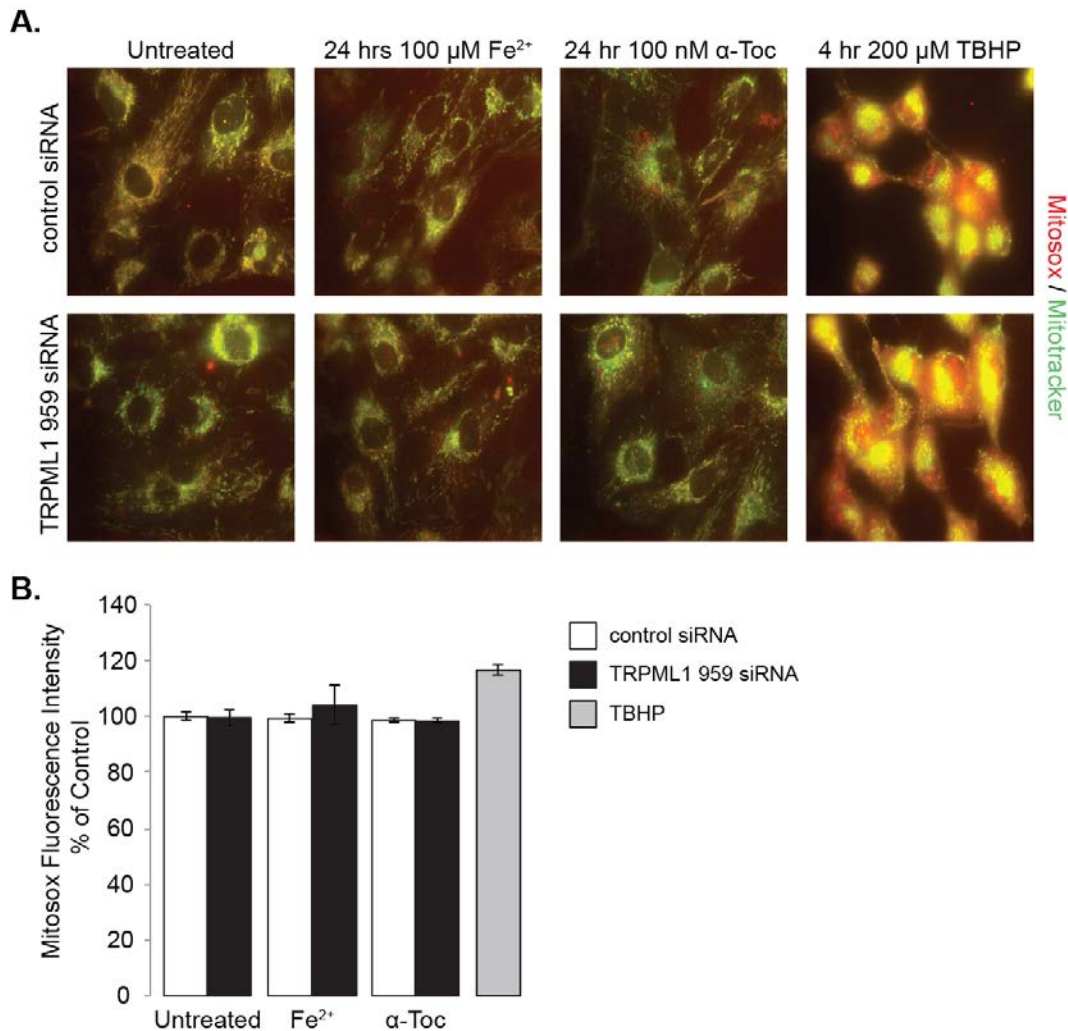


Figure 18 ROS in TRPML1 deficient RPE1 cells are not localized to mitochondria

(A) Mitochondrial superoxide generation was measured in live RPE1 cells transfected with control or TRPML1 959-siRNA for 72 hours prior to imaging. Cells were also treated with 100 μM Fe^{2+} or 100 nM $\alpha\text{-Toc}$ for 24 hours prior to imaging. As a positive control, cells were treated with 200 μM TBHP for 4 hours prior to imaging. Cells were loaded with MitoSOXTM Red and MitoTracker[®] Green FM according to manufacturer’s instructions. (B) Quantification of changes in superoxide production as a direct reflection of mean red fluorescence intensity expressed as % of control. n=3.

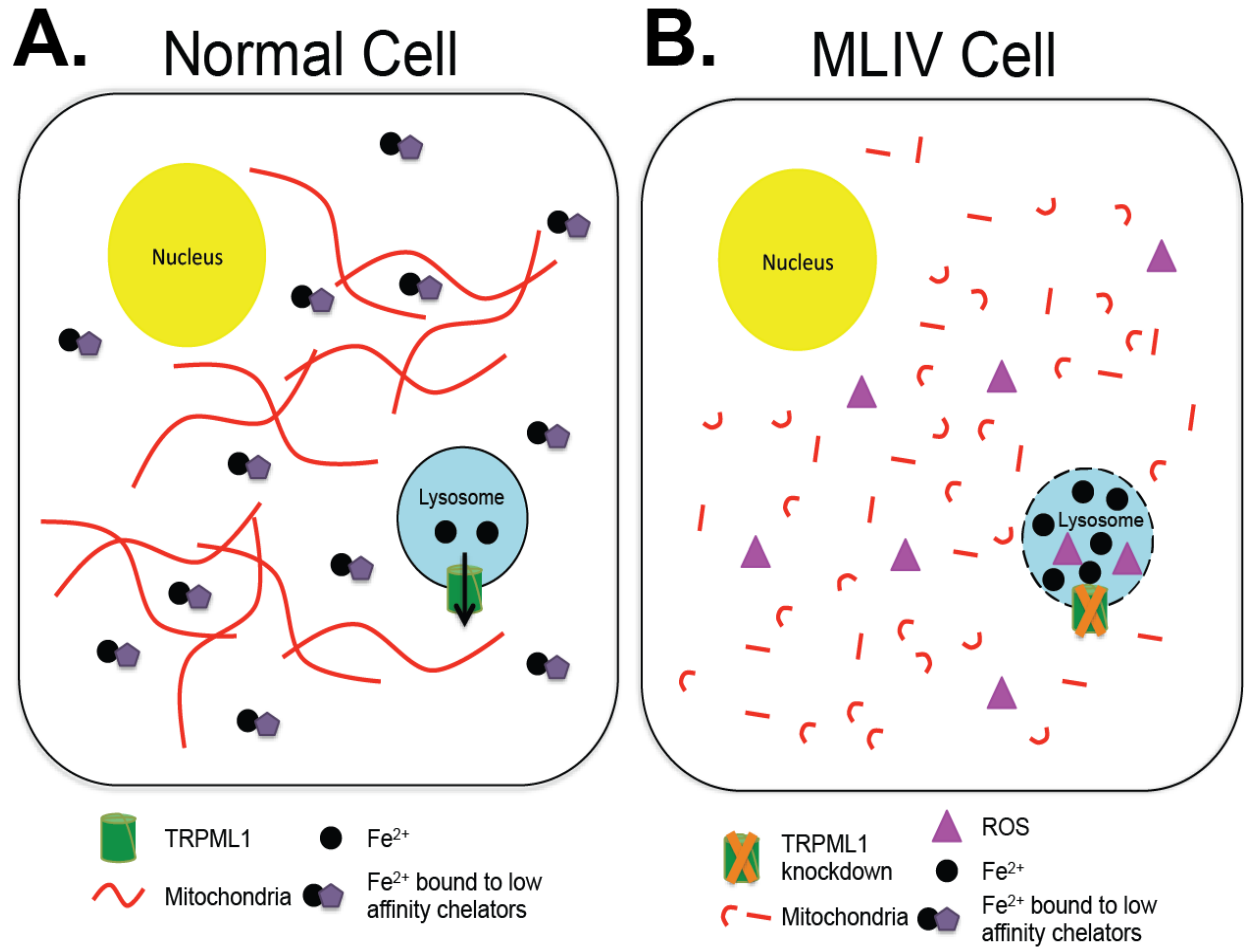


Figure 19 Model of TRPML1-deficiency in RPE1 cells induces ROS and mitochondrial fragmentation

(A) Under normal conditions, Fe^{2+} enters the lysosome via endocytosis of Fe^{2+} bound proteins. The proteins are degraded and Fe^{2+} is transported to the cytoplasm via TRPML1 ion channel. In the cytoplasm, Fe^{2+} binds to low affinity chelators. Under these conditions, mitochondria remain elongated. (B) In MLIV cells lacking TRPML1, Fe^{2+} that would normally be transported to the cytoplasm, accumulates in the lysosome and catalyzes Fenton reactions resulting in the production of ROS. ROS oxidize lipids, which may permeabilize the lysosomal membrane, allowing ROS to access the cytosol and induce mitochondrial fragmentation and loss of $\Delta\Psi_m$.

3.3 DISCUSSION

Whereas TRPML1 conductance properties and regulation are well understood, the functional impact of TRPML1 activity on the endocytic pathway and the cell as a whole is largely unclear. A popular explanation pins its function to Ca^{2+} release events that drive membrane fusion in the endocytic pathway (203). This explanation is supported by the fact that TRPML1 conducts Ca^{2+} . On the other hand, TRPML1 is also known to conduct Fe^{2+} and Zn^{2+} , and accumulation of these metals has been shown in TRPML1-deficient cells (58,88,103). My results provide additional insight into the pathogenesis of MLIV and suggest that TRPML1 regulates transition metal homeostasis within the lysosome in addition to processes beyond the lysosome.

Although our understanding of TRPML1's functional impact beyond the lysosome is limited, there is a fairly well developed body of data connecting TRPML1 loss to autophagy deficits in MLIV patient fibroblasts and mouse tissues (49,54). As discussed earlier, an important question remains whether or not cell deterioration in TRPML1-deficient cells, and ultimately MLIV, is a passive outcome of the loss of degradative and absorptive functions of the lysosome. An alternative explanation suggests that the loss of TRPML1 may promote active cell damaging, such as the mitochondrial fragmentation I see here. Identification of these processes may point towards additional avenues of therapeutic approaches for MLIV. It should be noted that TRPML1 is blocked by sphingomyelins and a TRPML1 component was proposed in diseases associated with sphingomyelin accumulation or mishandling (203). It is, therefore, possible that pathological effects of TRPML1 loss discussed here are applicable to a range of conditions.

Here I showed that TRPML1 loss is associated with mitochondrial fragmentation. The relatively short time to development and TRPML1-specificity of this phenotype suggests that this phenotype is an active event caused by the loss of TRPML1 and perhaps further aggravated by the

induced lysosomal deficits and/or Fe^{2+} accumulation associated with MLIV. The fact that this fragmentation is reversed by ROS reduction with an antioxidant is new. It suggests that ROS generated from TRPML1-deficient cells damages mitochondria. This is a unique observation connecting TRPML1 to processes outside the lysosome. ROS generation in my model is supported by qPCR experiments and lipid peroxidation assays, while ROS localization within lysosomes is supported by carboxy- H_2DCFDA assays. While new techniques arise to analyze ROS at the cellular level, specifics like where ROS are produced and where ROS are acting on proteins, lipids, and DNA can be determined.

Based on these results, and the previously published evidence of TRPML1 permeability to Fe^{2+} and Zn^{2+} , this supports the idea that TRPML1 is a lysosomal divalent cation channel, whose function is to regulate - directly or not - the distribution of transition metals between lysosomes and the cytoplasm. In the context of the experimental model used in this study, cell overload with transition metals and the loss of TRPML1 function likely resulted in metal accumulation in the lysosome. This speculation is supported by previously published data on Fe^{2+} and Zn^{2+} buildup in the lysosomes of TRPML1-deficient cells (58,88,103). A unique aspect of my study is the evidence that such a buildup is associated with ROS production. It appears that the generation of ROS in my system is strong enough to induce structural and physiological changes in mitochondria (Figure 19). Based on the fact that Fe^{2+} aggravated every aspect of TRPML1-KD phenotype discussed here, I propose that Fe^{2+} entrapment in the lysosomes and the resulting ROS production in TRPML1-KD cells are the key factors of cell damage in these cells. Autophagy inhibition prevents mitochondrial recycling and could lead to secondary damages such as ROS production. However my experiments using 3-MA to inhibit autophagic flux (Figure 6B) argue against this being the sole cause of ROS generation in my model.

Until the functional significance of the proposed model is tested in TRPML1-deficient animals, it is difficult to determine the potential significance of antioxidant treatment for ultra-structural and clinical aspects of MLIV pathogenesis. It does, however, provide a novel and specific avenue towards directly testing mechanisms, as well as developing approaches to alleviate symptoms of MLIV.

3.4 ACKNOWLEDGEMENTS

I thank Neel Andharia, Yi Wang, and Dr. Grace Farber (Colletti) for technical assistance, and Karina Peña and Dr. Ora Weisz for fruitful discussion. I thank Michael Meyer and Bratislav Janjic for their help with flow cytometry and data analysis. I thank Dr. Lew Jacobson for use of his fluorometer.

This work was supported by the National Institute of Health grant numbers HD058577, ES01678, and U54 RR022241-01 awarded to Kirill Kiselyov. This project used the University of Pittsburgh Cancer Institute Flow Cytometry Facility that is supported in part by a National Institute of Health award [number P30CA047904].

4.0 OXIDATIVE STRESS INDUCED BY TRPML1 DEFICIENCY ALTERS EXPRESSION OF REGULATORS OF MITOCHONDRIAL DYNAMICS AND REDUCES MITOCHONDRIAL METABOLISM

The work discussed in this Chapter is unpublished data of which I performed all of the experiments except for the microarray assay, which was performed by a previous graduate student in our lab Dr. Grace Colletti, and the JC-1 assay with GDAP1-KD, which was performed by a current graduate student in our lab, Karina Peña. Part of this work stems from a collaborative effort with Dr. Susan Slaughaupt's lab at Harvard Medical School.

4.1 INTRODUCTION

TRPML1 is a lysosomal ion channel encoded for by the gene *MCOLN1*. Mutations in the gene are associated with the lysosomal storage disorder Mucopolipidosis type IV (MLIV) (34). MLIV is a neurodevelopmental and neurodegenerative disease that more recently was found to induce activation of microglia (41). MLIV is characterized by the presence of electron dense storage bodies. Very little is known about the pathogenesis of MLIV, as the role of the ion channel TRPML1 is still being determined. Recent advances in TRPML1 biology indicate that it acts as a Ca^{2+} release channel to promote fusion of late endosomes and lysosomal membranes and has a role in transition metal homeostasis, as it functions to release Fe^{2+} and Zn^{2+} into the cytosol from the lysosomal lumen (23,58,62,88,103).

In addition to TRPML1's role in transition metal homeostasis, I recently indicated that the role of TRPML1 in the cell extends beyond the lysosome as it affects several parameters of mitochondrial function, including mitochondrial morphology, induction of ROS in response to the loss of TRPML1, which induces lipid peroxidation and mitochondrial depolarization(23). However, in disagreement with MLIV studies and some other model systems I do not observe any cell death (23). While changes in these parameters lend insight into the mechanism of MLIV pathogenesis, the molecular mechanisms regulating mitochondrial fragmentation in TRPML1-deficient cells are not known. Previous work in MLIV patient fibroblasts have indicated that autophagic deficits lead to the buildup of effete mitochondria, which is associated with loss of Ca^{2+} buffering capacity that could possibly lead to pro-apoptotic effects (24). As my previous results ruled out the possibility that mitochondrial fragmentation is the result of autophagic deficit, this scenario is not likely the sole cause of mitochondrial fragmentation.

To delineate the events associated with loss of TRPML1, production of ROS, mitochondrial permeabilization, and mitochondrial fragmentation I first confirmed the presence of oxidative stress in the MLIV mouse model. Next I examined alterations in gene expression upon the loss of TRPML1 to determine if any mitochondrial proteins are altered by the loss of TRPML1. Since our lab has previously performed a microarray analysis in HeLa cells after a 48 hour knockdown of TRPML1, I first examined gene expression changes in that data, and then performed qPCR analysis to confirm gene expression in my RPE1 model system (Unpublished data). Upon identification of any possible target genes, I confirmed that changes in gene expression were specific to the loss of TRPML1. To do this, I compared the results to a microarray performed in HeLa cells transfected with siRNA for the enzyme palmitoyl-protein-thioesterase 1 (PPT1), a gene mutated in infantile neuronal ceroid lipofuscinosis (INCL), another LSD (228). Additionally I ran

qPCR experiments on RPE1 cells transfected with PPT1 siRNA. I also confirmed my findings in MLIV patient fibroblasts. The potential candidate gene, *GDAP1* was identified. The identification of *GDAP1* as a candidate that links oxidative stress to mitochondrial fragmentation has provided additional insight into the regulation of MLIV pathogenesis.

4.2 RESULTS

4.2.1 RPE1 cell culture model of oxidative stress as a factor in MLIV pathogenesis extends to the MLIV mouse model

Recent data from our lab indicates that the loss of *TRPML1* in RPE1 cells results in the production of ROS (23). To confirm this phenotype in a more physiologically relevant model system, qPCR was performed on samples isolated from *MCOLN1*^{-/-} and *MCOLN1*^{+/+} mouse brain isolated at 2 and 6 months of age. This study was performed in a doubly blind manner to eliminate bias. As a read out of oxidative stress, I once again examined the mRNA levels of genes antioxidant/cytoprotective genes that are transcriptionally regulated by the master regulator of antioxidant and cytoprotective genes, Nrf2 (146,147). Figure 20 shows the qPCR analysis of *HO-1* and *NQO1* mRNA abundance in mouse brains at 2 and 6 months of age. Figure 20 indicates that *HO-1* mRNA levels are significantly increased at both 2 and 6 months of age, while *NQO1* is significantly upregulated only after 6 months of age. These results confirm the oxidative stress data obtained from my *TRPML1*-deficient RPE1 model.

4.2.2 Oxidative stress in TRPML1-deficient cells alters gene expression of a mitochondrial fission factor

To obtain a general overview of gene regulation in response to the down regulation of TRPML1 in HeLa cells, as an attempt to identify a candidate gene inducible by ROS and responsible for initiating mitochondrial fragmentation I examined the top up and down regulated genes from a microarray analysis on TRPML1-48 hour-KD cells. The 34 most up or down regulated genes, their cellular role, and their cellular localization are listed in Table 3. One of the genes, *GDAP1*, looked like the best possible candidate to fit my description, as it is activated by cellular oxidative stress and induces mitochondrial fragmentation. As discussed in section 1.5.3, GDAP1 is the ganglioside induced differentiation associated protein 1, which is involved in mitochondrial fission and is localized to the OMM (65,183,185). Interestingly, GDAP1 was first identified in a study where extracellular gangliosides were added to cell culture to induce differentiation (229). Over expression of GDAP1 has been shown to induce mitochondrial fragmentation, while not activating apoptosis (183,185). Mutations in *GDAP1* are associated with both dominant and recessive forms of Charcot-Marie-Tooth (CMT) neuropathies (185). GDAP1 is characterized as a new member of the glutathione S-transferase (GST) family based on sequence similarity (182). Whether or not it has GST activity is not known, but recent data indicates that GDAP1 expression was critical for protection against oxidative stress in response to low glutathione levels, as cells expressing mutant GDAP1 did not survive (187). This result indicates that GDAP1 may have a protective effect under oxidative stress conditions. Recent work with GDAP1L1, a GDAP1 paralog, suggests that GDAP1-family members act in a protective manner against stress caused by elevated levels of oxidized glutathione (185).

To confirm that *GDAP1* is actually expressed at elevated levels in a TRPML1 deficient model, I examined *GDAP1* mRNA expression in conjunction with *HMOX1* levels in MLIV patient fibroblasts. Figure 21 shows significantly elevated levels of *GDAP1* and *HMOX1* mRNA in the MLIV patient. This result indicates that loss of TRPML1 does indeed induce oxidative stress, which is somehow correlated to the expression of *GDAP1*.

To confirm that *GDAP1* is responsible for the mitochondrial phenotypes I observed in the TRPML1-deficient RPE1 cell model, I examined expression of two genes that maintain mitochondrial dynamics, *GDAP1* and *MFN1*. To ensure that the results I saw were specific to loss of TRPML1, I compared the results with PPT1-deficient RPE1 cells. Figure 22 showed the effective siRNA modulation of *MCOLN1*, *GDAP1*, and *PPT1*. Surprisingly, Figure 23A indicated that TRPML1-KD in RPE1 cells results in down regulation of *MFN1*. While this result cannot currently be explained, it is rather interesting as down regulation of *MFN1* would support a shift in mitochondrial dynamics towards fission. As I expected, in agreement with MLIV patient fibroblasts, Figure 23B indicated that TRPML1 KD in RPE1 cells results in up regulation of *GDAP1*. Loss of PPT1 in RPE1 cells did not result in significant changes in either *MFN1* or *GDAP1*.

To confirm that *GDAP1* upregulation occurred secondary to oxidative stress induced by TRPML1 loss in RPE1 cells, I utilized the antioxidant α -tocopherol. Treatment with α -tocopherol reversed the *GDAP1* upregulation indicating that *GDAP1* is upregulated in response to the oxidative stress burden in TRPML1 deficient cells. Supporting my hypothesis that a candidate gene is activated in response to oxidative stress induced by loss of TRPML1.

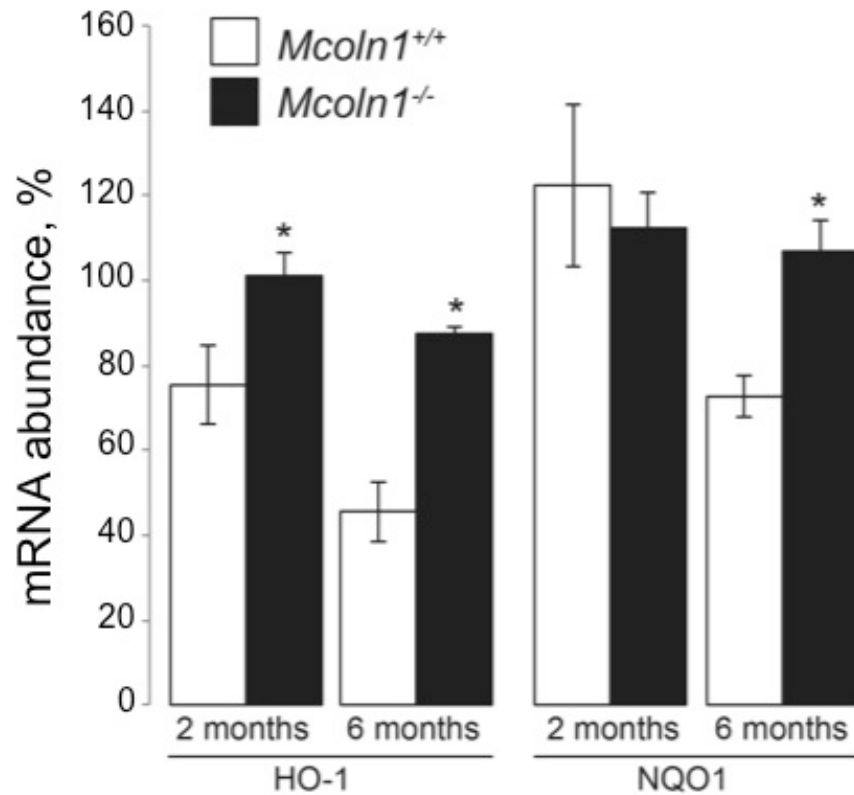


Figure 20 Oxidative stress in brain isolated from MLIV mouse model

(A) Analysis of *HO-1* and *NQO1* mRNA expression by qPCR. mRNA was obtained from whole brain homogenates of *Mcoln1*^{+/+} and *Mcoln1*^{-/-} mice at 2 or 6 months of age. Four separate samples were analyzed in a double blind manner for each condition. Data are normalized to *Mcoln1*^{-/-}, which was considered 100%. *HO-1* and *NQO1* mRNA levels were normalized to the house-keeping gene *RPL32*. * represents $p < 0.05$.

Table 3 Up and down regulated genes from microarray analysis of TRPML1-deficient HeLa cells

| | Gene | Cellular Role | Cellular Localization |
|-----------------------|---|--|----------------------------------|
| Down Regulated | ANAPC13 | Anaphase promoting complex subunit | Nucleus |
| | CIRBP | RNA binding protein | Nucleus |
| | HNRPH2 | Nuclear ribonucleoprotein | Nucleus/Cytosol |
| | MGC24039 | GEF for RAB39A and RAB39B | Cytosol |
| | RDH10 | Retinol dehydrogenase | ER |
| | RPL15 | Ribosomal Protein | Cytosol |
| | SNCG | Synuclein family protein | Cytoskeleton/Cytosol |
| Up Regulated | BCAR3 | Signal transduction | Cytosol |
| | BIVM | Basic immunoglobulin-like variable motif containing | Nucleus |
| | CAP2 | Adenylyl cyclase associated protein | Plasma Membrane |
| | CPLX1 | Complexin- Exocytosis | Cytosol |
| | ERO1L | Endoplasmic Oxidoreductin- Disulfide bond formation | ER |
| | GDAP1 | Mitochondrial Fission/Neuronal development | Mitochondria |
| | HCN3 | Voltage gated cation channel | Plasma Membrane |
| | IRAK2 | Interleukin-1 receptor associated kinase 2/ up regulation of NF-κB | Cytosol/Endosome/Plasma Membrane |
| | KRT17 | Keratin | Cytoskeleton |
| | KRT80 | Keratin | Cytosol |
| | MAL2 | Lipid raft component | Plasma Membrane/Endosome |
| | PAQR4 | Progesterin and AdipoQ receptor member | Plasma Membrane/Mitochondria |
| | PTBP2 | Exon splicing regulation | Nucleus/Cytosol |
| | PTPLB | 3-Hydroxyacyl-CoA Dehydratase | ER |
| | QSOX2 | Sulfhydryl oxidase/quiescin-6 family member | Extracellular |
| | RAI14 | Retinoic Acid Induced Protein 14 | Nucleus |
| | SCG2 | Neuroendocrine secretory granule protein | Extracellular |
| | SIX4 | Nuclear homeoprotein | Nucleus/Cytosol |
| | SLC2A3 | Glucose Transporter | Plasma Membrane |
| | SLC25A19 | Mitochondrial thiamine pyrophosphate carrier | Mitochondria |
| SNAP25 | t-SNARE-exocytosis | Cytosol/Endosome/Plasma Membrane | |
| SOCS2 | Regulates cytokine signal transduction | Cytosol | |
| TMEM145 | Transmembrane protein | Plasma Membrane | |
| VEGF | Neurosecretory Protein | Extracellular | |
| WDR22 | Associated with E3 ubiquitin ligase complex | Nucleus/Mitochondria | |

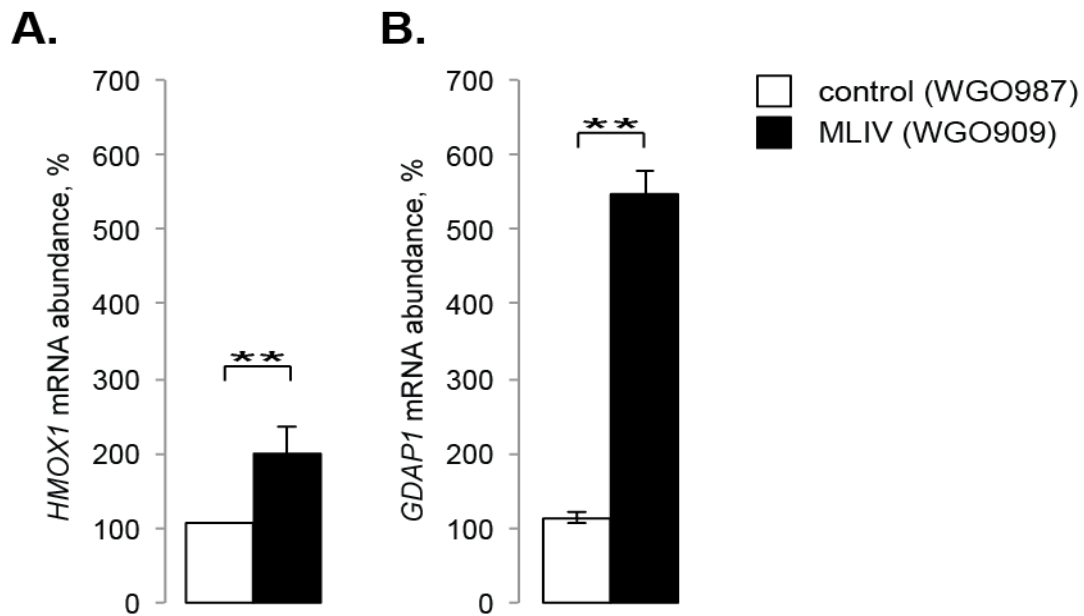


Figure 21 Oxidative stress in MLIV patient fibroblasts induces transcription of *GDAP1*, a key player in mitochondrial fragmentation

(A) qPCR analysis of *HMOX1* and (B) *GDAP1* mRNA levels in fibroblasts isolated from an MLIV patient and related control, shown as % of control. n=2, ** indicates P<0.01.

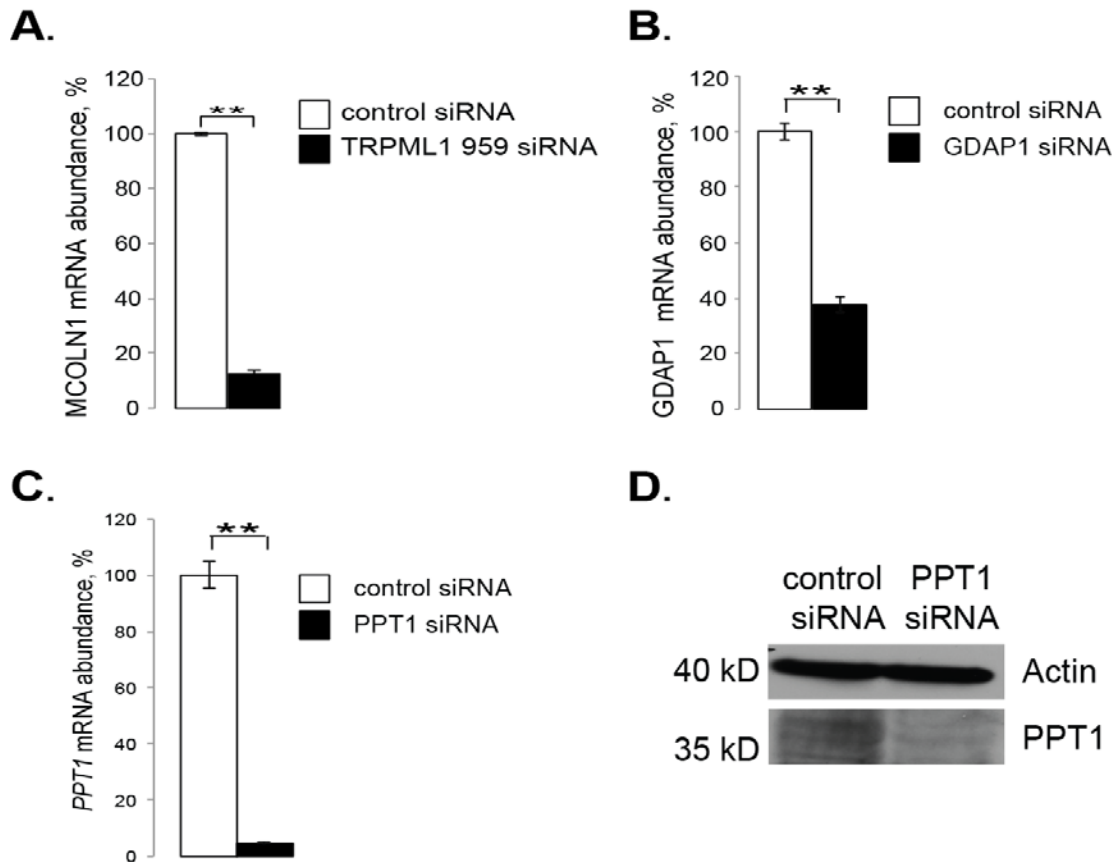


Figure 22 siRNA modulation of TRPML1, GDAP1, and PPT1 in RPE1 cells

(A) qPCR analysis of *MCOLN1* mRNA levels in RPE1 cells transfected with control, TRPML1 959, or TRPML1 745-siRNA. (B) qPCR analysis of *GDAP1* mRNA levels in RPE1 cells transfected with control or GDAP1 siRNA. (C) qPCR analysis of *PPT1* mRNA levels in RPE1 cells transfected with control or PPT1 siRNA. For all transfections, RNA was isolated 72 hours post transfection. Data shown as % of control-KD cells, n=3, ** indicates P<0.01. (D) Western blot analysis of PPT1 protein levels in cells transfected with control and PPT1 siRNA.

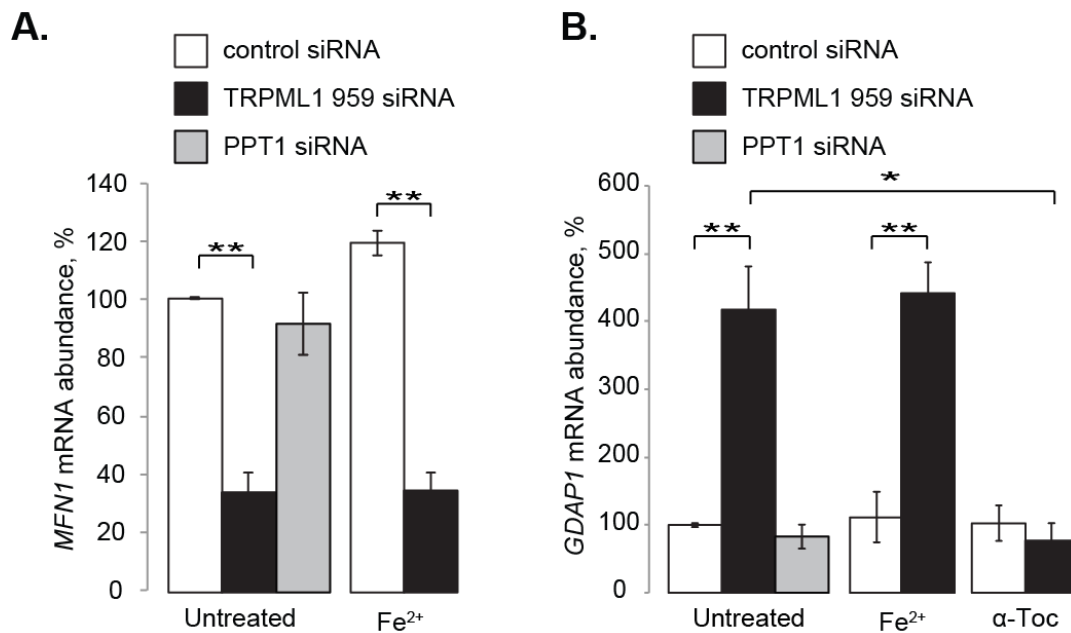


Figure 23 Changes in *MFN1* and *GDAP1* mRNA levels are specific to TRPML1 functional status in RPE1 cells and not general lysosomal dysfunction

(A) qPCR analysis of *MFN1* and (B) *GDAP1* mRNA levels in RPE1 cells transfected with control, TRPML1 959, or PPT1 siRNA for 72 hours prior to RNA isolation. Cells were also treated with 100 μM Fe²⁺ for 48 hours or (B) 100 nM α-Toc for 24 hours prior to RNA isolation. Data shown as % of untreated control cells, n=3, * indicates P<0.05 and ** indicates P<0.01.

4.2.3 Oxidative stress in TRPML1-deficient RPE1 cells decreases mitochondrial metabolic function

To confirm the second part of my hypothesis, that a candidate gene is transcriptionally activated and induces changes in mitochondrial morphology and function, I first examined the effects that loss of TRPML1 had on mitochondrial metabolism and glycolytic function. As our lab recently published data showing that loss of TRPML1 results in the production of ROS that actively damage the cell, indicated by mitochondrial fragmentation and loss of mitochondrial membrane potential, I was interested in determining if these changes altered the ability of the mitochondria to utilize oxygen to produce ATP. To test this hypothesis, I measured mitochondrial metabolism utilizing the Seahorse Extracellular Flux Analyzer in cells deficient of TRPML1. Using this assay, I was able to obtain a comprehensive analysis of basal cellular oxygen consumption rates, which provided information about mitochondrial health and information about the glycolytic function of the cell with regards to conversion of pyruvate to lactic acid. While experiments were only performed in control, TRPML1, and TRPML1+Fe²⁺-KD RPE1 cells, future experiments will have to be repeated to examine the status of cells with and without GDAP1. Experiments in Figure 24A indicated that there were no significant differences in cellular glycolytic function between any condition, while Figure 24B and Figure 24C indicates that loss of TRPML1 results in significantly lower basal oxygen consumption rates, significantly lower ATP-linked oxygen consumption, and significantly lower maximal respiration rates in both TRPML1-deficient RPE1 cells with and without Fe²⁺. To determine if the increased expression of GDAP1 in TRPML1-deficient cells is responsible for altering mitochondrial membrane potential, a JC-1 fluorometric assay was performed. Figure 25 showed that in TRPML1-deficient RPE1 cells, mitochondria are depolarized by 25% of control. GDAP1-deficient RPE1 cells are similar to control potential. Surprisingly,

Figure 25 showed that cells deficient for both TRPML1 and GDAP1, mitochondrial depolarization is rescued. Suggesting that the second part of my hypothesis is true, that GDAP1 is induced by ROS in response to loss of TRPML1, which then induces mitochondrial damage. It will be interesting to see if the double knockouts can rescue mitochondrial metabolism and morphology.

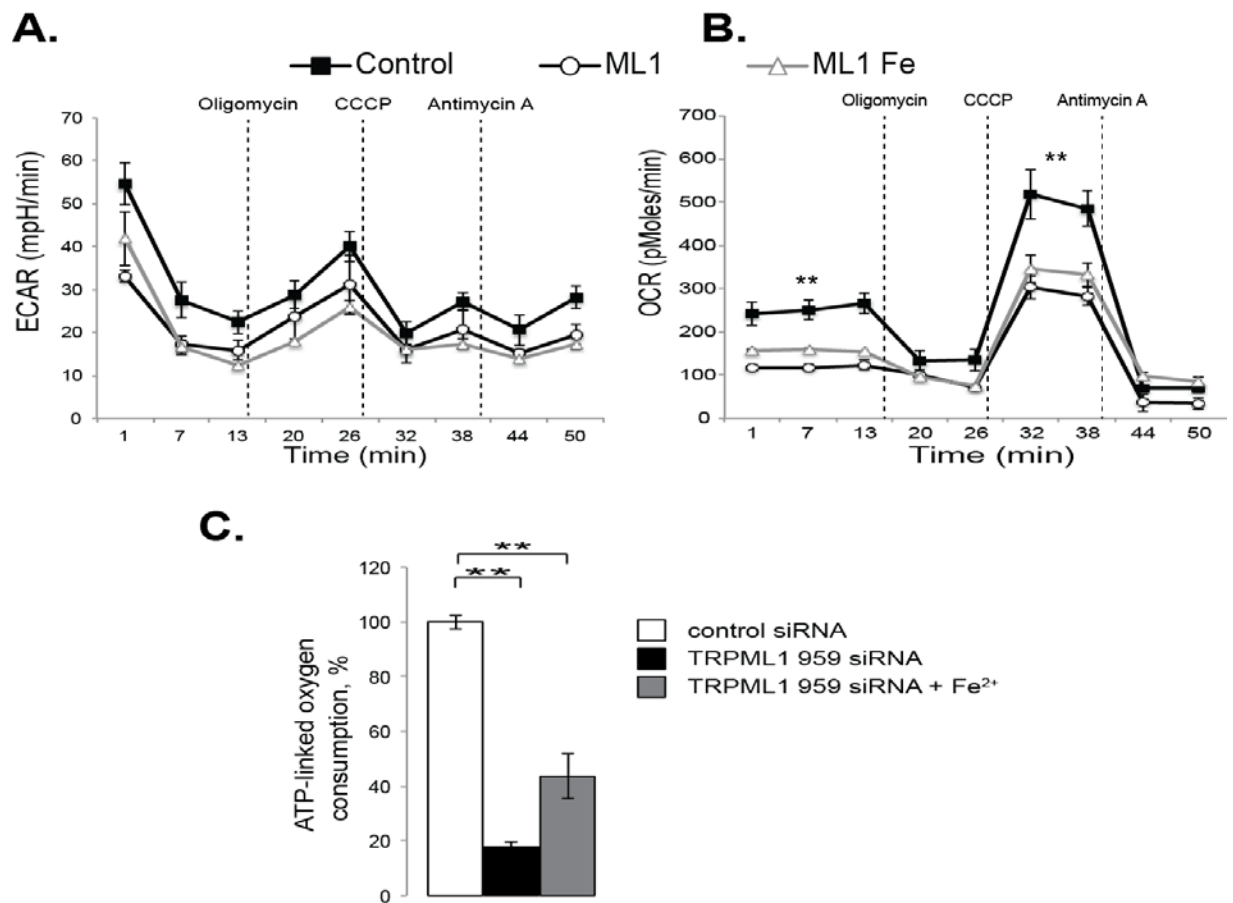


Figure 24 Oxidative stress in TRPML1-deficient RPE1 cells inhibits mitochondrial metabolic function

(A) Extracellular acidification rates (ECAR) and (B) Oxygen consumption rates (OCR) were measured using the XF24 analyzer prior to addition of chemicals to obtain the basal respiration rate, and after each addition of oligomycin, CCCP, and antimycin A. (C) ATP-linked OCR rates were calculated between control and treatment by averaging the drop in OCR following oligomycin. ** indicates $P < 0.01$.

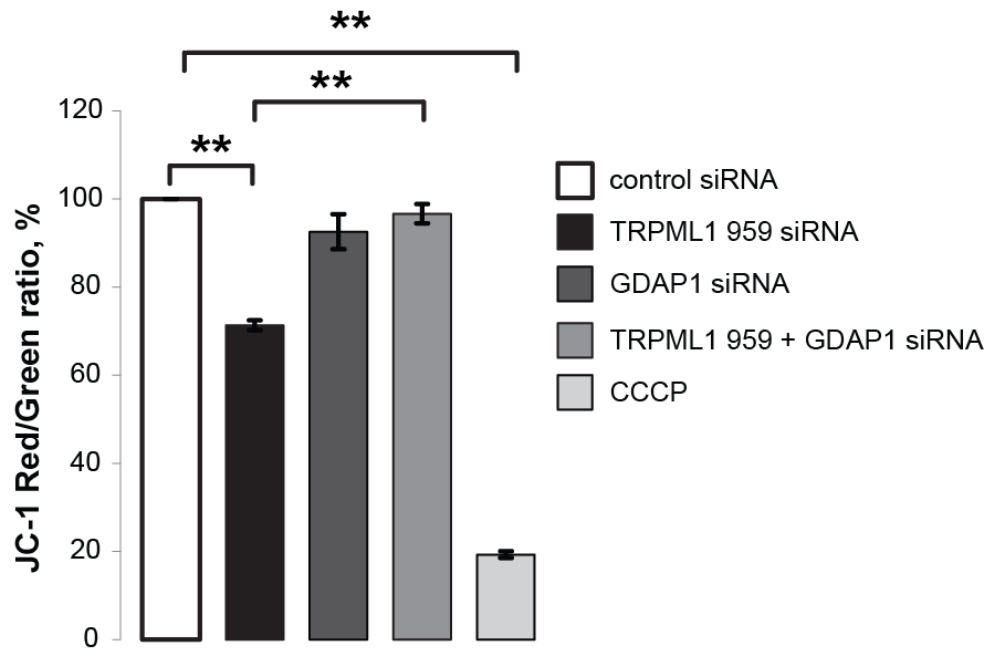


Figure 25 Mitochondrial depolarization in TRPML1-deficient RPE1 cells is dependent on upregulation of GDAP1

Analysis of mitochondrial depolarization in RPE1 cells transfected with control, TRPML1, GDAP1, or TRPML1 + GDAP1 siRNA 72 hours prior to experiment. As a positive control, cells were treated with 10 μ M CCCP for 15 minutes prior to experiment. Data are shown as % of control-KD cells, n=3, ** indicates P<0.005.

4.3 DISCUSSION

In an effort to verify the oxidative stress observed in my previous publication, I examined *HO-1* and *NQO1* levels in brain samples from MLIV mice, the results from this experiment and the one performed in MLIV patient fibroblasts indicate that the RPE1 model of oxidative stress induced by loss of TRPML1 are recapitulated in other models. In an attempt to identify the molecular mechanisms of MLIV pathogenesis, I analyzed previous microarrays in search of a gene candidate that was activated by ROS and altered mitochondrial morphology. The results I obtained from the microarray were extremely promising, as *GDAP1* fit both descriptions. It is known to function in mitochondrial fragmentation and was recently shown to be regulated in response to oxidative stress (182,187). Not only did the gene candidate appear on the microarray, but *GDAP1*'s expression in both MLIV patient fibroblasts and TRPML1 RPE1 cells was also elevated.

Two of the most promising and interesting aspects of this study are the fact that α -tocopherol reversed the *GDAP1* upregulation indicating that *GDAP1* is upregulated in response to the oxidative stress burden in TRPML1 deficient cells. And the fact that double knockdown of *GDAP1* and TRPML1 in the same cells reversed the mitochondrial depolarization observed in TRPML1-deficient RPE1 cells alone. Both of these results support my hypothesis that TRPML1 loss induces oxidative stress, which increased the expression of *GDAP1*, a protein that regulates mitochondrial morphology and as seen here mitochondrial membrane potential. Future experiments measuring mitochondrial metabolism and examining mitochondrial morphology will provide more information about the role *GDAP1* plays in mitochondrial morphology with regards to TRPML1's functional status.

4.4 ACKNOWLEDGEMENTS

I thank Karina Peña for technical assistance with the JC-1 assay, Aaron Gusdon for help with the Seahorse assay and analysis, and Dr. Lew Jacobson for use of his fluorometer.

This work was supported by the National Institute of Health grant numbers HD058577, ES01678, and U54 RR022241-01 awarded to Kirill Kiselyov.

5.0 CONCLUSION AND FUTURE DIRECTIONS

Until recently, the centric view of the lysosome was an organelle that participated solely in cellular digestion. With the recent discovery of TFEB, the master regulator of lysosomal biogenesis, autophagy, and lysosomal function, the role of the lysosome has grown drastically (4,17,20,21,114,230,231). While the role of the lysosome in the cell is constantly expanding, evidence from our lab suggests that the lysosome functions as a cytoprotective organelle that works to sequester cytotoxic material, such as transition metals, thus preventing cellular damage to other organelles (23,103,232). The majority of my thesis work over the past five years has focused on the involvement of TRPML1 in the cytoprotective function of the lysosome. The results of this work are summarized below.

This work has led to a better understanding of TRPML1's role in lysosomal transition metal homeostasis with regards to Fe^{2+} and has also provided new developments into the molecular mechanisms of MLIV pathogenesis. Additionally, these studies provide a novel therapeutic approach for alleviating ultra-structural and clinical aspects of MLIV pathogenesis. While the functional significance and efficacy of these treatments still need to be evaluated in MLIV animal models, it is likely that the use of these treatments could prolong the lifespan of animals and/or decrease the rate of MLIV disease progression, as similar studies have shown success in the treatment of other LSDs (233). Since a handful of LSDs have increased levels of ROS, this therapeutic treatment may extend to several other LSDs. While several questions about the exact role of TRPML1 within the lysosome remain unanswered, my work suggests that the role of TRPML1 within the cell extends beyond the lysosome.

5.1 TRPML1 LOSS RESULTS IN ROS ACCUMULATION

In Chapter 3, I performed experiments indicating that Fe^{2+} retention in lysosomes of TRPML1-deficient cells catalyzes the formation of ROS in lysosomes. Based on the evidence that TRPML1-deficient cells accumulate lysosomal Fe^{2+} and the recent discovery that TRPML1 acts as an endolysosomal Fe^{2+} release channel, I hypothesized that in the absence of a functional TRPML1 channel, Fe^{2+} retained in the lysosome will have detrimental effects on the cell (58). Since lysosomally localized Fe^{2+} can participate in Fenton chemistry, I first examined the possibility that it could catalyze ROS within the lysosome. To test this hypothesis, I utilized a cell culture model of MLIV, where TRPML1 levels were modulated in RPE1 cells using a siRNA-based approach. Using this system, I determined that the loss of TRPML1 results in the accumulation of ROS, as measured by increases in *HMOX1* mRNA levels. While my system simulates an “acute” loss of TRPML1, as TRPML1 was knocked down for only 72 hours, I wanted to determine if Fe^{2+} levels present in “chronic” models of MLIV potentiate the production of ROS. To test this hypothesis, I exposed TRPML1-deficient cells to 100 μM Fe^{2+} for 24 hours and found that ROS levels were even higher, as measured by a larger increase in *HMOX1* mRNA levels compared to TRPML1-KD alone. To support my finding that loss of TRPML1 results in the production of ROS, I measured the levels of lipid peroxidation and found more oxidation in TRPML1-deficient cells. Surprisingly, all of these changes that occur in TRPML1-deficient cells as a result of ROS production can be reversed by the addition of the antioxidant α -tocopherol. This result was very exciting and suggests the possibility that therapeutic antioxidant treatment may alleviate some symptoms of MLIV pathogenesis.

In support of these results, I wanted to confirm the possibility that oxidative stress is a key factor in MLIV pathogenesis. To test this hypothesis, I examined levels of *HMOX1* mRNA in

MLIV patient fibroblasts and found it to be elevated, confirming my findings in the TRPML1-deficient RPE1 model. Additionally, as a collaboration with Susan Slaugenhaupt's lab at Harvard Medical School, I obtained brain samples from 2 and 6 month old MLIV mouse models and performed doubly blind analysis to examine the induction of oxidative stress. In *MCOLN1*^{-/-} samples, I observed elevated levels of *HO-1* and *NQO1*, another gene regulated by Nrf2, suggesting that oxidative stress indeed plays a role in MLIV pathogenesis. The establishment of these findings were very exciting, as they suggest that symptoms associated with MLIV pathogenesis in all of these model systems may respond to antioxidant therapeutic treatments.

As few reliable methods are available to directly measure levels of ROS within the cell, I relied on an indirect measurement of ROS by measuring the mRNA levels of a gene known to be upregulated in response to oxidative stress and the presence of ROS. Since different types of ROS can induce oxidative stress and activate Nrf2 to promote transcription of antioxidant/cytoprotective genes, this measurement likely encompasses several types of ROS (147,149).

To support the idea that ROS were catalyzed by Fenton chemistry in the lysosome and are directly linked to TRPML1's functional status and the secondary accumulation of lysosomal Fe²⁺, I confirmed that ROS were lysosomally localized using immunofluorescence and carboxy-H₂DCFDA dye. Experiments performed in Chapter 3 confirmed that ROS generation was likely localized to the lysosome, as mitochondrial superoxide production was not detected in any condition. In several models of oxidative stress, ROS generated within the lysosome leads to peroxidation of membrane lipids and ultimately results in destabilization of the membrane and eventual lysosomal membrane permeabilization (LMP) (234,235). The resulting LMP then allows lysosomal contents to leak out into the cytoplasm, where lysosomal enzymes have the potential to activate caspases and the apoptotic cascade to initiate cell death (234).

Measurement of both Annexin V binding and Caspase 3 activity indicated no activation of apoptotic cell death cascades in TRPML1-deficient RPE1 cells regardless of Fe^{2+} status. This suggests that accumulation of ROS in lysosomes deficient of TRPML1 is not enough to induce cell death in the RPE1 model of MLIV. Interestingly, the absence of cell death initiation may be cell type specific, as data from our lab previously indicated that TRPML1 deficiency in HeLa cells results in the release of Cathepsin B from the lysosome which promotes cytochrome C release from the mitochondria and activation of Caspase-3, likely inducing eventual cell death (189). While there seems to be cell type specific differences between these cell model systems, how ROS impact the integrity of lysosomes upon modulation of TRPML1 and whether antioxidant treatment can alleviate MLIV symptoms will ultimately need to be analyzed in MLIV patient cells or the MLIV mouse model.

5.2 MITOCHONDRIAL HEALTH IN MLIV

In the remainder of Chapter 3 and Chapter 4, I performed experiments indicating that ROS produced in TRPML1-deficient cells induced cellular dysfunction outside of the lysosome, specifically within the mitochondria. The results in this section suggest that loss of TRPML1 in RPE1 cells results in changes in mitochondrial morphology that is directly related to the production of ROS.

Here I showed that TRPML1 loss is associated with mitochondrial fragmentation. The relatively short time to development and TRPML1-specificity of this phenotype suggests that this phenotype is an active event caused by the loss of TRPML1 and perhaps further aggravated by the induced lysosomal deficits and/or Fe^{2+} accumulation associated with MLIV. The fact that this

fragmentation is reversed by ROS reduction with the antioxidant α -tocopherol is new. It suggests that ROS generated from TRPML1-deficient cells damages mitochondria. This is a unique observation connecting TRPML1 to processes outside of the lysosome.

In conjunction with this, Chapter 4 supports the idea that TRPML1 loss induces oxidative stress, which increased the expression of GDAP1 and decreased the expression of MFN1, both are proteins that regulates mitochondrial morphology. Additionally, TRPML1 loss also reduced mitochondrial membrane potential. This alone adds a whole new dimension to what I know about the molecular mechanisms leading to MLIV pathology. Not only can I reverse this process with antioxidants, I now have a protein target, which is down stream of the loss of TRPML1 that I can target to alleviate mitochondrial damage. The model in Figure 26 summarizes the results from Chapter 3 and Chapter 4. While little is known about the exact function of GDAP1 in mitochondrial dynamics, future research will focus on identifying how GDAP1 senses the oxidative stress burden and in return alters mitochondrial morphology.

Since MLIV patient cells have been shown to have defects in autophagy, it is possible that fragmented and damaged mitochondria may accumulate in TRPML1-deficient cells since they are unable to be recycled via autophagy and lysosomal degradation (49,236). My data indicates that the production of ROS in the lysosome are at least partly responsible for the presence of fragmented dysfunctional mitochondria, as this phenotype is reversible with the antioxidant α -tocopherol. This observation that ROS are responsible for causing the associated mitochondrial dysfunction seems to be unique to MLIV, as other LSDs, such as the Mucopolysacchridoses, have been shown to induce mitochondrial dysfunction as a direct result of autophagic dysfunction (237).

While data in Chapter 3, indicates that apoptotic cascades are not initiated in my RPE1 model, perhaps due to the short time of TRPML1 modulation, mitochondrial dysfunction in MLIV

patient fibroblasts has been associated with loss of mitochondrial Ca^{2+} buffering capacity (23,24). As loss of mitochondrial Ca^{2+} buffering capacity is associated with increased sensitivity to apoptosis (238,239). It is possible that in other cell types mitochondrial dysfunction induced by TRPML1 deficiency may activate apoptosis, as was previously seen by our lab in HeLa cells (189). While the centric view of MLIV pathology is shifting towards microglial and astrocyte activation rather than neuronal death, which revealed the lack of cell death, future research identifying the impact of oxidative stress and mitochondrial dysfunction in the central nervous system of MLIV mice will provide valuable insight into the status of apoptotic cascade initiation.

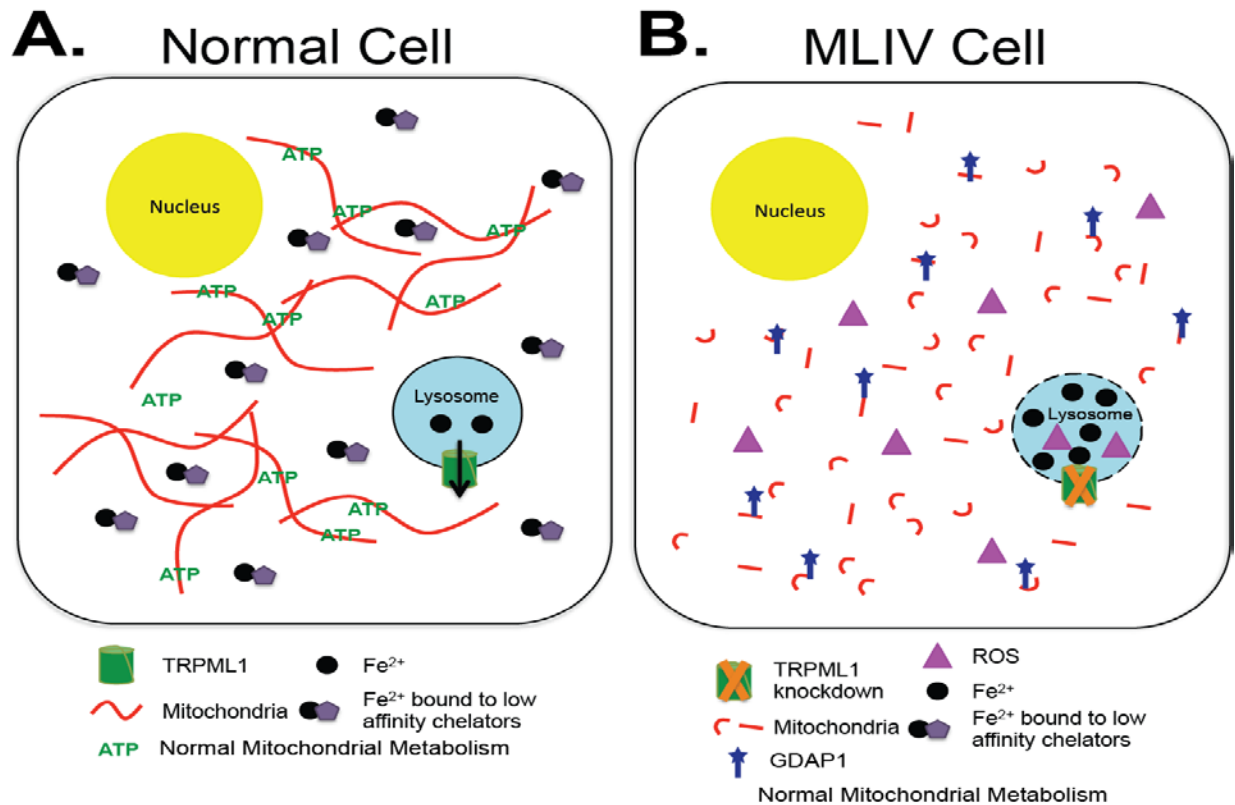


Figure 26 Model of TRPML1 deficiency in RPE1 cells

(A) Under normal conditions, Fe²⁺ enters the lysosome via endocytosis of Fe²⁺ bound proteins. The proteins are degraded and Fe²⁺ is transported to the cytoplasm via TRPML1 ion channel. In the cytoplasm, Fe²⁺ binds to low affinity chelators. Under these conditions, mitochondria remain elongated and are capable of normal metabolism. (B) In MLIV cells, which lack TRPML1, Fe²⁺ that is normally transported to the cytoplasm, accumulates in the lysosome and catalyzes Fenton reactions resulting in the production of ROS. ROS oxidize lipids, which can permeabilize the lysosomal membrane, allowing ROS to access the cytosol and induce mitochondrial fragmentation and loss of $\Delta\Psi_m$. Increased levels of oxidative stress upon loss of TRPML1 induce GDAP1 dependent mitochondrial fragmentation and result in reduced mitochondrial metabolism. While not depicted, several of these perturbations are reversible via the addition of the antioxidant α -tocopherol.

APPENDIX A

THE COMPARISON OF THE LOSS OF TWO LYSOSOMAL PROTEINS ASSOCIATED WITH MITOCHONDRIAL DYSFUNCTION TO IDENTIFY A MECHANISM REGULATING LYSOSOMAL AND MITOCHONDRIAL HEALTH

The work discussed in this section is unpublished.

A.1 OVERVIEW

Previously I have focused my work on the loss of TRPML1, to investigate this mechanism in a broader fashion I have also focused on the loss of ATP13A2. ATP13A2 is a member of the P5 subfamily of ATPases involved in lysosomal cation transport and mutations in this gene are associated with Parkinson's disease (197). I hypothesize that loss of a lysosomal protein is sufficient to directly cause mitochondrial damage. The alternative hypothesis is that accumulation of bad mitochondria occurs as an indirect mechanism induced by inhibition of autophagy. To test this aim, I started by confirming that the loss of both TRPML1 and ATP13A2 result in mitochondrial dysfunction characterized by loss of mitochondrial membrane potential.

As multiple neurodegenerative disorders, including other lysosomal storage diseases and Parkinson's disease, show defective lysosomal function, accumulation of transition metals, and buildup of unhealthy mitochondria, I am currently trying to identify a broad target that can be used

to alleviate these symptoms. Recently, it has been shown that overexpression of TFEB, the transcription factor known to regulate lysosomal and autophagic biogenesis as well as secretion, can successfully alleviate storage phenotypes by upregulating exocytosis, specifically in Pompe disease (114). Whether or not overexpression of TFEB can alleviate the lysosomal linked mitochondrial damage in neurodegenerative disorders has not been studied. To test the hypothesis that TFEB overexpression can alleviate mitochondrial damage induced by loss of lysosomal proteins, I will overexpress TFEB in cells that are deficient for multiple lysosomal proteins associated with neurodegenerative disorders and examine if mitochondrial dysfunction and damage is rescued by TFEB overexpression. For these experiments I will examine mitochondrial membrane potential. If TFEB overexpression can alleviate mitochondrial damage, I expect to see membrane potential return to control levels, suggesting that overexpression of TFEB is a successful treatment for mitochondrial damage associated with neurodegenerative diseases. However, if TFEB overexpression is not sufficient to rescue these phenotypes, I will pursue other avenues such as the activation of TRPML1, which should also prevent mitochondrial damage by sequestering transition metals like iron in the lysosome.

These studies will not only provide future direction for treatment of MLIV, in addition to my previously suggested treatments with antioxidants, but the results obtained from this study will allow us to more broadly treat neurodegenerative disorders where both the lysosome and mitochondria are dysfunctional.

A.2 PRELIMINARY DATA

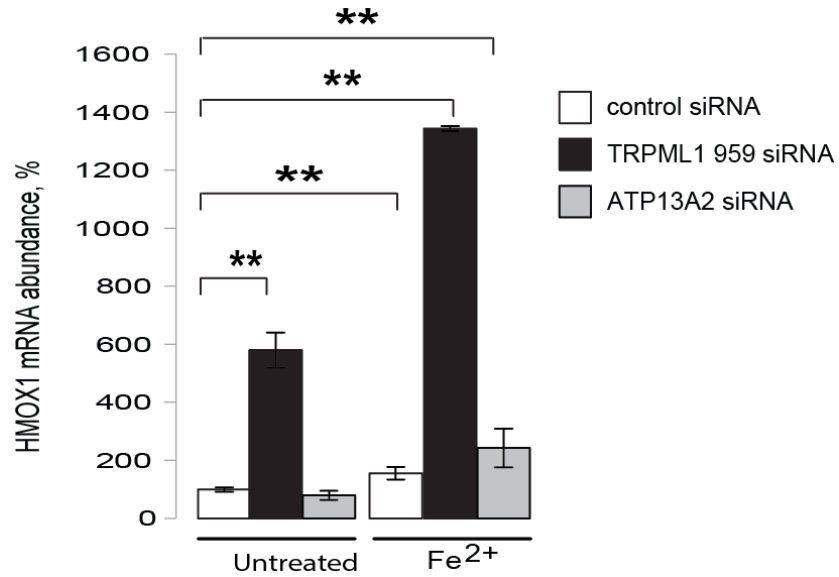


Figure 27 Oxidative stress is induced in TRPML1-deficient RPE1 cells, but not ATP13A2-deficient RPE1 cells

HMOX1 mRNA expression assessed by qPCR in control, TRPML1, and ATP13A2-KD cells. Data were normalized to values detected in untreated control-KD cells, which were taken as 100%. Data are means \pm S.E.M. n=3, ** P<0.01.

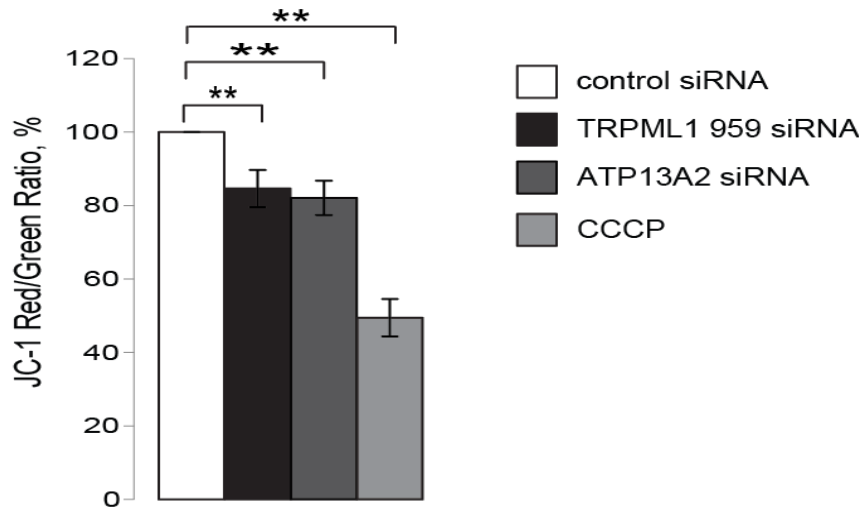


Figure 28 Loss of TRPML1 and ATP13A2 in RPE1 cells induces mitochondrial depolarization

Analysis of mitochondrial depolarization in RPE1 cells transfected with control, TRPML1, ATP13A2 siRNA 72 hours prior to experiment. As a positive control, cells were treated with 10 μ M CCCP for 15 minutes prior to experiment. Data are shown as % of control-KD cells, n=3, ** indicates $P < 0.01$.

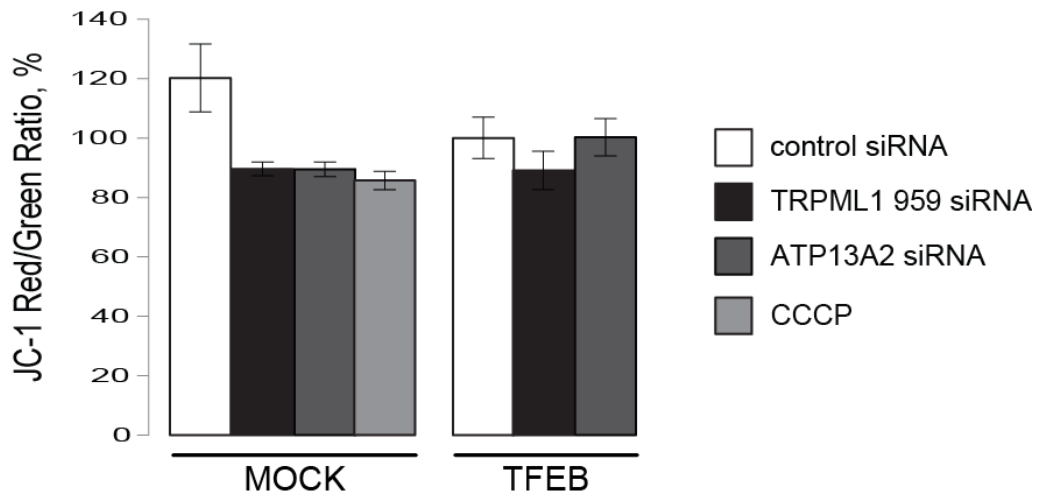


Figure 29 Mitochondrial depolarization is rescued by TFEB overexpression in ATP13A2-deficient HEK cells

Analysis of mitochondrial depolarization in HEK cells transfected with MOCK or TFEB plasmid, followed by transfection with control, TRPML1, ATP13A2 siRNA 72 hours prior to experiment. As a positive control, cells were treated with 10 μ M CCCP for 15 minutes prior to experiment. Data are shown as % of control-KD cells, n=3.

APPENDIX B

OXIDATIVE STRESS IN TRPML1-DEFICIENT RPE1 CELLS ACTIVATES INFLAMMATORY PATHWAY TRANSCRIPTIONAL REGULATION

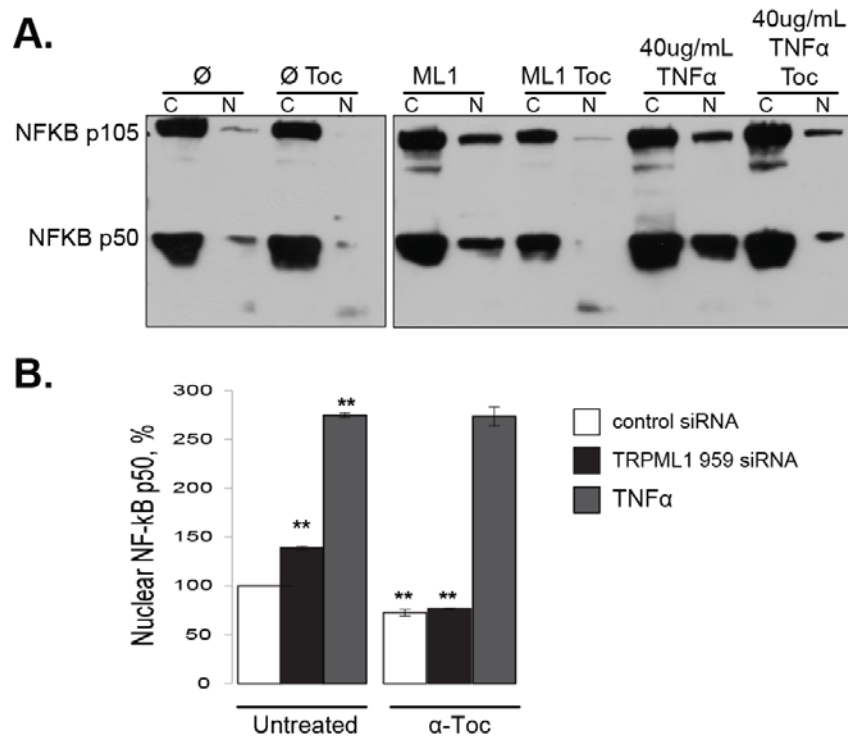


Figure 30 TRPML1 deficiency in RPE1 cells induces NF- κB p50 nuclear translocation in an ROS dependent manner

(A) Western blot analysis of RPE1 cells transfected with control or TRPML1-siRNA 72 hours prior to analysis. As a positive control, cells were treated with 40 ug/mL of TNF- α for 8 hours. As a means of reducing oxidative stress, cells were pretreated with 100 nM α -Toc for 24 hours prior to analysis. (B) Quantitative analysis of NF- κ B p50 nuclear translocation normalized to actin and shown as % of control. n=3, **indicates P<0.01.

APPENDIX C

CHARACTERIZING THE CELLULAR RESPONSE TO DEFECTS IN ENDOCYTTIC TRAFFICKING

The work discussed in this section is unpublished data.

Endocytosis is an essential process in all cells. It is used to absorb nutrients, regulate protein surface expression, and functions in membrane remodeling and cell signaling. It is unclear how this process is regulated and if cells are able to gauge defects in this pathway. I propose that cells have specific regulatory networks to monitor and respond to trafficking defects along the endocytic pathway. To test this hypothesis, I have established a system in which I can modulate different steps of the endocytic pathway to produce trafficking defects. To modulate aspects of endocytosis, siRNA was used to target the following proteins, RAB5A, RAB7A, TRPML1 and 3, PPT1 and TPC. Western blotting and quantitative real-time PCR confirmed significant down regulation of both protein and mRNA levels. To confirm the presence of trafficking defects, I plan to perform fluorescent trafficking assays using the fluid phase endocytic marker dextran and quantitative radioactive assays. Once trafficking defects are identified, I plan to measure the genomic response using microarray analysis to assemble gene expression profiles. Gene expression profiles will be compared between all endocytic trafficking defects to determine if similar genes are altered. Furthermore, to identify common regulatory elements responsible for the genomic response, I will compare transcription factors associated with up and down regulated genes. The results of this

study will provide insight into how the endocytic pathway is regulated when the pathway is disrupted.

C.1 INTRODUCTION

Regulatory gene networks are responsible for monitoring organelle biogenesis and cellular stress responses within the cell (166). Endocytosis is a highly complex process responsible for nutrient absorption, membrane remodeling, and cell signaling (240). How this pathway is regulated is not well understood. Recently, a regulatory gene network (CLEAR network) associated with the latter portion of the endocytic pathway was identified. This network is responsible for regulating lysosomal biogenesis through activation of the master transcription factor EB (TFEB) (166). Not all genes coding for endocytic proteins contain TFEB binding sites, which suggests that TFEB is not the only transcription factor regulating endocytosis. Little is known about what signals feed into this pathway and what is responsible for the continual movement of cargo through the endocytic pathway. I propose that acute knockdown of endocytic proteins followed by gene expression assays will identify specific regulatory networks that gauge the status of endocytic compartments and respond to trafficking defects along the endocytic pathway.

When the endocytic pathway is not functioning properly to deliver and digest cargo, it can result in the accumulation of storage bodies in the cytoplasm, which are a characteristic of storage diseases. Interestingly, storage diseases are commonly associated with neurodegeneration due to cell death. Multiple storage diseases, including Mucopolysaccharidosis type IV, Infantile Neuronal Lipofuscinosis, and Charcot-Marie-Tooth disease type 2B, are associated with protein malfunction in the endocytic pathway, more specifically with defects in TRPML1, PPT1, and RAB7A

respectively (28,241,242). I propose that genomic responses to problems in the endocytic pathway may contribute to the pathological manifestations of storage diseases. I will test this suggestion by acutely knocking down proteins that are implicated in storage diseases and endocytic function. These experiments will lend insight into how cells respond at the genomic level to defects at different points along the endocytic pathway. This study will provide a more accurate depiction of trafficking defects generated as a direct result of disrupting the function of important endocytic proteins. The results of this study will provide valuable information about the genomic response associated with different lysosomal storage disorders and diseases associated with the disruption of the endocytic pathway. This study will also provide analysis of the localization and activity of transcription factors directly responsible for the cellular response to trafficking defects.

C.1.1 Endocytosis

Endocytosis is an essential process in all cells. It is used to absorb nutrients, regulate protein surface expression, and functions in membrane remodeling, cell signaling, and intracellular transport (240). In order for cells to perform these tasks, they need to maintain trafficking throughout the entire pathway (240). The endocytic pathway is composed of multiple compartments, each with a unique function. This process is highly complex and relies on multiple proteins to coordinate specific events, such as vesicle movement, maturation, and fusion/fission events. During internalization, cargo is initially delivered to the EE, where it is either sorted for degradation or recycled back to the plasma membrane (240). The early endosome contains the small GTPase RAB5A, which mediates fusion between clathrin coated vesicles and early endosomes (Figure 31) (243). As cargo transits through the pathway, the EE fuses with the LE, where cargo begins to undergo degradation (240). As trafficking continues, the LE fuses with the

lysosome, where degradation is completed prior to absorption of nutrients and materials (240). Fusion of the EE and LE as well as fusion of the LE and lysosome is regulated by the small GTPase RAB7A (Figure 31) (243). It is unclear how this trafficking process is regulated, but previous studies have identified key proteins and phosphoinositides that when mutated or knocked down result in the formation of storage bodies (190,244-247). The presence of storage bodies, indicating a delay or block in endocytosis, is a hallmark of LSD (248). Utilizing the specificity of RAB proteins, I can establish defects that specifically disrupt the function of distinct compartments along the endocytic pathway.

To determine how endocytosis is regulated, specific aspects of trafficking will be disrupted by inhibiting protein synthesis, decreasing levels of phosphoinositides, or treating cells with pharmacological compounds. The molecules displayed in Figure 31 were selected for modulation because they play an important role in endocytic events and/or are implicated in storage diseases. The first candidate is TRPML1, an inwardly rectifying cation channel, activated by PI(3,5)P₂ (79). TRPML1 localizes to the lysosome and is thought to regulate fusion/fission between the late endosome and lysosome (86). Mutations in the gene *MCOLN1*, encoding for TRPML1, are associated with Mucopolysaccharidosis IV and result in neurodegeneration characterized by developmental delays, retinal degeneration, and motor and cognitive deficiencies (28). The second candidate is TRPML3, a pH regulated Ca²⁺ channel localized to the endocytic pathway (245). Overexpression studies of MCOLN3, the gene encoding TRPML3, suggests that it plays an important role in endosomal function because it results in enlargement and clustering of endosomes (200,245). Alternatively, impairment of TRPML3 results in defective membrane trafficking and endosomal acidification (245). The third candidate is TPC1, a Ca²⁺ permeable channel activated by NAADP localized to endo/lysosomal compartments (249). The release of Ca²⁺ from the lysosome may also

facilitate fusion/fission events. The fourth candidate is PI(3,5)P₂, a phosphoinositide localized to the LE and lysosome (246). Recent publications have identified it as the main activator of TRPML1 (79). The loss of PI(3,5)P₂ results in enlarged endo/lysosomes (79). PI(3,5)P₂ is produced from PI(3)P via the kinase PIKfyve/PIP5K3 (246). To decrease levels of PI(3,5)P₂, the kinase will be targeted using siRNA. The fifth candidate is RAB5A, a small GTPase localized to the early endosome. RAB5A is responsible for mediating fusion between internalized vesicles and early endosomes (244). The sixth candidate is RAB7A, another small GTPase responsible for facilitating vesicle fusion/fission between the EE and LE and the LE and the lysosome (247). RAB7A has also been shown to be necessary for lysosomal degradation of an endocytic receptor complex, EGF-EGFR (247). Mutations in RAB7A are associated with Charcot-Marie-Tooth Type 2B Neuropathy, which is characterized by muscle weakness and wasting along with sensory loss (241). The seventh candidate is PPT1, a lysosomal enzyme thought to be involved in the degradation of lipid-modified proteins (228). Like TRPML1, mutations in PPT1 are associated with a lysosomal storage disorder, known as Infantile Neuronal ceroid lipofuscinosis (242).

Aside from modulating endocytosis by RNA silencing, multiple pharmacological compounds are commercially available to target specific aspects of the endocytic pathway. Calcium is an important molecule in many cellular processes and recent publications have indicated a role for Ca²⁺ release in endo/lysosomal fusion (250). As a means of inhibiting this event, a Ca²⁺ chelator, BAPTA-AM is used to cause trafficking defects by inhibiting vesicle fusion/fission (190). Another aspect of endocytosis necessary for trafficking is the proper acidification of endocytic compartments. Compartmental acidification is maintained by vacuolar H⁺-ATPase pumps, inhibition of this pump was shown to slow delivery to late endosomes/lysosomes (240). Bafilomycin A1, a compound that blocks lysosomal acidification,

can inhibit the H⁺-ATPase pump (240). The lysosome is the final destination for all cargo that enters the endocytic pathway to be degraded. It contains multiple acid hydrolase enzymes used to digest nutrients and breakdown cellular debris and waste (240). Leupeptin, a serine/cysteine protease inhibitor, is used to inhibit the degradative properties of lysosomal enzymes therefore preventing degradation of protein substrates (251). Specifically modulating different aspects of the endocytic pathway using siRNA or pharmacological compounds will allow us to determine if a single regulatory gene network is responsible for gauging the status of the entire endocytic pathway. Anticipated results of modulating proteins along the endocytic pathway are indicated in Table 4.

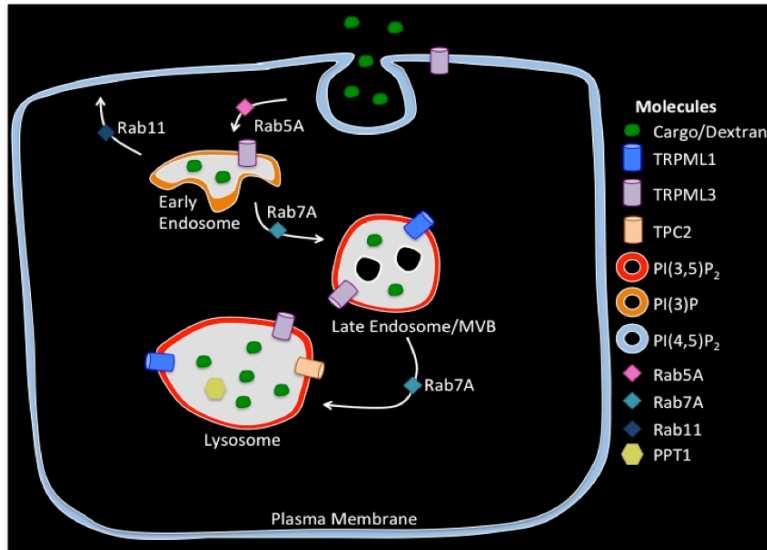


Figure 31 Localization of proteins and phosphoinositides associated with endocytic traffic

(A) The distribution of PI(4,5)P₂, PI(3)P₂, and PI(3,5)P₂ associated with the plasma membrane and membranes of the early endosome and late endosome/lysosome are represented by blue, orange, and yellow outlines, respectively. Green circles represent cargo/probes for fluid phase endocytosis.

Table 4 Anticipated trafficking defects produced as a result of modulating endocytic proteins

| Gene | Protein | Anticipated Defect |
|--------------------|---------|---|
| MCOLN1 | TRPML1 | Disrupt fusion/fission of late endosome and lysosome by preventing Ca ²⁺ release. |
| MCOLN3 | TRPML3 | Disrupt fusion/fission of endosomes and lysosomes by preventing Ca ²⁺ release. |
| TPCN2 | TPC2 | Block NAADP induced Ca ²⁺ release from lysosome affecting fusion/fission. |
| RAB5A | RAB5A | Disrupt fusion of plasma membrane and early endosomes. |
| RAB7A | RAB7A | Disrupt vesicle trafficking in late endosomes and also between late endosomes and lysosomes. |
| PPT1 | PPT1 | Disrupt lysosomal function by blocking degradation of lipid-modified proteins. |
| PIP5K3/ PIKfyve | PIP5K3 | Decrease levels of PI(3,5)P ₂ to disrupt lysosomal TRPML1 channel to disrupt fusion/fission. |

C.1.2 Regulatory Gene Networks

Regulatory gene networks have recently been implicated for monitoring several biological processes including stress responses. One example of a regulatory gene network is the activation of the unfolded protein response within the endoplasmic reticulum that activates the transcription factor Atf6 (252). Regulatory gene networks also play a role in organelle biogenesis and maturation processes. As previously mentioned, the first regulatory gene network associated with the endocytic pathway was recently discovered. This network, known as the CLEAR (Coordinated Lysosomal Expression and Regulation) network, regulates biogenesis and function of the lysosome (19). The CLEAR network is activated upon conditions of starvation or lysosomal disruptions. Both conditions activate the master transcription factor, TFEB, which enters the nucleus and binds to a consensus sequence within the promoter known as the CLEAR sequence (19). This results in the transcription of lysosomal genes necessary for lysosomal biogenesis (19). The function and activity of the endocytic pathway is well established, but little is known about how this pathway utilizes signaling to regulate trafficking. The identification of the CLEAR network suggests that regulatory gene networks monitor the endocytic pathway.

C.2 RESULTS

C.2.1 Establish and characterize distinct trafficking defects by modulating endocytic proteins and phosphoinositides

To establish a toolbox of endocytic disruptions that will be used to examine the cellular response to trafficking defects I have knocked down several candidate proteins. They include TRPML1, TPC1, PPT1, RAB7A, RAB5A, FIG4, VAC14, and PIP5K3. Figure 32A shows the quantification of mRNA levels after siRNA KD using q-PCR, while Figure 32B shows protein levels using Western blot analysis. The results from these figures indicate that siRNA down regulation results in decreased mRNA and protein levels. These initial results also indicate that siRNA is an effective method for targeting specific endocytic proteins.

As a means of monitoring endocytosis, fluorescent probes conjugated to dextran are internalized through fluid phase endocytosis. Upon internalization, the assay is stopped at specific timepoints by fixing the cells. Once fixed, the cells are assayed by immunofluorescent staining with antibodies specific to an endocytic compartment. The antibodies that are typically used include, EEA1 (BD-Transduction Laboratories) to stain the EE, M6PR (AbCam) to stain the LE, and LAMP-1 (Santa Cruz Biotechnology) to stain lysosomes. This assay provides “snapshots” of the endocytic pathway by comparing the localization of fluorescent dextran with specific endocytic markers. Previous publications studying lysosomal storage disorders examine the uptake of fluorescent dextran with long load and chase times (53). Using this procedure TRPML1 KD, PIP5K3 KD and control KD cells were loaded with Texas red dextran for 3 hour, followed by chase of either 0 or 6 hours. The results from this assay are shown in Figure 33A and quantified in Figure 33B. This procedure revealed similar co-localization between dextran and the lysosomal

marker LAMP-1 after a 6 hour chase for all treatments. Although this data alone suggests that there may not be a trafficking delay because dextran is still delivered to the lysosome, the resolution of this protocol may not be good enough to see a delay. If this is the case, this procedure is not optimal for my study because I am interested in localizing trafficking defects to both early and late compartments along the endocytic pathway. To confirm the presence or absence of minute trafficking delays, I need an assay that is more sensitive to detect delays at earlier time points in the endocytic pathway. To do this, I have developed a revised protocol that utilizes short load (5 minute) and chase (0, 20, 60 minute) times to get a better representation of each endocytic compartment, rather than just the lysosome. Figure 34 shows the revised protocol is sensitive enough to resolve trafficking between specific endocytic compartments including the EE and lysosome. Using this assay, I will be able to monitor trafficking defects throughout the entire endocytic pathway and specifically pinpoint the location of any trafficking defects. Future work will involve performing individual trafficking assays in combination with different siRNA.

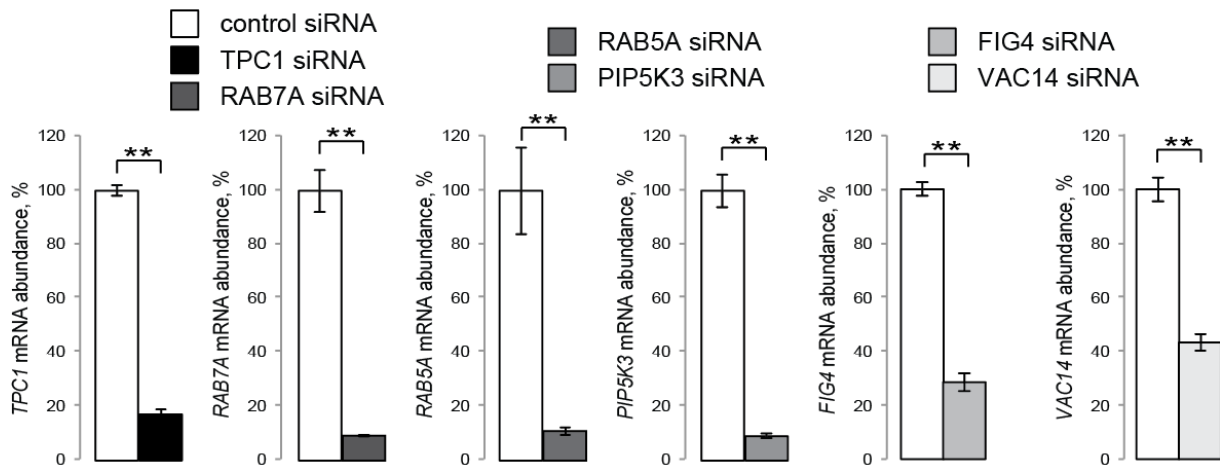
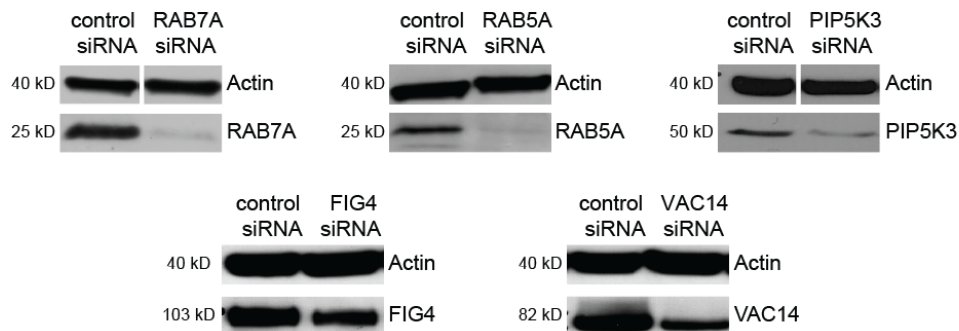
A.**B.**

Figure 32 siRNA-mediated down regulation of endocytic proteins

(A) HeLa cells were transfected with respective siRNA 48 hours prior to isolation of RNA. Total RNA was isolated and cDNA was synthesized and probed using primers spanning exons. Experimental samples were normalized to housekeeping gene, β -Actin. $**P < 0.01$. (B) HeLa cells were transfected with respective siRNA and lysates were collected 48 hours after transfection and subjected to Western blot analysis using the respective antibodies. Protein levels were normalized to β -Actin. Note TRPML1 and PPT1 in RPE1 cells were also analyzed using this method. These results are shown in Figure 22.

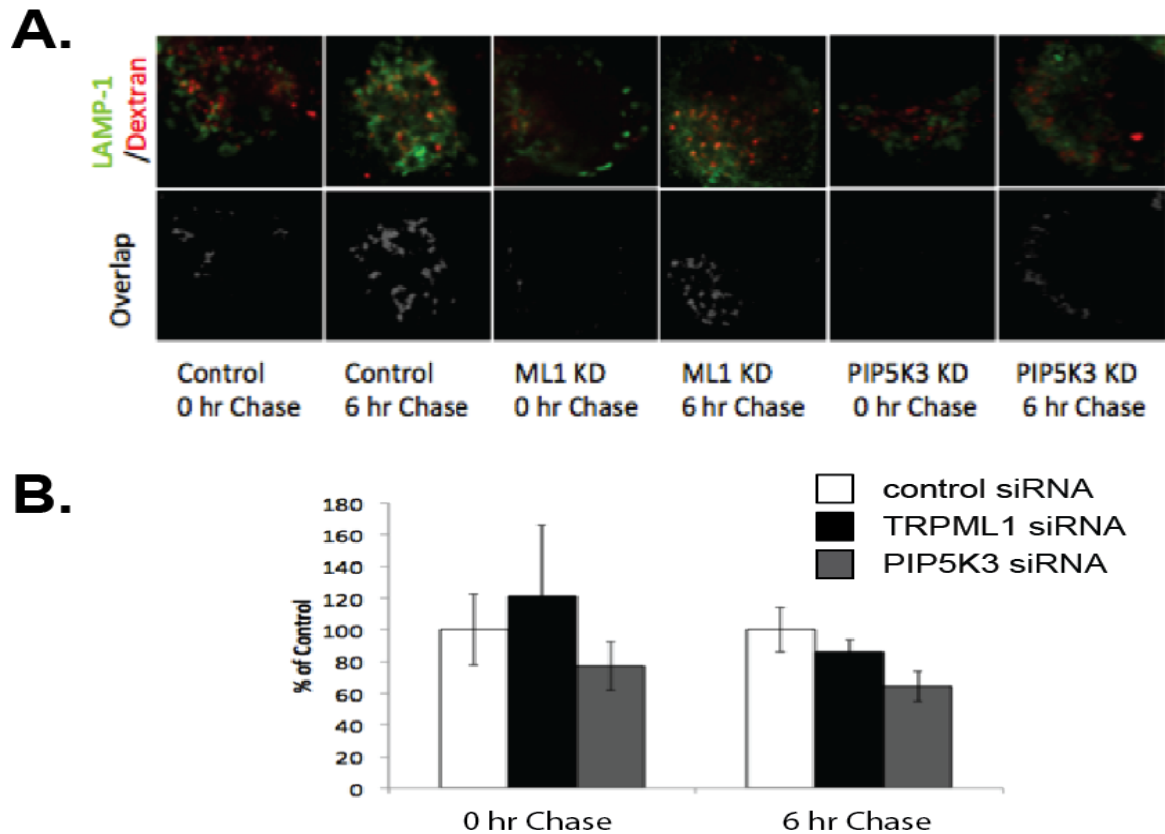


Figure 33 Texas red dextran delivery to lysosomes after long load and long chase times does not provide enough resolution to distinguish trafficking delays in TRPML1 and PIP5K3 deficient cells

(A) HeLa cells were treated with Control, TRPML1, or PIP5K3 siRNA for 48 hours then loaded for 3 hours with Texas Red (TR) dextran. Following a 3 hour load, cells were washed with regular media and fixed (0 hour chase) or chased for an additional 6 hours. Cells were then fixed and processed for immunofluorescence. Delivery of TR dextran to lysosomes was measured by quantifying the percent overlap between TR dextran and the lysosomal marker, LAMP-1. (B) Graphical representation of the quantifications are shown and are expressed as the percent overlap \pm SEM for cells under each condition. n=5.

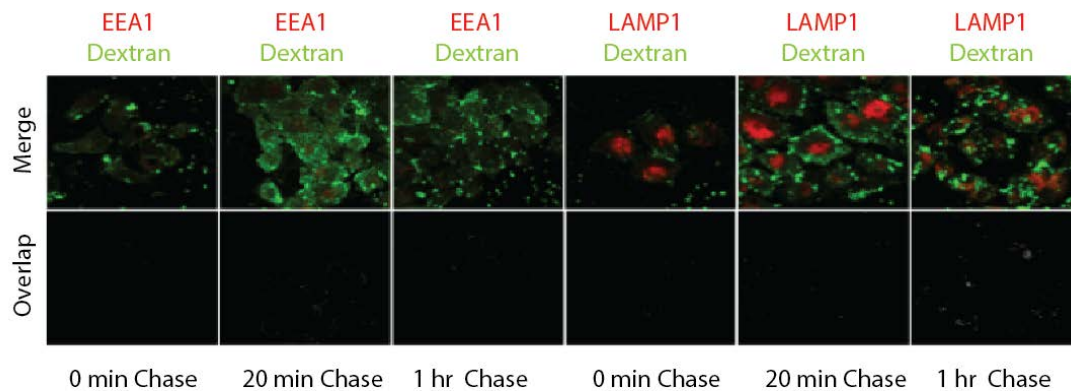


Figure 34 Trafficking assays with Alexa Fluor 488 dextran using short load and chase times can be used to pinpoint the time it takes for cargo to be delivered to the early endosome and lysosome in control cells

HeLa cells transfected with control siRNA were loaded for 5 minutes with Alexa Fluor 488 (A488) dextran. Following a 5 minute load, cells were washed with regular media and fixed (0 minute chase) or chased for either an additional 20 minutes or 1 hour. Cells were then fixed and processed for immunofluorescence. Delivery of A488 dextran to early endosomes was measured by quantifying the percent overlap between A488 dextran and the early endosomal marker, EEA1. While delivery to the lysosome was measured using the lysosomal marker, LAMP-1.

C.3 DISCUSSION AND FUTURE DIRECTIONS

The goal of this project is to determine if the cell is able to sense a disruption in endocytic trafficking. More specifically, with the results of this project, I will be able to establish a cellular response model for endocytic trafficking defects and determine if the cell responds in a general manner to all endocytic assaults or in a manner that is specific to the location of the defect along the endocytic pathway. Upon analysis of the transcription factors identified using the microarray analysis I will determine which regulatory networks are acting in response to defects and how these networks are activated.

C.3.1 Endocytic trafficking assays are sensitive enough to detect defects in endocytosis

My results confirm that siRNA modulation can effectively down regulate mRNA and protein levels of several endocytic proteins. Using this technique to modulate protein expression, I was able to examine endocytic trafficking by monitoring fluid phase endocytosis of the fluorescent probe, dextran. Performing this assay with long load and long chases, indicates that there may be trafficking defects present upon modulation of TRPML1 and PIP5K3 KD, but these assays are not sensitive enough to resolve the localization of the trafficking defect. As a way to better resolve the specific location of each trafficking defect along the endocytic pathway, I developed a protocol that utilized short load and short chase times in combination with EE and LE markers to determine the rate at which cargo travels through each compartment. My assays performed in control cells indicate that the sensitivity of this protocol can be used to examine modulations to the endocytic pathway and help to specifically localize the trafficking defect. Future work in our lab will focus on this.

C.3.2 Acute TRPML1 modulation does not result in changes in gene expression in TFEB regulated genes

Our lab has initiated preliminary analysis of the cellular response to modulations of key endocytic proteins. Microarray analysis has been completed for 48 hour KD of TRPML1 in comparison to control cells. TRPML1 is a lysosomal protein and therefore the KD may cause lysosomal disruption triggering the activation of TFEB and the up or down regulation of CLEAR network associated genes. The microarray data obtained indicates that the expression of several genes changed upon knocking down TRPML1. Interestingly, none of the genes that were up or down regulated are associated with the CLEAR network. This indicates that either 48 hour KD of TRPML1 does not cause sufficient lysosomal disruption to activate TFEB or that another novel regulatory gene network may be activated in response to TRPML1 KD. Analysis of the transcription factors associated with the genes that are up and down regulated in TRPML1 deficient cells revealed several possible transcription factors that may be responsible for the cellular response. The transcription factor that was most frequently associated with genes that had differential expression was NF- κ B. To determine if NF- κ B is the transcription factor responsible for the cellular response to TRPML1 KD, I need to perform microarray analysis on other endocytic disruptions to see if NF- κ B regulated genes are also up or down regulated upon KD. Future work will involve performing microarray analysis with other siRNA modulations of the endocytic pathway. To answer whether individual endocytic compartments are regulated by the same transcription factor or if each compartment utilizes a unique and specific transcription factor for the cellular response, I can compare the data from several endocytic disruptions. Additionally, I can use this data to differentiate between responses that are due to knocking down a specific protein compared to responses that are due to general disruptions of endocytosis.

BIBLIOGRAPHY

1. De Duve, C., Pressman, B. C., Gianetto, R., Wattiaux, R., and Appelmans, F. (1955) Tissue fractionation studies. 6. Intracellular distribution patterns of enzymes in rat-liver tissue. *The Biochemical journal* **60**, 604-617
2. Appelqvist, H., Waster, P., Kagedal, K., and Ollinger, K. (2013) The lysosome: from waste bag to potential therapeutic target. *Journal of molecular cell biology* **5**, 214-226
3. Alroy, J., Garganta, C., and Wiederschain, G. (2014) Secondary biochemical and morphological consequences in lysosomal storage diseases. *Biochemistry. Biokhimiia* **79**, 619-636
4. Sardiello, M., Palmieri, M., di Ronza, A., Medina, D. L., Valenza, M., Gennarino, V. A., Di Malta, C., Donaudy, F., Embrione, V., Polishchuk, R. S., Banfi, S., Parenti, G., Cattaneo, E., and Ballabio, A. (2009) A gene network regulating lysosomal biogenesis and function. *Science* **325**, 473-477
5. Saftig, P., Schroder, B., and Blanz, J. (2010) Lysosomal membrane proteins: life between acid and neutral conditions. *Biochemical Society transactions* **38**, 1420-1423
6. Schulze, H., Kolter, T., and Sandhoff, K. (2009) Principles of lysosomal membrane degradation: Cellular topology and biochemistry of lysosomal lipid degradation. *Biochimica et biophysica acta* **1793**, 674-683
7. Granger, B. L., Green, S. A., Gabel, C. A., Howe, C. L., Mellman, I., and Helenius, A. (1990) Characterization and cloning of lgp110, a lysosomal membrane glycoprotein from mouse and rat cells. *The Journal of biological chemistry* **265**, 12036-12043
8. Lloyd-Evans, E., and Platt, F. M. (2011) Lysosomal Ca(2+) homeostasis: role in pathogenesis of lysosomal storage diseases. *Cell calcium* **50**, 200-205
9. Mindell, J. A. (2012) Lysosomal acidification mechanisms. *Annual review of physiology* **74**, 69-86
10. Rodriguez, A., Webster, P., Ortego, J., and Andrews, N. W. (1997) Lysosomes behave as Ca²⁺-regulated exocytic vesicles in fibroblasts and epithelial cells. *The Journal of cell biology* **137**, 93-104
11. Settembre, C., Fraldi, A., Medina, D. L., and Ballabio, A. (2013) Signals from the lysosome: a control centre for cellular clearance and energy metabolism. *Nature reviews. Molecular cell biology* **14**, 283-296
12. Jin, M., and Klionsky, D. J. (2014) Regulation of autophagy: modulation of the size and number of autophagosomes. *FEBS letters* **588**, 2457-2463
13. Kimura, S., Noda, T., and Yoshimori, T. (2008) Dynein-dependent movement of autophagosomes mediates efficient encounters with lysosomes. *Cell structure and function* **33**, 109-122
14. Segatori, L. (2014) Impairment of homeostasis in lysosomal storage disorders. *IUBMB life* **66**, 472-477
15. Roczniak-Ferguson, A., Petit, C. S., Froehlich, F., Qian, S., Ky, J., Angarola, B., Walther, T. C., and Ferguson, S. M. (2012) The transcription factor TFEB links mTORC1 signaling to transcriptional control of lysosome homeostasis. *Science signaling* **5**, ra42

16. Pena-Llopis, S., Vega-Rubin-de-Celis, S., Schwartz, J. C., Wolff, N. C., Tran, T. A., Zou, L., Xie, X. J., Corey, D. R., and Brugarolas, J. (2011) Regulation of TFEB and V-ATPases by mTORC1. *The EMBO journal* **30**, 3242-3258
17. Sardiello, M., and Ballabio, A. (2009) Lysosomal enhancement: a CLEAR answer to cellular degradative needs. *Cell cycle* **8**, 4021-4022
18. Settembre, C., Zoncu, R., Medina, D. L., Vetrini, F., Erdin, S., Erdin, S., Huynh, T., Ferron, M., Karsenty, G., Vellard, M. C., Facchinetti, V., Sabatini, D. M., and Ballabio, A. (2012) A lysosome-to-nucleus signalling mechanism senses and regulates the lysosome via mTOR and TFEB. *The EMBO journal* **31**, 1095-1108
19. Palmieri, M., Impey, S., Kang, H., di Ronza, A., Pelz, C., Sardiello, M., and Ballabio, A. (2011) Characterization of the CLEAR network reveals an integrated control of cellular clearance pathways. *Human molecular genetics* **20**, 3852-3866
20. Settembre, C., and Ballabio, A. (2011) TFEB regulates autophagy: an integrated coordination of cellular degradation and recycling processes. *Autophagy* **7**, 1379-1381
21. Song, W., Wang, F., Savini, M., Ake, A., di Ronza, A., Sardiello, M., and Segatori, L. (2013) TFEB regulates lysosomal proteostasis. *Human molecular genetics* **22**, 1994-2009
22. Hollak, C. E., and Wijburg, F. A. (2014) Treatment of lysosomal storage disorders: successes and challenges. *Journal of inherited metabolic disease* **37**, 587-598
23. Coblentz, J., St Croix, C., and Kiselyov, K. (2014) Loss of TRPML1 promotes production of reactive oxygen species: is oxidative damage a factor in mucopolipidosis type IV? *The Biochemical journal* **457**, 361-368
24. Jennings, J. J., Jr., Zhu, J. H., Rbaibi, Y., Luo, X., Chu, C. T., and Kiselyov, K. (2006) Mitochondrial aberrations in mucopolipidosis Type IV. *The Journal of biological chemistry* **281**, 39041-39050
25. Venkatachalam, K., Long, A. A., Elsaesser, R., Nikolaeva, D., Broadie, K., and Montell, C. (2008) Motor deficit in a Drosophila model of mucopolipidosis type IV due to defective clearance of apoptotic cells. *Cell* **135**, 838-851
26. Bargal, R., Avidan, N., Ben-Asher, E., Olender, Z., Zeigler, M., Frumkin, A., Raas-Rothschild, A., Glusman, G., Lancet, D., and Bach, G. (2000) Identification of the gene causing mucopolipidosis type IV. *Nature genetics* **26**, 118-123
27. Bassi, M. T., Manzoni, M., Monti, E., Pizzo, M. T., Ballabio, A., and Borsani, G. (2000) Cloning of the gene encoding a novel integral membrane protein, mucopolipidin-and identification of the two major founder mutations causing mucopolipidosis type IV. *American journal of human genetics* **67**, 1110-1120
28. Sun, M., Goldin, E., Stahl, S., Falardeau, J. L., Kennedy, J. C., Acierno, J. S., Jr., Bove, C., Kaneski, C. R., Nagle, J., Bromley, M. C., Colman, M., Schiffmann, R., and Slaugenhaupt, S. A. (2000) Mucopolipidosis type IV is caused by mutations in a gene encoding a novel transient receptor potential channel. *Human molecular genetics* **9**, 2471-2478
29. Wakabayashi, K., Gustafson, A. M., Sidransky, E., and Goldin, E. (2011) Mucopolipidosis type IV: an update. *Molecular genetics and metabolism* **104**, 206-213
30. Berman, E. R., Livni, N., Shapira, E., Merin, S., and Levij, I. S. (1974) Congenital corneal clouding with abnormal systemic storage bodies: a new variant of mucopolipidosis. *The Journal of pediatrics* **84**, 519-526
31. Bach, G., Webb, M. B., Bargal, R., Zeigler, M., and Ekstein, J. (2005) The frequency of mucopolipidosis type IV in the Ashkenazi Jewish population and the identification of 3 novel MCOLN1 mutations. *Human mutation* **26**, 591

32. Altarescu, G., Sun, M., Moore, D. F., Smith, J. A., Wiggs, E. A., Solomon, B. I., Patronas, N. J., Frei, K. P., Gupta, S., Kaneski, C. R., Quarrell, O. W., Slaugenhaupt, S. A., Goldin, E., and Schiffmann, R. (2002) The neurogenetics of mucopolipidosis type IV. *Neurology* **59**, 306-313
33. Kogot-Levin, A., Zeigler, M., Ornoy, A., and Bach, G. (2009) Mucopolipidosis type IV: the effect of increased lysosomal pH on the abnormal lysosomal storage. *Pediatric research* **65**, 686-690
34. Bach, G. (2001) Mucopolipidosis type IV. *Molecular genetics and metabolism* **73**, 197-203
35. Geer, J. S., Skinner, S. A., Goldin, E., and Holden, K. R. (2010) Mucopolipidosis type IV: a subtle pediatric neurodegenerative disorder. *Pediatric neurology* **42**, 223-226
36. Bindu, P. S., Gayathri, N., Yasha, T. C., Kooroor, J. M., Subasree, R., Rao, S., Panda, S., and Pal, P. K. (2008) A variant form of mucopolipidosis IV: report on 4 patients from the Indian subcontinent. *Journal of child neurology* **23**, 1443-1446
37. Mirabelli-Badenier, M., Severino, M., Tappino, B., Tortora, D., Camia, F., Zanaboni, C., Brera, F., Priolo, E., Rossi, A., Biancheri, R., Di Rocco, M., and Filocamo, M. (2014) A novel homozygous MCOLN1 double mutant allele leading to TRP channel domain ablation underlies Mucopolipidosis IV in an Italian Child. *Metabolic brain disease*
38. Chen, C. C., Keller, M., Hess, M., Schiffmann, R., Urban, N., Wolfgardt, A., Schaefer, M., Bracher, F., Biel, M., Wahl-Schott, C., and Grimm, C. (2014) A small molecule restores function to TRPML1 mutant isoforms responsible for mucopolipidosis type IV. *Nature communications* **5**, 4681
39. Newman, N. J., Starck, T., Kenyon, K. R., Lessell, S., Fish, I., and Kolodny, E. H. (1990) Corneal surface irregularities and episodic pain in a patient with mucopolipidosis IV. *Archives of ophthalmology* **108**, 251-254
40. Riedel, K. G., Zwaan, J., Kenyon, K. R., Kolodny, E. H., Hanninen, L., and Albert, D. M. (1985) Ocular abnormalities in mucopolipidosis IV. *American journal of ophthalmology* **99**, 125-136
41. Grishchuk, Y., Sri, S., Rudinskiy, N., Ma, W., Stember, K. G., Cottle, M. W., Sapp, E., Difiglia, M., Muzikansky, A., Betensky, R. A., Wong, A. M., Bacskai, B. J., Hyman, B. T., Kelleher, R. J., Cooper, J. D., and Slaugenhaupt, S. A. (2014) Behavioral deficits, early gliosis, dysmyelination and synaptic dysfunction in a mouse model of mucopolipidosis IV. *Acta neuropathologica communications* **2**, 133
42. Schiffmann, R., Dwyer, N. K., Lubensky, I. A., Tsokos, M., Sutliff, V. E., Latimer, J. S., Frei, K. P., Brady, R. O., Barton, N. W., Blanchette-Mackie, E. J., and Goldin, E. (1998) Constitutive achlorhydria in mucopolipidosis type IV. *Proceedings of the National Academy of Sciences of the United States of America* **95**, 1207-1212
43. Bonavita, S., Virta, A., Jeffries, N., Goldin, E., Tedeschi, G., and Schiffmann, R. (2003) Diffuse neuroaxonal involvement in mucopolipidosis IV as assessed by proton magnetic resonance spectroscopic imaging. *Journal of child neurology* **18**, 443-449
44. Frei, K. P., Patronas, N. J., Crutchfield, K. E., Altarescu, G., and Schiffmann, R. (1998) Mucopolipidosis type IV: characteristic MRI findings. *Neurology* **51**, 565-569
45. Walkley, S. U., Sikora, J., Micsenyi, M., Davidson, C., and Dobrenis, K. (2010) Lysosomal compromise and brain dysfunction: examining the role of neuroaxonal dystrophy. *Biochemical Society transactions* **38**, 1436-1441
46. Schiffmann, R., Mayfield, J., Swift, C., and Nestrasil, I. (2014) Quantitative neuroimaging in mucopolipidosis type IV. *Molecular genetics and metabolism* **111**, 147-151

47. Smith, J. A., Chan, C. C., Goldin, E., and Schiffmann, R. (2002) Noninvasive diagnosis and ophthalmic features of mucopolipidosis type IV. *Ophthalmology* **109**, 588-594
48. Alroy, J., and Ucci, A. A. (2006) Skin biopsy: a useful tool in the diagnosis of lysosomal storage diseases. *Ultrastructural pathology* **30**, 489-503
49. Vergarajauregui, S., Connelly, P. S., Daniels, M. P., and Puertollano, R. (2008) Autophagic dysfunction in mucopolipidosis type IV patients. *Human molecular genetics* **17**, 2723-2737
50. Slaugenhaupt, S. A., Acierno, J. S., Jr., Helbling, L. A., Bove, C., Goldin, E., Bach, G., Schiffmann, R., and Gusella, J. F. (1999) Mapping of the mucopolipidosis type IV gene to chromosome 19p and definition of founder haplotypes. *American journal of human genetics* **65**, 773-778
51. Goldin, E., Blanchette-Mackie, E. J., Dwyer, N. K., Pentchev, P. G., and Brady, R. O. (1995) Cultured skin fibroblasts derived from patients with mucopolipidosis 4 are auto-fluorescent. *Pediatric research* **37**, 687-692
52. Bargal, R., and Bach, G. (1997) Mucopolipidosis type IV: abnormal transport of lipids to lysosomes. *Journal of inherited metabolic disease* **20**, 625-632
53. Chen, C. S., Bach, G., and Pagano, R. E. (1998) Abnormal transport along the lysosomal pathway in mucopolipidosis, type IV disease. *Proceedings of the National Academy of Sciences of the United States of America* **95**, 6373-6378
54. Venugopal, B., Browning, M. F., Curcio-Morelli, C., Varro, A., Michaud, N., Nanthakumar, N., Walkley, S. U., Pickel, J., and Slaugenhaupt, S. A. (2007) Neurologic, gastric, and ophthalmologic pathologies in a murine model of mucopolipidosis type IV. *American journal of human genetics* **81**, 1070-1083
55. Folkerth, R. D., Alroy, J., Lomakina, I., Skutelsky, E., Raghavan, S. S., and Kolodny, E. H. (1995) Mucopolipidosis IV: morphology and histochemistry of an autopsy case. *Journal of neuropathology and experimental neurology* **54**, 154-164
56. Bozzato, A., Barlati, S., and Borsani, G. (2008) Gene expression profiling of mucopolipidosis type IV fibroblasts reveals deregulation of genes with relevant functions in lysosome physiology. *Biochimica et biophysica acta* **1782**, 250-258
57. Stenson, P. D., Mort, M., Ball, E. V., Shaw, K., Phillips, A., and Cooper, D. N. (2014) The Human Gene Mutation Database: building a comprehensive mutation repository for clinical and molecular genetics, diagnostic testing and personalized genomic medicine. *Human genetics* **133**, 1-9
58. Dong, X. P., Cheng, X., Mills, E., Delling, M., Wang, F., Kurz, T., and Xu, H. (2008) The type IV mucopolipidosis-associated protein TRPML1 is an endolysosomal iron release channel. *Nature* **455**, 992-996
59. Raychowdhury, M. K., Gonzalez-Perrett, S., Montalbetti, N., Timpanaro, G. A., Chasan, B., Goldmann, W. H., Stahl, S., Cooney, A., Goldin, E., and Cantiello, H. F. (2004) Molecular pathophysiology of mucopolipidosis type IV: pH dysregulation of the mucopolipin-1 cation channel. *Human molecular genetics* **13**, 617-627
60. Falardeau, J. L., Kennedy, J. C., Acierno, J. S., Jr., Sun, M., Stahl, S., Goldin, E., and Slaugenhaupt, S. A. (2002) Cloning and characterization of the mouse Mcoln1 gene reveals an alternatively spliced transcript not seen in humans. *BMC genomics* **3**, 3
61. Slaugenhaupt, S. A. (2002) The molecular basis of mucopolipidosis type IV. *Current molecular medicine* **2**, 445-450
62. Cheng, X., Shen, D., Samie, M., and Xu, H. (2010) Mucopolipins: Intracellular TRPML1-3 channels. *FEBS letters* **584**, 2013-2021

63. Fares, H., and Greenwald, I. (2001) Regulation of endocytosis by CUP-5, the *Caenorhabditis elegans* mucolipin-1 homolog. *Nature genetics* **28**, 64-68
64. Zheng, J. (2013) Molecular mechanism of TRP channels. *Comprehensive Physiology* **3**, 221-242
65. Nilius, B., and Owsianik, G. (2011) The transient receptor potential family of ion channels. *Genome biology* **12**, 218
66. Dong, X. P., Wang, X., and Xu, H. (2010) TRP channels of intracellular membranes. *Journal of neurochemistry* **113**, 313-328
67. Pryor, P. R., Reimann, F., Gribble, F. M., and Luzio, J. P. (2006) Mucolipin-1 is a lysosomal membrane protein required for intracellular lactosylceramide traffic. *Traffic* **7**, 1388-1398
68. Kim, H. J., Soyombo, A. A., Tjon-Kon-Sang, S., So, I., and Muallem, S. (2009) The Ca(2+) channel TRPML3 regulates membrane trafficking and autophagy. *Traffic* **10**, 1157-1167
69. Vergarajauregui, S., and Puertollano, R. (2006) Two di-leucine motifs regulate trafficking of mucolipin-1 to lysosomes. *Traffic* **7**, 337-353
70. Zeevi, D. A., Frumkin, A., Offen-Glasner, V., Kogot-Levin, A., and Bach, G. (2009) A potentially dynamic lysosomal role for the endogenous TRPML proteins. *The Journal of pathology* **219**, 153-162
71. Flores, E. N., and Garcia-Anoveros, J. (2011) TRPML2 and the evolution of mucolipins. *Advances in experimental medicine and biology* **704**, 221-228
72. Venkatachalam, K., Hofmann, T., and Montell, C. (2006) Lysosomal localization of TRPML3 depends on TRPML2 and the mucopolidosis-associated protein TRPML1. *The Journal of biological chemistry* **281**, 17517-17527
73. Curcio-Morelli, C., Zhang, P., Venugopal, B., Charles, F. A., Browning, M. F., Cantiello, H. F., and Slaugenhaupt, S. A. (2010) Functional multimerization of mucolipin channel proteins. *Journal of cellular physiology* **222**, 328-335
74. Zeevi, D. A., Lev, S., Frumkin, A., Minke, B., and Bach, G. (2010) Heteromultimeric TRPML channel assemblies play a crucial role in the regulation of cell viability models and starvation-induced autophagy. *Journal of cell science* **123**, 3112-3124
75. Wang, W., Zhang, X., Gao, Q., and Xu, H. (2014) TRPML1: an ion channel in the lysosome. *Handbook of experimental pharmacology* **222**, 631-645
76. Abe, K., and Puertollano, R. (2011) Role of TRP channels in the regulation of the endosomal pathway. *Physiology* **26**, 14-22
77. Vergarajauregui, S., Oberdick, R., Kiselyov, K., and Puertollano, R. (2008) Mucolipin 1 channel activity is regulated by protein kinase A-mediated phosphorylation. *The Biochemical journal* **410**, 417-425
78. Alam, J., Wicks, C., Stewart, D., Gong, P., Touchard, C., Otterbein, S., Choi, A. M., Burow, M. E., and Tou, J. (2000) Mechanism of heme oxygenase-1 gene activation by cadmium in MCF-7 mammary epithelial cells. Role of p38 kinase and Nrf2 transcription factor. *The Journal of biological chemistry* **275**, 27694-27702
79. Dong, X. P., Shen, D., Wang, X., Dawson, T., Li, X., Zhang, Q., Cheng, X., Zhang, Y., Weisman, L. S., Dellinger, M., and Xu, H. (2010) PI(3,5)P(2) controls membrane trafficking by direct activation of mucolipin Ca(2+) release channels in the endolysosome. *Nature communications* **1**, 38

80. Zhang, X., Li, X., and Xu, H. (2012) Phosphoinositide isoforms determine compartment-specific ion channel activity. *Proceedings of the National Academy of Sciences of the United States of America* **109**, 11384-11389
81. Zhang, Y., McCartney, A. J., Zolov, S. N., Ferguson, C. J., Meisler, M. H., Sutton, M. A., and Weisman, L. S. (2012) Modulation of synaptic function by VAC14, a protein that regulates the phosphoinositides PI(3,5)P(2) and PI(5)P. *The EMBO journal* **31**, 3442-3456
82. Qian, F., and Noben-Trauth, K. (2005) Cellular and molecular function of mucolipins (TRPML) and polycystin 2 (TRPP2). *Pflugers Archiv : European journal of physiology* **451**, 277-285
83. Kiselyov, K., Chen, J., Rbaibi, Y., Oberdick, D., Tjon-Kon-Sang, S., Shcheynikov, N., Muallem, S., and Soyombo, A. (2005) TRP-ML1 is a lysosomal monovalent cation channel that undergoes proteolytic cleavage. *The Journal of biological chemistry* **280**, 43218-43223
84. Miedel, M. T., Weixel, K. M., Bruns, J. R., Traub, L. M., and Weisz, O. A. (2006) Posttranslational cleavage and adaptor protein complex-dependent trafficking of mucolipin-1. *The Journal of biological chemistry* **281**, 12751-12759
85. Puertollano, R., and Kiselyov, K. (2009) TRPMLs: in sickness and in health. *American journal of physiology. Renal physiology* **296**, F1245-1254
86. Colletti, G. A., and Kiselyov, K. (2011) Trpml1. *Advances in experimental medicine and biology* **704**, 209-219
87. Pagano, R. E. (2003) Endocytic trafficking of glycosphingolipids in sphingolipid storage diseases. *Philosophical transactions of the Royal Society of London. Series B, Biological sciences* **358**, 885-891
88. Eichelsdoerfer, J. L., Evans, J. A., Slaugenhaupt, S. A., and Cuajungco, M. P. (2010) Zinc dyshomeostasis is linked with the loss of mucopolidosis IV-associated TRPML1 ion channel. *The Journal of biological chemistry* **285**, 34304-34308
89. Choi, D. W., and Koh, J. Y. (1998) Zinc and brain injury. *Annual review of neuroscience* **21**, 347-375
90. Frederickson, C. J., Koh, J. Y., and Bush, A. I. (2005) The neurobiology of zinc in health and disease. *Nature reviews. Neuroscience* **6**, 449-462
91. Kurz, T., Eaton, J. W., and Brunk, U. T. (2011) The role of lysosomes in iron metabolism and recycling. *The international journal of biochemistry & cell biology* **43**, 1686-1697
92. McCord, M. C., and Aizenman, E. (2014) The role of intracellular zinc release in aging, oxidative stress, and Alzheimer's disease. *Frontiers in aging neuroscience* **6**, 77
93. Terman, A., and Kurz, T. (2013) Lysosomal iron, iron chelation, and cell death. *Antioxidants & redox signaling* **18**, 888-898
94. Vallee, B. L., and Falchuk, K. H. (1993) The biochemical basis of zinc physiology. *Physiological reviews* **73**, 79-118
95. Valko, M., Leibfritz, D., Moncol, J., Cronin, M. T., Mazur, M., and Telser, J. (2007) Free radicals and antioxidants in normal physiological functions and human disease. *The international journal of biochemistry & cell biology* **39**, 44-84
96. Pourahmad, J., Ross, S., and O'Brien, P. J. (2001) Lysosomal involvement in hepatocyte cytotoxicity induced by Cu(2+) but not Cd(2+). *Free radical biology & medicine* **30**, 89-97
97. Stroikin, Y., Dalen, H., Loof, S., and Terman, A. (2004) Inhibition of autophagy with 3-methyladenine results in impaired turnover of lysosomes and accumulation of lipofuscin-like material. *European journal of cell biology* **83**, 583-590

98. Terman, A., and Brunk, U. T. (2004) Lipofuscin. *The international journal of biochemistry & cell biology* **36**, 1400-1404
99. Brunk, U. T., Jones, C. B., and Sohal, R. S. (1992) A novel hypothesis of lipofuscinogenesis and cellular aging based on interactions between oxidative stress and autophagocytosis. *Mutation research* **275**, 395-403
100. Terman, A., Kurz, T., Navratil, M., Arriaga, E. A., and Brunk, U. T. (2010) Mitochondrial turnover and aging of long-lived postmitotic cells: the mitochondrial-lysosomal axis theory of aging. *Antioxidants & redox signaling* **12**, 503-535
101. Schneider, J. L., and Cuervo, A. M. (2014) Autophagy and human disease: emerging themes. *Current opinion in genetics & development* **26C**, 16-23
102. Collins, J. F., Prohaska, J. R., and Knutson, M. D. (2010) Metabolic crossroads of iron and copper. *Nutrition reviews* **68**, 133-147
103. Kukic, I., Lee, J. K., Coblentz, J., Kelleher, S. L., and Kiselyov, K. (2013) Zinc-dependent lysosomal enlargement in TRPML1-deficient cells involves MTF-1 transcription factor and ZnT4 (Slc30a4) transporter. *The Biochemical journal* **451**, 155-163
104. Dusek, P., Jankovic, J., and Le, W. (2012) Iron dysregulation in movement disorders. *Neurobiology of disease* **46**, 1-18
105. Andrews, N. C., and Schmidt, P. J. (2007) Iron homeostasis. *Annual review of physiology* **69**, 69-85
106. Morgan, E. H., and Oates, P. S. (2002) Mechanisms and regulation of intestinal iron absorption. *Blood cells, molecules & diseases* **29**, 384-399
107. Blair, B. G., Larson, C. A., Adams, P. L., Abada, P. B., Pesce, C. E., Safaei, R., and Howell, S. B. (2011) Copper transporter 2 regulates endocytosis and controls tumor growth and sensitivity to cisplatin in vivo. *Molecular pharmacology* **79**, 157-166
108. Howell, S. B., Safaei, R., Larson, C. A., and Sailor, M. J. (2010) Copper transporters and the cellular pharmacology of the platinum-containing cancer drugs. *Molecular pharmacology* **77**, 887-894
109. Llanos, R. M., and Mercer, J. F. (2002) The molecular basis of copper homeostasis copper-related disorders. *DNA and cell biology* **21**, 259-270
110. Ugarte, M., Osborne, N. N., Brown, L. A., and Bishop, P. N. (2013) Iron, zinc, and copper in retinal physiology and disease. *Survey of ophthalmology* **58**, 585-609
111. Harris, E. D. (2000) Cellular copper transport and metabolism. *Annual review of nutrition* **20**, 291-310
112. Song, W., Wang, F., Lotfi, P., Sardiello, M., and Segatori, L. (2014) 2-Hydroxypropyl-beta-cyclodextrin promotes transcription factor EB-mediated activation of autophagy: implications for therapy. *The Journal of biological chemistry* **289**, 10211-10222
113. Medina, D. L., Fraldi, A., Bouche, V., Annunziata, F., Mansueto, G., Spampanato, C., Puri, C., Pignata, A., Martina, J. A., Sardiello, M., Palmieri, M., Polishchuk, R., Puertollano, R., and Ballabio, A. (2011) Transcriptional activation of lysosomal exocytosis promotes cellular clearance. *Developmental cell* **21**, 421-430
114. Spampanato, C., Feeney, E., Li, L., Cardone, M., Lim, J. A., Annunziata, F., Zare, H., Polishchuk, R., Puertollano, R., Parenti, G., Ballabio, A., and Raben, N. (2013) Transcription factor EB (TFEB) is a new therapeutic target for Pompe disease. *EMBO molecular medicine* **5**, 691-706

115. Dehay, B., Bove, J., Rodriguez-Muela, N., Perier, C., Recasens, A., Boya, P., and Vila, M. (2010) Pathogenic lysosomal depletion in Parkinson's disease. *The Journal of neuroscience : the official journal of the Society for Neuroscience* **30**, 12535-12544
116. Tsunemi, T., Ashe, T. D., Morrison, B. E., Soriano, K. R., Au, J., Roque, R. A., Lazarowski, E. R., Damian, V. A., Masliah, E., and La Spada, A. R. (2012) PGC-1alpha rescues Huntington's disease proteotoxicity by preventing oxidative stress and promoting TFEB function. *Science translational medicine* **4**, 142ra197
117. Schiffmann, R. (2006) Neuropathy and Fabry disease: pathogenesis and enzyme replacement therapy. *Acta neurologica Belgica* **106**, 61-65
118. Dangel, M. E., Bremer, D. L., and Rogers, G. L. (1985) Treatment of corneal opacification in mucopolipidosis IV with conjunctival transplantation. *American journal of ophthalmology* **99**, 137-141
119. Altarescu, G., Hill, S., Wiggs, E., Jeffries, N., Kreps, C., Parker, C. C., Brady, R. O., Barton, N. W., and Schiffmann, R. (2001) The efficacy of enzyme replacement therapy in patients with chronic neuronopathic Gaucher's disease. *The Journal of pediatrics* **138**, 539-547
120. Lund, T. C. (2013) Hematopoietic stem cell transplant for lysosomal storage diseases. *Pediatric endocrinology reviews : PER* **11 Suppl 1**, 91-98
121. Prasad, V. K., and Kurtzberg, J. (2010) Cord blood and bone marrow transplantation in inherited metabolic diseases: scientific basis, current status and future directions. *British journal of haematology* **148**, 356-372
122. Seregin, S. S., and Amalfitano, A. (2011) Gene therapy for lysosomal storage diseases: progress, challenges and future prospects. *Current pharmaceutical design* **17**, 2558-2574
123. Brady, R. O. (2003) Enzyme replacement therapy: conception, chaos and culmination. *Philosophical transactions of the Royal Society of London. Series B, Biological sciences* **358**, 915-919
124. Desnick, R. J., and Schuchman, E. H. (2012) Enzyme replacement therapy for lysosomal diseases: lessons from 20 years of experience and remaining challenges. *Annual review of genomics and human genetics* **13**, 307-335
125. Platt, F. M. (2014) Sphingolipid lysosomal storage disorders. *Nature* **510**, 68-75
126. Hawkins-Salsbury, J. A., Reddy, A. S., and Sands, M. S. (2011) Combination therapies for lysosomal storage disease: is the whole greater than the sum of its parts? *Human molecular genetics* **20**, R54-60
127. Li, J., O, W., Li, W., Jiang, Z. G., and Ghanbari, H. A. (2013) Oxidative stress and neurodegenerative disorders. *International journal of molecular sciences* **14**, 24438-24475
128. Koskenkorva-Frank, T. S., Weiss, G., Koppenol, W. H., and Burckhardt, S. (2013) The complex interplay of iron metabolism, reactive oxygen species, and reactive nitrogen species: insights into the potential of various iron therapies to induce oxidative and nitrosative stress. *Free radical biology & medicine* **65**, 1174-1194
129. Campeau, P. M., Rafei, M., Boivin, M. N., Sun, Y., Grabowski, G. A., and Galipeau, J. (2009) Characterization of Gaucher disease bone marrow mesenchymal stromal cells reveals an altered inflammatory secretome. *Blood* **114**, 3181-3190
130. Deganuto, M., Pittis, M. G., Pines, A., Dominissini, S., Kelley, M. R., Garcia, R., Quadrifoglio, F., Bembi, B., and Tell, G. (2007) Altered intracellular redox status in Gaucher disease fibroblasts and impairment of adaptive response against oxidative stress. *Journal of cellular physiology* **212**, 223-235

131. Hachiya, Y., Hayashi, M., Kumada, S., Uchiyama, A., Tsuchiya, K., and Kurata, K. (2006) Mechanisms of neurodegeneration in neuronal ceroid-lipofuscinoses. *Acta neuropathologica* **111**, 168-177
132. Heine, C., Tyynela, J., Cooper, J. D., Palmer, D. N., Elleder, M., Kohlschutter, A., and Braulke, T. (2003) Enhanced expression of manganese-dependent superoxide dismutase in human and sheep CLN6 tissues. *The Biochemical journal* **376**, 369-376
133. Jeyakumar, M., Thomas, R., Elliot-Smith, E., Smith, D. A., van der Spoel, A. C., d'Azzo, A., Perry, V. H., Butters, T. D., Dwek, R. A., and Platt, F. M. (2003) Central nervous system inflammation is a hallmark of pathogenesis in mouse models of GM1 and GM2 gangliosidosis. *Brain : a journal of neurology* **126**, 974-987
134. Kim, S. J., Zhang, Z., Lee, Y. C., and Mukherjee, A. B. (2006) Palmitoyl-protein thioesterase-1 deficiency leads to the activation of caspase-9 and contributes to rapid neurodegeneration in INCL. *Human molecular genetics* **15**, 1580-1586
135. Reddy, J. V., Ganley, I. G., and Pfeffer, S. R. (2006) Clues to neuro-degeneration in Niemann-Pick type C disease from global gene expression profiling. *PloS one* **1**, e19
136. Shen, J. S., Meng, X. L., Moore, D. F., Quirk, J. M., Shayman, J. A., Schiffmann, R., and Kaniski, C. R. (2008) Globotriaosylceramide induces oxidative stress and up-regulates cell adhesion molecule expression in Fabry disease endothelial cells. *Molecular genetics and metabolism* **95**, 163-168
137. Villani, G. R., Di Domenico, C., Musella, A., Cecere, F., Di Napoli, D., and Di Natale, P. (2009) Mucopolysaccharidosis IIIB: oxidative damage and cytotoxic cell involvement in the neuronal pathogenesis. *Brain research* **1279**, 99-108
138. Zampieri, S., Mellon, S. H., Butters, T. D., Nevyjel, M., Covey, D. F., Bembi, B., and Dardis, A. (2009) Oxidative stress in NPC1 deficient cells: protective effect of allopregnanolone. *Journal of cellular and molecular medicine* **13**, 3786-3796
139. Vitner, E. B., Platt, F. M., and Futerman, A. H. (2010) Common and uncommon pathogenic cascades in lysosomal storage diseases. *The Journal of biological chemistry* **285**, 20423-20427
140. Shukla, V., Mishra, S. K., and Pant, H. C. (2011) Oxidative stress in neurodegeneration. *Advances in pharmacological sciences* **2011**, 572634
141. Turrens, J. F. (2003) Mitochondrial formation of reactive oxygen species. *The Journal of physiology* **552**, 335-344
142. Wang, X., Fang, H., Huang, Z., Shang, W., Hou, T., Cheng, A., and Cheng, H. (2013) Imaging ROS signaling in cells and animals. *Journal of molecular medicine* **91**, 917-927
143. Gutteridge, J. M., and Halliwell, B. (2000) Free radicals and antioxidants in the year 2000. A historical look to the future. *Annals of the New York Academy of Sciences* **899**, 136-147
144. Holmstrom, K. M., and Finkel, T. (2014) Cellular mechanisms and physiological consequences of redox-dependent signalling. *Nature reviews. Molecular cell biology* **15**, 411-421
145. Droge, W. (2002) Free radicals in the physiological control of cell function. *Physiological reviews* **82**, 47-95
146. Bataille, A. M., and Manautou, J. E. (2012) Nrf2: a potential target for new therapeutics in liver disease. *Clinical pharmacology and therapeutics* **92**, 340-348
147. van der Wijst, M. G., Brown, R., and Rots, M. G. (2014) Nrf2, the master redox switch: The Achilles' heel of ovarian cancer? *Biochimica et biophysica acta*

148. Yanaka, A., Zhang, S., Tauchi, M., Suzuki, H., Shibahara, T., Matsui, H., Nakahara, A., Tanaka, N., and Yamamoto, M. (2005) Role of the nrf-2 gene in protection and repair of gastric mucosa against oxidative stress. *Inflammopharmacology* **13**, 83-90
149. Baird, L., and Dinkova-Kostova, A. T. (2011) The cytoprotective role of the Keap1-Nrf2 pathway. *Archives of toxicology* **85**, 241-272
150. Son, Y., Lee, J. H., Chung, H. T., and Pae, H. O. (2013) Therapeutic roles of heme oxygenase-1 in metabolic diseases: curcumin and resveratrol analogues as possible inducers of heme oxygenase-1. *Oxidative medicine and cellular longevity* **2013**, 639541
151. Dinkova-Kostova, A. T., and Talalay, P. (2010) NAD(P)H:quinone acceptor oxidoreductase 1 (NQO1), a multifunctional antioxidant enzyme and exceptionally versatile cytoprotector. *Archives of biochemistry and biophysics* **501**, 116-123
152. Levtchenko, E., de Graaf-Hess, A., Wilmer, M., van den Heuvel, L., Monnens, L., and Blom, H. (2005) Altered status of glutathione and its metabolites in cystinotic cells. *Nephrology, dialysis, transplantation : official publication of the European Dialysis and Transplant Association - European Renal Association* **20**, 1828-1832
153. Perry, T. L., Godin, D. V., and Hansen, S. (1982) Parkinson's disease: a disorder due to nigral glutathione deficiency? *Neuroscience letters* **33**, 305-310
154. Guthrie, H. D., and Welch, G. R. (2007) Use of fluorescence-activated flow cytometry to determine membrane lipid peroxidation during hypothermic liquid storage and freeze-thawing of viable boar sperm loaded with 4, 4-difluoro-5-(4-phenyl-1,3-butadienyl)-4-bora-3a,4a-diaza-s-indacene-3-undecanoic acid. *Journal of animal science* **85**, 1402-1411
155. Spickett, C. M., Wiswedel, I., Siems, W., Zarkovic, K., and Zarkovic, N. (2010) Advances in methods for the determination of biologically relevant lipid peroxidation products. *Free radical research* **44**, 1172-1202
156. Guo, H., Aleyasin, H., Dickinson, B. C., Haskew-Layton, R. E., and Ratan, R. R. (2014) Recent advances in hydrogen peroxide imaging for biological applications. *Cell & bioscience* **4**, 64
157. Duan, Y., Gross, R. A., and Sheu, S. S. (2007) Ca²⁺-dependent generation of mitochondrial reactive oxygen species serves as a signal for poly(ADP-ribose) polymerase-1 activation during glutamate excitotoxicity. *The Journal of physiology* **585**, 741-758
158. Zielonka, J., and Kalyanaraman, B. (2010) Hydroethidine- and MitoSOX-derived red fluorescence is not a reliable indicator of intracellular superoxide formation: another inconvenient truth. *Free radical biology & medicine* **48**, 983-1001
159. Szabadkai, G., Simoni, A. M., Chami, M., Wieckowski, M. R., Youle, R. J., and Rizzuto, R. (2004) Drp-1-dependent division of the mitochondrial network blocks intraorganellar Ca²⁺ waves and protects against Ca²⁺-mediated apoptosis. *Molecular cell* **16**, 59-68
160. Chen, H., and Chan, D. C. (2005) Emerging functions of mammalian mitochondrial fusion and fission. *Human molecular genetics* **14 Spec No. 2**, R283-289
161. Kasahara, A., and Scorrano, L. (2014) Mitochondria: from cell death executioners to regulators of cell differentiation. *Trends in cell biology*
162. Kim, I., Rodriguez-Enriquez, S., and Lemasters, J. J. (2007) Selective degradation of mitochondria by mitophagy. *Archives of biochemistry and biophysics* **462**, 245-253
163. Campello, S., and Scorrano, L. (2010) Mitochondrial shape changes: orchestrating cell pathophysiology. *EMBO reports* **11**, 678-684
164. Ribas, V., Garcia-Ruiz, C., and Fernandez-Checa, J. C. (2014) Glutathione and mitochondria. *Frontiers in pharmacology* **5**, 151

165. Novak, I. (2012) Mitophagy: a complex mechanism of mitochondrial removal. *Antioxidants & redox signaling* **17**, 794-802
166. Palmer, C. S., Osellame, L. D., Stojanovski, D., and Ryan, M. T. (2011) The regulation of mitochondrial morphology: intricate mechanisms and dynamic machinery. *Cellular signalling* **23**, 1534-1545
167. Tanaka, A. (2010) Parkin-mediated selective mitochondrial autophagy, mitophagy: Parkin purges damaged organelles from the vital mitochondrial network. *FEBS letters* **584**, 1386-1392
168. Gomes, L. C., and Scorrano, L. (2013) Mitochondrial morphology in mitophagy and macroautophagy. *Biochimica et biophysica acta* **1833**, 205-212
169. Kageyama, Y., Zhang, Z., Roda, R., Fukaya, M., Wakabayashi, J., Wakabayashi, N., Kensler, T. W., Reddy, P. H., Iijima, M., and Sesaki, H. (2012) Mitochondrial division ensures the survival of postmitotic neurons by suppressing oxidative damage. *The Journal of cell biology* **197**, 535-551
170. Knott, A. B., Perkins, G., Schwarzenbacher, R., and Bossy-Wetzel, E. (2008) Mitochondrial fragmentation in neurodegeneration. *Nature reviews. Neuroscience* **9**, 505-518
171. Rambold, A. S., and Lippincott-Schwartz, J. (2011) Mechanisms of mitochondria and autophagy crosstalk. *Cell cycle* **10**, 4032-4038
172. Mizushima, N., and Komatsu, M. (2011) Autophagy: renovation of cells and tissues. *Cell* **147**, 728-741
173. Gomes, L. C., Di Benedetto, G., and Scorrano, L. (2011) Essential amino acids and glutamine regulate induction of mitochondrial elongation during autophagy. *Cell cycle* **10**, 2635-2639
174. Rambold, A. S., Kostecky, B., Elia, N., and Lippincott-Schwartz, J. (2011) Tubular network formation protects mitochondria from autophagosomal degradation during nutrient starvation. *Proceedings of the National Academy of Sciences of the United States of America* **108**, 10190-10195
175. Wu, S., Zhou, F., Zhang, Z., and Xing, D. (2011) Mitochondrial oxidative stress causes mitochondrial fragmentation via differential modulation of mitochondrial fission-fusion proteins. *The FEBS journal* **278**, 941-954
176. da Silva, A. F., Mariotti, F. R., Maximo, V., and Campello, S. (2014) Mitochondria dynamism: of shape, transport and cell migration. *Cellular and molecular life sciences : CMLS* **71**, 2313-2324
177. Loson, O. C., Song, Z., Chen, H., and Chan, D. C. (2013) Fis1, Mff, MiD49, and MiD51 mediate Drp1 recruitment in mitochondrial fission. *Molecular biology of the cell* **24**, 659-667
178. Scott, I., and Youle, R. J. (2010) Mitochondrial fission and fusion. *Essays in biochemistry* **47**, 85-98
179. Gomes, L. C., Di Benedetto, G., and Scorrano, L. (2011) During autophagy mitochondria elongate, are spared from degradation and sustain cell viability. *Nature cell biology* **13**, 589-598
180. Wagner, K. M., Ruegg, M., Niemann, A., and Suter, U. (2009) Targeting and function of the mitochondrial fission factor GDAP1 are dependent on its tail-anchor. *PloS one* **4**, e5160

181. Mandemakers, W., Morais, V. A., and De Strooper, B. (2007) A cell biological perspective on mitochondrial dysfunction in Parkinson disease and other neurodegenerative diseases. *Journal of cell science* **120**, 1707-1716
182. Marco, A., Cuesta, A., Pedrola, L., Palau, F., and Marin, I. (2004) Evolutionary and structural analyses of GDAP1, involved in Charcot-Marie-Tooth disease, characterize a novel class of glutathione transferase-related genes. *Molecular biology and evolution* **21**, 176-187
183. Pedrola, L., Espert, A., Wu, X., Claramunt, R., Shy, M. E., and Palau, F. (2005) GDAP1, the protein causing Charcot-Marie-Tooth disease type 4A, is expressed in neurons and is associated with mitochondria. *Human molecular genetics* **14**, 1087-1094
184. Pla-Martin, D., Rueda, C. B., Estela, A., Sanchez-Piris, M., Gonzalez-Sanchez, P., Traba, J., de la Fuente, S., Scorrano, L., Renau-Piqueras, J., Alvarez, J., Satrustegui, J., and Palau, F. (2013) Silencing of the Charcot-Marie-Tooth disease-associated gene GDAP1 induces abnormal mitochondrial distribution and affects Ca²⁺ homeostasis by reducing store-operated Ca²⁺ entry. *Neurobiology of disease* **55**, 140-151
185. Niemann, A., Huber, N., Wagner, K. M., Somandin, C., Horn, M., Lebrun-Julien, F., Angst, B., Pereira, J. A., Halfter, H., Welzl, H., Feltri, M. L., Wrabetz, L., Young, P., Wessig, C., Toyka, K. V., and Suter, U. (2014) The Gdap1 knockout mouse mechanistically links redox control to Charcot-Marie-Tooth disease. *Brain : a journal of neurology* **137**, 668-682
186. Hayes, J. D., and Pulford, D. J. (1995) The glutathione S-transferase supergene family: regulation of GST and the contribution of the isoenzymes to cancer chemoprotection and drug resistance. *Critical reviews in biochemistry and molecular biology* **30**, 445-600
187. Noack, R., Frede, S., Albrecht, P., Henke, N., Pfeiffer, A., Knoll, K., Dehmel, T., Meyer Zu Horste, G., Stettner, M., Kieseier, B. C., Summer, H., Golz, S., Kochanski, A., Wiedau-Pazos, M., Arnold, S., Lewerenz, J., and Methner, A. (2012) Charcot-Marie-Tooth disease CMT4A: GDAP1 increases cellular glutathione and the mitochondrial membrane potential. *Human molecular genetics* **21**, 150-162
188. Xu, W., Barrientos, T., and Andrews, N. C. (2013) Iron and copper in mitochondrial diseases. *Cell metabolism* **17**, 319-328
189. Colletti, G. A., Miedel, M. T., Quinn, J., Andharia, N., Weisz, O. A., and Kiselyov, K. (2012) Loss of lysosomal ion channel transient receptor potential channel mucolipin-1 (TRPML1) leads to cathepsin B-dependent apoptosis. *The Journal of biological chemistry* **287**, 8082-8091
190. Miedel, M. T., Rbaibi, Y., Guerriero, C. J., Colletti, G., Weixel, K. M., Weisz, O. A., and Kiselyov, K. (2008) Membrane traffic and turnover in TRP-ML1-deficient cells: a revised model for mucopolidosis type IV pathogenesis. *The Journal of experimental medicine* **205**, 1477-1490
191. Livak, K. J., and Schmittgen, T. D. (2001) Analysis of relative gene expression data using real-time quantitative PCR and the 2(-Delta Delta C(T)) Method. *Methods* **25**, 402-408
192. Wang, A. L., Boulton, M. E., Dunn, W. A., Jr., Rao, H. V., Cai, J., Lukas, T. J., and Neufeld, A. H. (2009) Using LC3 to monitor autophagy flux in the retinal pigment epithelium. *Autophagy* **5**, 1190-1193
193. Cheng, W. Y., Tong, H., Miller, E. W., Chang, C. J., Remington, J., Zucker, R. M., Bromberg, P. A., Samet, J. M., and Hofer, T. P. (2010) An integrated imaging approach to

- the study of oxidative stress generation by mitochondrial dysfunction in living cells. *Environmental health perspectives* **118**, 902-908
194. White, R. J., and Reynolds, I. J. (1996) Mitochondrial depolarization in glutamate-stimulated neurons: an early signal specific to excitotoxin exposure. *The Journal of neuroscience : the official journal of the Society for Neuroscience* **16**, 5688-5697
 195. Jang, W., Park, H. H., Lee, K. Y., Lee, Y. J., Kim, H. T., and Koh, S. H. (2014) 1,25-dihydroxyvitamin D Attenuates L-DOPA-Induced Neurotoxicity in Neural Stem Cells. *Molecular neurobiology*
 196. Choi, S. W., Gerencser, A. A., and Nicholls, D. G. (2009) Bioenergetic analysis of isolated cerebrocortical nerve terminals on a microgram scale: spare respiratory capacity and stochastic mitochondrial failure. *Journal of neurochemistry* **109**, 1179-1191
 197. Gusdon, A. M., Zhu, J., Van Houten, B., and Chu, C. T. (2012) ATP13A2 regulates mitochondrial bioenergetics through macroautophagy. *Neurobiology of disease* **45**, 962-972
 198. Qian, W., and Van Houten, B. (2010) Alterations in bioenergetics due to changes in mitochondrial DNA copy number. *Methods* **51**, 452-457
 199. Zhou, W., Choi, M., Margineantu, D., Margaretha, L., Hesson, J., Cavanaugh, C., Blau, C. A., Horwitz, M. S., Hockenbery, D., Ware, C., and Ruohola-Baker, H. (2012) HIF1alpha induced switch from bivalent to exclusively glycolytic metabolism during ESC-to-EpiSC/hESC transition. *The EMBO journal* **31**, 2103-2116
 200. Martina, J. A., Lelouvier, B., and Puertollano, R. (2009) The calcium channel mucolipin-3 is a novel regulator of trafficking along the endosomal pathway. *Traffic* **10**, 1143-1156
 201. Karacsonyi, C., Miguel, A. S., and Puertollano, R. (2007) Mucolipin-2 localizes to the Arf6-associated pathway and regulates recycling of GPI-APs. *Traffic* **8**, 1404-1414
 202. Dong, X. P., Wang, X., Shen, D., Chen, S., Liu, M., Wang, Y., Mills, E., Cheng, X., Delling, M., and Xu, H. (2009) Activating mutations of the TRPML1 channel revealed by proline-scanning mutagenesis. *The Journal of biological chemistry* **284**, 32040-32052
 203. Shen, D., Wang, X., Li, X., Zhang, X., Yao, Z., Dibble, S., Dong, X. P., Yu, T., Lieberman, A. P., Showalter, H. D., and Xu, H. (2012) Lipid storage disorders block lysosomal trafficking by inhibiting a TRP channel and lysosomal calcium release. *Nature communications* **3**, 731
 204. Bach, G. (2005) Mucolipin I: endocytosis and cation channel--a review. *Pflugers Archiv : European journal of physiology* **451**, 313-317
 205. LaPlante, J. M., Sun, M., Falardeau, J., Dai, D., Brown, E. M., Slaugenhaupt, S. A., and Vassilev, P. M. (2006) Lysosomal exocytosis is impaired in mucopolidosis type IV. *Molecular genetics and metabolism* **89**, 339-348
 206. Kiselyov, K., Soyombo, A., and Muallem, S. (2007) TRPopathies. *The Journal of physiology* **578**, 641-653
 207. Barnett, A., and Brewer, G. J. (2011) Autophagy in aging and Alzheimer's disease: pathologic or protective? *Journal of Alzheimer's disease : JAD* **25**, 385-394
 208. Kiselyov, K., and Muallem, S. (2008) Mitochondrial Ca²⁺ homeostasis in lysosomal storage diseases. *Cell calcium* **44**, 103-111
 209. Settembre, C., Fraldi, A., Rubinsztein, D. C., and Ballabio, A. (2008) Lysosomal storage diseases as disorders of autophagy. *Autophagy* **4**, 113-114

210. Hegde, M. L., Hegde, P. M., Rao, K. S., and Mitra, S. (2011) Oxidative genome damage and its repair in neurodegenerative diseases: function of transition metals as a double-edged sword. *Journal of Alzheimer's disease : JAD* **24 Suppl 2**, 183-198
211. Huang, X. P., O'Brien, P. J., and Templeton, D. M. (2006) Mitochondrial involvement in genetically determined transition metal toxicity I. Iron toxicity. *Chemico-biological interactions* **163**, 68-76
212. Mehta, R., Templeton, D. M., and O'Brien P, J. (2006) Mitochondrial involvement in genetically determined transition metal toxicity II. Copper toxicity. *Chemico-biological interactions* **163**, 77-85
213. Morgan, M. J., and Liu, Z. G. (2011) Crosstalk of reactive oxygen species and NF-kappaB signaling. *Cell research* **21**, 103-115
214. Salminen, A., Kaarniranta, K., and Kauppinen, A. (2012) Inflammaging: disturbed interplay between autophagy and inflammasomes. *Aging* **4**, 166-175
215. Szydłowska, K., and Tymianski, M. (2010) Calcium, ischemia and excitotoxicity. *Cell calcium* **47**, 122-129
216. Valerio, L. G. (2007) Mammalian iron metabolism. *Toxicology mechanisms and methods* **17**, 497-517
217. Merin, S., Livni, N., Berman, E. R., and Yatziv, S. (1975) Mucopolidosis IV: ocular, systemic, and ultrastructural findings. *Investigative ophthalmology* **14**, 437-448
218. Kiselyov, K., Jennigs, J. J., Jr., Rbaibi, Y., and Chu, C. T. (2007) Autophagy, mitochondria and cell death in lysosomal storage diseases. *Autophagy* **3**, 259-262
219. Barth, S., Glick, D., and Macleod, K. F. (2010) Autophagy: assays and artifacts. *The Journal of pathology* **221**, 117-124
220. Ott, M., Gogvadze, V., Orrenius, S., and Zhivotovsky, B. (2007) Mitochondria, oxidative stress and cell death. *Apoptosis : an international journal on programmed cell death* **12**, 913-922
221. Venugopal, B., Mesires, N. T., Kennedy, J. C., Curcio-Morelli, C., Laplante, J. M., Dice, J. F., and Slaugenhaupt, S. A. (2009) Chaperone-mediated autophagy is defective in mucopolidosis type IV. *Journal of cellular physiology* **219**, 344-353
222. Takamura, A., Higaki, K., Kajimaki, K., Otsuka, S., Ninomiya, H., Matsuda, J., Ohno, K., Suzuki, Y., and Nanba, E. (2008) Enhanced autophagy and mitochondrial aberrations in murine G(M1)-gangliosidosis. *Biochemical and biophysical research communications* **367**, 616-622
223. Pacheco, C. D., Kunkel, R., and Lieberman, A. P. (2007) Autophagy in Niemann-Pick C disease is dependent upon Beclin-1 and responsive to lipid trafficking defects. *Human molecular genetics* **16**, 1495-1503
224. Cao, Y., Espinola, J. A., Fossale, E., Massey, A. C., Cuervo, A. M., MacDonald, M. E., and Cotman, S. L. (2006) Autophagy is disrupted in a knock-in mouse model of juvenile neuronal ceroid lipofuscinosis. *The Journal of biological chemistry* **281**, 20483-20493
225. Mortiboys, H., Thomas, K. J., Koopman, W. J., Klaffke, S., Abou-Sleiman, P., Olpin, S., Wood, N. W., Willems, P. H., Smeitink, J. A., Cookson, M. R., and Bandmann, O. (2008) Mitochondrial function and morphology are impaired in parkin-mutant fibroblasts. *Annals of neurology* **64**, 555-565
226. Benard, G., and Rossignol, R. (2008) Ultrastructure of the mitochondrion and its bearing on function and bioenergetics. *Antioxidants & redox signaling* **10**, 1313-1342

227. Nishio, K., Ishida, N., Saito, Y., Ogawa-Akazawa, Y., Shichiri, M., Yoshida, Y., Hagihara, Y., Noguchi, N., Chirico, J., Atkinson, J., and Niki, E. (2011) alpha-Tocopheryl phosphate: uptake, hydrolysis, and antioxidant action in cultured cells and mouse. *Free radical biology & medicine* **50**, 1794-1800
228. Gupta, P., Soyombo, A. A., Atashband, A., Wisniewski, K. E., Shelton, J. M., Richardson, J. A., Hammer, R. E., and Hofmann, S. L. (2001) Disruption of PPT1 or PPT2 causes neuronal ceroid lipofuscinosis in knockout mice. *Proceedings of the National Academy of Sciences of the United States of America* **98**, 13566-13571
229. Liu, H., Nakagawa, T., Kanematsu, T., Uchida, T., and Tsuji, S. (1999) Isolation of 10 differentially expressed cDNAs in differentiated Neuro2a cells induced through controlled expression of the GD3 synthase gene. *Journal of neurochemistry* **72**, 1781-1790
230. Feeney, E. J., Spanpanato, C., Puertollano, R., Ballabio, A., Parenti, G., and Raben, N. (2013) What else is in store for autophagy? Exocytosis of autolysosomes as a mechanism of TFEB-mediated cellular clearance in Pompe disease. *Autophagy* **9**, 1117-1118
231. Settembre, C., Di Malta, C., Polito, V. A., Garcia Arencibia, M., Vetrini, F., Erdin, S., Erdin, S. U., Huynh, T., Medina, D., Colella, P., Sardiello, M., Rubinsztein, D. C., and Ballabio, A. (2011) TFEB links autophagy to lysosomal biogenesis. *Science* **332**, 1429-1433
232. Kucic, I., Kelleher, S. L., and Kiselyov, K. (2014) Zn²⁺ efflux through lysosomal exocytosis prevents Zn²⁺-induced toxicity. *Journal of cell science* **127**, 3094-3103
233. Beck, M. (2010) Therapy for lysosomal storage disorders. *IUBMB life* **62**, 33-40
234. Repnik, U., Hafner Cesen, M., and Turk, B. (2014) Lysosomal membrane permeabilization in cell death: Concepts and challenges. *Mitochondrion*
235. Wong-Ekkabut, J., Xu, Z., Triampo, W., Tang, I. M., Tieleman, D. P., and Monticelli, L. (2007) Effect of lipid peroxidation on the properties of lipid bilayers: a molecular dynamics study. *Biophysical journal* **93**, 4225-4236
236. Venkatachalam, K., Wong, C. O., and Montell, C. (2013) Feast or famine: role of TRPML in preventing cellular amino acid starvation. *Autophagy* **9**, 98-100
237. Archer, L. D., Langford-Smith, K. J., Bigger, B. W., and Fildes, J. E. (2014) Mucopolysaccharide diseases: a complex interplay between neuroinflammation, microglial activation and adaptive immunity. *Journal of inherited metabolic disease* **37**, 1-12
238. Boitier, E., Rea, R., and Duchen, M. R. (1999) Mitochondria exert a negative feedback on the propagation of intracellular Ca²⁺ waves in rat cortical astrocytes. *The Journal of cell biology* **145**, 795-808
239. Parekh, A. B. (2003) Store-operated Ca²⁺ entry: dynamic interplay between endoplasmic reticulum, mitochondria and plasma membrane. *The Journal of physiology* **547**, 333-348
240. Mukherjee, S., Ghosh, R. N., and Maxfield, F. R. (1997) Endocytosis. *Physiological reviews* **77**, 759-803
241. Verhoeven, K., De Jonghe, P., Coen, K., Verpoorten, N., Auer-Grumbach, M., Kwon, J. M., FitzPatrick, D., Schmedding, E., De Vriendt, E., Jacobs, A., Van Gerwen, V., Wagner, K., Hartung, H. P., and Timmerman, V. (2003) Mutations in the small GTP-ase late endosomal protein RAB7 cause Charcot-Marie-Tooth type 2B neuropathy. *American journal of human genetics* **72**, 722-727
242. Vesa, J., Hellsten, E., Verkruyse, L. A., Camp, L. A., Rapola, J., Santavuori, P., Hofmann, S. L., and Peltonen, L. (1995) Mutations in the palmitoyl protein thioesterase gene causing infantile neuronal ceroid lipofuscinosis. *Nature* **376**, 584-587

243. Stenmark, H. (2009) Rab GTPases as coordinators of vesicle traffic. *Nature reviews. Molecular cell biology* **10**, 513-525
244. Chen, P. I., Kong, C., Su, X., and Stahl, P. D. (2009) Rab5 isoforms differentially regulate the trafficking and degradation of epidermal growth factor receptors. *The Journal of biological chemistry* **284**, 30328-30338
245. Lelouvier, B., and Puertollano, R. (2011) Mucolipin-3 regulates luminal calcium, acidification, and membrane fusion in the endosomal pathway. *The Journal of biological chemistry* **286**, 9826-9832
246. Shen, D., Wang, X., and Xu, H. (2011) Pairing phosphoinositides with calcium ions in endolysosomal dynamics: phosphoinositides control the direction and specificity of membrane trafficking by regulating the activity of calcium channels in the endolysosomes. *BioEssays : news and reviews in molecular, cellular and developmental biology* **33**, 448-457
247. Vanlandingham, P. A., and Ceresa, B. P. (2009) Rab7 regulates late endocytic trafficking downstream of multivesicular body biogenesis and cargo sequestration. *The Journal of biological chemistry* **284**, 12110-12124
248. Ballabio, A., and Gieselmann, V. (2009) Lysosomal disorders: from storage to cellular damage. *Biochimica et biophysica acta* **1793**, 684-696
249. Patel, S., and Muallem, S. (2011) Acidic Ca(2+) stores come to the fore. *Cell calcium* **50**, 109-112
250. Kiselyov, K., Yamaguchi, S., Lyons, C. W., and Muallem, S. (2010) Aberrant Ca²⁺ handling in lysosomal storage disorders. *Cell calcium* **47**, 103-111
251. Seglen, P. O., Grinde, B., and Solheim, A. E. (1979) Inhibition of the lysosomal pathway of protein degradation in isolated rat hepatocytes by ammonia, methylamine, chloroquine and leupeptin. *European journal of biochemistry / FEBS* **95**, 215-225
252. Kohno, K. (2010) Stress-sensing mechanisms in the unfolded protein response: similarities and differences between yeast and mammals. *Journal of biochemistry* **147**, 27-33